Oscillatory cortical activities in the human brain

Habilitationsschrift

vorgelegt von

Matthias M. Müller

an der Sozialwissenschaftlichen Fakultät

der Universität Konstanz

1997

Preface

When I started my work on cortical oscillatory activities, only little was known about these responses. Induced gamma band responses had been reported in animal studies, but there was not a single experiment in the human brain. With respect to the steady-state responses, it was known that they exist and for the auditory modality the superposition theory was practically accepted, i.e. auditory steady-state responses result from the superposition of transient middle latency components. While conducting the P300 experiments (see section 2.1.2 and 2.1.3), there was a first verbal report (or rather, a rumor) that Scott Makeig had shown that the P300 influences the auditory steady-state response. As for the visual steady-state response, there were only reports on the existence of the so-called "photic driving". In sum, it was quite unclear where the scientific journey would end up. However, it was the Zeitgeist of oscillatory cortical activities and more and more reports on these rhythms were being published. During the last years, I had the opportunity to work with many experts in the field who taught me experimental and analysis techniques which were to become the bread and butter of my work. I also had the unique opportunity to work at the Cuban Center of Neuroscience in Havana for a period of four weeks and to stay at the Department of Neuroscience at the Univesity of California in San Diego for one year. Both visits were supported by a grant from the Deutsche Forschungsgemeinschaft. Additional grants from the Human Frontier Science Program, the University of Konstanz and the Deutsche Forschungsgemeinschaft made this work possible.

First, I'm grateful to Thomas Elbert who was and still is a constant source of knowledge and ideas and he increasingly became my mentor over the last years. He has supported me in gaining my own experiences in this field. Warm thanks also to Brigitte Rockstroh for her support, her fight to get my current position at the University of Konstanz and her constant confidence in my scientific work. Thanks to Scott Makeig, who introduced me to the secrets of Complex Event Related Potentials analysis. During my stay in Havana, it was Mitchell and Pedro Valdes Sosa who taught me to use the Discrete Gabor Transform, and helped me to conduct my first experiments on the induced gamma band responses. However, these first steps in the world of induced gamma band response would have never been possible without the help of my friend Jorge Bosch, who spent several nights with me in front of the computer to calculate an analysis or to finish a program.

This was already the case in Havana, but even more so while he was in Konstanz; working instead of enjoying the good German Weizenbier.

During my stay in San Diego, Steve Hillyard inspired me and critically discussed all suggestions I made with devotion. I'm grateful to all I have learned from him during my stay, which has certainly changed my scientific thinking. In Steve Hillyard's lab, it was Wolfgang Teder who helped me soldering the stimulation equipment, Matt Marlow who did all the programming, Carlos Nava who helped me to organize and record the subjects and Lourdes Anllo-Vento who introduced me to the secrets of the analysis program and helped me whenever I had a question. Without their help, I would have never been able to conduct such a series of experiments within one year. While in San Diego, I also had the privilege of working with Terry Picton, who introduced me to new ideas in analyzing the steady-state visual evoked potentials and conducted the source analysis by means of VARETA. Thanks for the significant input into the present work and his tremendous patience, when the data transfer from and to Toronto worked other than optimally.

In the MSI lab at the Scripps Clinic in San Diego, I was able to conduct the MEG study, which will be presented in the present work and an additional MEG study, which is currently undergoing the analysis procedure. Many thanks to Lacy Kurelowech, Patti Quint, and Joslyne Foley for their support, which went way beyond assistance in data recording. And, finally, I would also like to thank Ted Bullock for the various discussions we had in San Diego with regard to the induced gamma band response.

In Konstanz, it was Thomas Gruber who wrote most of the stimulation and analysis programs and who supervises the analysis in the meantime. Thanks to his constant reliable work and his patience when I sometimes changed my mind from day to day with respect to the requirements of the diverse programs. Many thanks also to Gudrun Hanzo, who helped me with data recording and analysis, and Patrick Berg, who adapted his analysis programs to the special needs of my experiments. Thanks to Betina Duval and Stefan Beißwengert, who recorded the subjects and did most of the analysis for the third induced gamma-band experiment while I was in San Diego. Since the beginning of 1997, I'm happy to have a new team of motivated and reliabely students working with me. Thanks to Heike Meyer, Eva Bona, Nikolaus Ronning and Nina Waiblinger. I also thank Lisa Green

for her editorial assistance; without her help, reading the present work would have elicited a large number of N400s.

It was and still is the love of Annette Sterr which helped me over the years to concentrate and to continue my scientific work. Thanks for all the patience and understanding, especially while writing this work, when I spent the evenings, nights and weekends in front of the computer. I also have to thank her for all the scientific support and help in data recording and data analysis.

Last but not least, I have to thank the clerk of the weather, who managed to provide the most miserable weather in ages during the spring and early summer period of 1997. This has allowed me to concentrate on writing and prevented me from spending the weekends in the mountains searching further inspiration while flying my paraglider in one of the most picturesque mountain sceneries of Europe, the Appenzellerland.

Matthias Müller
Konstanz, August 1997

Contents

1. Introduction

Oscillatory cortical activities in the human brain do not form a homogeneous class of phenomena. Rather, they are diverse in many ways with respect to their significance and their underlying mechanisms. The present work presents a series of experiments on oscillatory brain responses in the auditory and visual modality to investigate (1) where the attentional modulations take place in the brain (primary or secondary sensory cortex), (2) the co-operative interactions between the primary auditory cortex and other brain regions, (3) the neural generators of various types of driven oscillatory activities in the visual modality, (4) temporal characteristics of visual spatial attention, (5) synchronized oscillatory activities as a basic mechanism of feature binding and stimulus representation, (6) the difference between frequency bands and their possible functional meanings, and (7) the attentional modulation of these synchronized oscillatory responses.

Cortical brain activity as measured by means of the electroencephalogram (EEG) is related to specific transient waveforms and amplitude components (Regan, 1989). These components are present in event related potentials (ERPs) which are elicited by discrete and discontinuous stimuli. However, if the time between the stimuli is shortened, a so-called steady-state response consisting of a sinusoidal oscillatory waveform at the stimulus frequency or multiples thereof can be recorded. A further different source of information on cortical processes is gained by decomposing the signal into specific frequency bands. Historically, the frequency components of the EEG are divided into the following bands: (1) *Delta:* 0.5-3.5 Hz, (2) *Theta*: 4-7.5 Hz, (3) *Alpha*: 8-12 Hz, (4) *Beta*: 13-20 Hz, and, (5) *Gamma*: above 20 Hz (Berger, 1929; Walter, 1959).

In recent years, research in the EEG frequency domain focused more and more on rhythmical and oscillatory cortical activities in the gamma band range, which summarizes different responses. In 1992, Galambos introduced the following classification with respect to gamma band responses (GBRs, Galambos, 1992):

1. *Evoked gamma band responses*. Elicited and precisely time-locked to a stimulus. This category should be further devided into (a) *transient evoked gamma band responses* and (b) *driven responses* like the 40 Hz auditory steady-state response. Figure 1.1a illustrates an example of an auditory transient evoked gamma band response, Figure 1.1b shows an example of an auditory steady-state response.

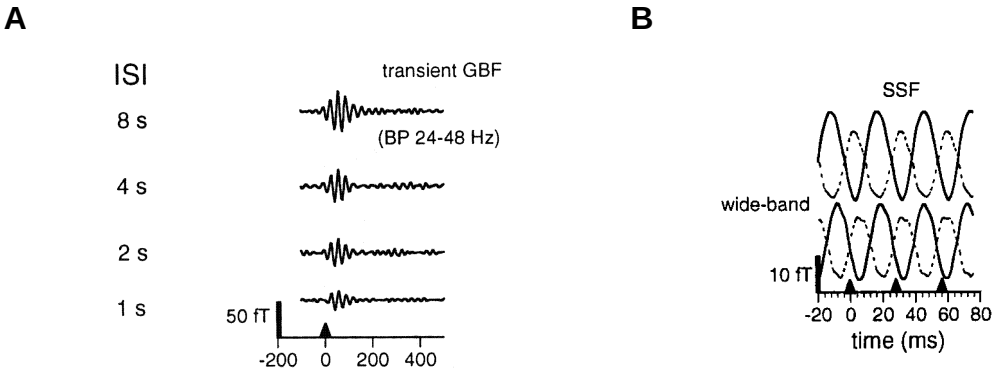

Figure 1.1. (A) example of a transient gamma band field, time locked to tone onset at four different stimulus rates. *(B)* Auditory steady-state field at two stimulation frequencies, centered around 40 Hz. *Note:* ISI = Inter Stimulus Interval, solid lines of (B) show the posterior, dashed lines the anterior extrema of the magnetic field. Derived from (Pantev, Elbert, Makeig, Hampson, Eulitz, & Hoke, 1993).

In contrast to the auditory steady-state response, the visual steady-state evoked potential can be elicited with a variety of frequencies (see section 1.1.3 and 2.1). Therefore, it does not seem appropriate to list visual steady-state evoked potentials under Galambos' evoked gamma band responses category.

2. *Induced gamma band rhythms*. Initiated by but not time- and phase-locked to a stimulus. Figure 1.2 depicts an example of induced gamma band responses in local field potentials of area 17 and 18 of the cat.

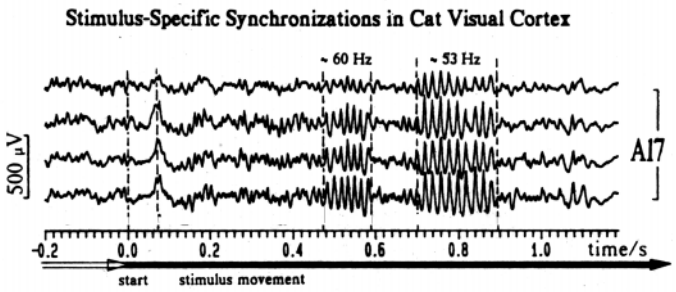

Figure 1.2. Induced gamma band activity in single sweep local field potentials of area 17 of the cat. The stimulus was a drifting grating. Movement started at t = 0. Derived from (Eckhorn, Reitboeck, Arndt, & Dicke, 1990)

In addition to the first two types of gamma band responses, Galambos has specified two more types. However, these responses will not be investigated in the present work and are listed for the sake of completeness.

3. *Spontaneous gamma rhythms*. Occur in the EEG and are not related to any stimulus[1].

4. *Emitted gamma band oscillations*. Gamma band activity time-locked to a stimulus that has been omitted[2].

Steady-state evoked responses and induced gamma responses represent two different cortical activities which may have different functional meanings. For both responses, the underlying mechanisms are not fully understood (see below). There is some evidence, however, that steady-state responses represent either a superposition of transient components resulting in a similar information from both types of responses in a linear system, or non-linear dynamical patterns providing complementary information about sensory processes and functioning (Pantev, et al., 1993; Pantev, Roberts, Elbert, Ross, & Wienbruch, 1996, see also section 1.1.1).

---

[1] For an example see Steriade, M., Amzica, F., & Contreras, D. (1996). Synchroization of fast (30-40 Hz) spontaneous rhythms during brain activation. *The Journal of Neuroscience, 16,* 392-417.

[2] For an example see Bullock, T. H., Karamürsel, S., Achimowicz, J. Z., McClune, M. C., & Basar-Eroglu, C. (1994). Dynamic properties of human visual evoked and omitted stimulus potentials. *Electroencephalography and Clinical Neurophysiology, 91,* 42-53.

In the present work, steady-state responses are evoked in the auditory and visual modality. In the auditory modality, it will be investigated whether information processing in the primary auditory cortex is altered by attentional manipulations. With respect to the steady-state visual evoked potential, the question is whether the location of the generator varies as a function of stimulation frequency, and whether steady-state visual evoked potentials are altered by visual spatial attention. In addition, the localization of the visual spatial attention effect will be studied. Visually evoked potentials are not suitable for measuring the temporal characteristics of attentional processes. However, these characteristics will be investigated for the first time on the cortical level by means of the steady-state visual evoked potential to get a better understanding of the temporal characteristics when a human subject is requested to shift attention from one object to another.

From the present view, induced gamma band responses may be related to the computational operation of the cerebral cortex to bind consistent relations among incoming signals together (Singer, 1995). Singer (1995) suggested two mechanisms of how the brain copes with the tremendous amount of feature constellations. "First, hard-wired neurons detect and represent relations that are particularly frequent and important. Second, dynamic grouping mechanisms, which allow for a flexible recombination of responses from hard-wired neurons, enable higher order relations to be analyzed and represent successively within the same hardware" (page 758).

The present work will deal with the dynamic grouping mechanisms and will test whether induced gamma band responses (1) can be measured non-invasively by means of the EEG, a prerequisite for a funtional discussion, (2) are related to the features of the stimulus, (3) are neither related to an artifact due to muscle activity nor higher harmonics of lower frequency bands (in particular the alpha band), giving support to the notion that they are of functional relevance, and, (4) can be modulated by visual spatial attention.

In the following chapters of the first section, a brief review of the relevant literature with respect to the current work on the auditory, visual SSR and the induced GBR is provided. The rational of the respective experiments is presented in the second section. The second section is divided into studies of the (1) auditory SSR, (2) visual SSR and (3) visually induced GBR. Each of

these sections ends with a general discussion of the experiments described. In total, 11 experiments, three auditory, four visual SSR and four visually induced GBR experiments, were conducted. The last section of the present work provides a general discussion of the conducted experiments.

1.1. Steady-state responses (SSR)

The steady-state evoked potential is a continuous brain response that is elicited by a repetitive stimulus presented at a fixed rate. The SSR can be recorded from the scalp as a nearly sinusoidal oscillatory waveform having the same fundamental frequency as the driving stimulus and often includes higher harmonics (Regan, 1989). A steady-state evoked potential has been reported in the visual (Müller, Teder, & Hillyard, 1997; Regan, 1989; Silberstein, Ciorciari, & Pipingas, 1995), auditory (Galambos, 1992; Hari, Hämäläinen, & Joutsiniemi, 1989; Makeig, 1989; Müller, Rockstroh, Berg, Wagner, Elbert, & Makeig, 1994; Otavio & Picton, 1995; Pantev, et al., 1996; Picton, Vajsar, Rodriguez, & Campbell, 1987), and somatosensory modalities (Snyder, 1992; Szczepaniak & Moller, 1993).

1.1.1. Auditory steady-state responses

In 1981, Galambos and co-workers (Galambos, Makeig, & Talmachoff, 1981) described a cortical activity which can be elicited by a 40-Hz stimulus train of tones. This 40-Hz evoked potential, or steady-state response, was of particular interest since it did not habituate but was altered by various general states of arousal, i.e., an amplitude reduction under anesthesia and while asleep (Galambos, et al., 1981). The mechanism which generates the auditory steady-state response is still under debate. Since auditory SSRs reach maximum amplitude when tone pulses are presented at a repetition rate near 40 Hz until recently, it was more or less accepted that the auditory SSR is produced mainly by the superposition of middle latency response (MLR) features of the event related potential evoked roughly 10-60 ms after a tone (Hari, et al., 1989; Mäkelä & Hari, 1987; Otavio & Picton, 1995; Picton, Champagne, & Kellett, 1992; Plourde, Stapells, & Picton, 1991). Magnetoencephalographic studies indicate that major generators of both the MLR and SSR are located bilaterally in the primary auditory cortices (Hari, et al., 1989; Mäkelä & Hari, 1987; Pantev, et al., 1993). Just recently Pantev and

co-workers (Pantev, et al., 1996) questioned the superposition theory. Their argumentation was based on the finding that the first prominent positive deflection of the MLR, the so-called Pam (m = magnetic, since magnetoencephalographic recordings were obtained) resembled an opposite tonotopic organization as compared to the steady-state fields, elicited by the same carrier frequencies. They argued further, that only a few subjects have shown clear Na, Nb or Pa middle latency components which were suggested to be the basic MLR components to superimpose. However, all subjects have exhibited a clear steady-state field (Pantev, Bertrand, Eulitz, Verkindt, Hampson, Schuierer, et al., 1995). These two findings led the authors to the conclusion that the SSR cannot be generated by a superposition of middle latency components. Although the authors have challenged the superposition theory, the sources of the steady-state fields elicited by different carrier frequencies were all found in the primary auditory cortex (Pantev, et al., 1995).

1.1.2. Auditory steady-state response and slow cortical potentials[3]

Knowledge of co-operative interactions between separate brain regions is crucial to understanding brain and central nervous system function. In a series of studies, Makeig and Galambos (1989; Makeig & Inlow, 1993) demonstrated systematic and relatively long-lasting variations in the amplitude and phase of the SSR following the presentation of foreground auditory stimuli. Perturbations in the amplitude and phase of an ongoing SSR timelocked to a distinct stimulus, such as occasional omissions of a pulse interspersed within the continuous 40-Hz stimulus train, can be measured conveniently in the frequency domain, yielding a complex time series, the "complex event-related potential" (CERP, Makeig and Galambos, 1989). SSR phase shifts are equivalent to latency shifts of the entire SSR wave form: positive-going phase advances correspond to latency decreases, and negative-going phase retards to latency increases (see 2.1.1). By varying attentional demands in an oddball paradigm, Makeig (1994) demonstrated a CERP phase advance following rare tones, regardless of whether the subject

[3] This section is an adapted version of the articles: Müller, M.M.; Rockstroh, B.; Berg, P.; Wagner, M., Elbert, T.; Makeig, S. In: Pantev, C., Elbert, T. & Lütkenhöner, B. (Hrsg). *Oscillatory event related brain dynamics.* Nato ASI Series, Plenum Press, New York, 1994, and an article entitled "Effects of voluntary movements on early auditory brain responses" by Makeig, S., Müller, M.M., Rockstroh, B., published in *Experimental Brain Research* , 1996, 110, 487-492.

was attending to the stimuli or not. In contrast, an above-baseline peak in SSR amplitude with a 400-msec latency occurred only when subjects directed their attention to the target stimuli. Rohrbaugh and colleagues (1990) also found a phase advance in the SSR during a 200-msec period following a foreground stimulus in an orienting paradigm. Since this phase advance occurred parallel to the development of a negative slow wave in the event-related potential, the authors interpreted both phenomena, the SSR phase advance and the negative slow wave, as reflecting a transient sensitization during orienting to the foreground stimuli (Rohrbaugh, Varner, Paige, Eckardt, & Ellingson, 1990a; Rohrbaugh, Varner, Paige, Eckhardt, & Ellingson, 1990b).

These studies indicate that more or less automatic sensory input processing (reflected by the SSR) is modulated by controlled processes, such as directing attention towards target detection, etc.. In a series of experiments, Hackley (1993) came to the conclusion that the earliest sensory analyses can be assumed to be automatic, i.e. there is no attentional modulation of such responses as the evoked retinal and VIIIth nerve potential, auditory brain stem ERPs, subcortical and early cortical ERPs, or transmission within the sensory-specific limb of the postauricular reflex. However, on a cortical level, early responses can be modified by attention. Attending to an oddball stimulus that alters the cortical responding should change parallel responses, such as the SSR. In light of this, the first two studies, presented in the experimental section 2.1, explored the interaction between auditory input processing and foreground task performance by varying attention tasks within an oddball paradigm.

The third experiment was conducted to examine whether an auditory SSR is influenced by voluntary movements. When human subjects are asked to make discrete finger or toe movements at relatively long, self-paced time intervals, a steadily-increasing negative event-related potential (ERP) component appears on the frontocentral scalp 1-2 s before each movement. This so-called readiness or Bereitschaftspotential (BP) (Deecke, Scheid, & Kornhuber, 1969) is thought to be generated in both the primary and supplementary motor cortex (Deecke, Kornhuber, Schreiber, Lang, Lang, Kornhuber, et al., 1986; Deecke, Lang, Heller, Hufnagl, & Kornhuber, 1987; Deecke, et al., 1969; Ikeda, Shibasaki, Nagamine, Terada, Kaji, Fukuyama, et al., 1994; Neshige, Lüders, & Shibasaki, 1988; Shibasaki, Barrett, Halliday, & Halliday, 1980). The BP and the ensuing postmovement ERP define a

roughly 2 sec. period during which planning, execution and updating of psychomotor brain processes relating to discrete movements are manifest. Task-irrelevant auditory, visual, and somatosensory stimuli presented near to voluntary movements generally evoke smaller responses than during rest (Hazemann, Audin, & Lille, 1975; Tapia, Cohen, & Starr, 1987). However, the interaction of early auditory evoked responses with motor preparation has not been well-studied, and there is no consensus that any auditory evoked response components earlier than about 180 ms (P200) after stimulus onset are affected (Hazemann, et al., 1975; Tapia, et al., 1987). SSR perturbations during planning and executing of self cued motor responses would indicate an interaction with early auditory evoked responses, located in the primary auditory cortex.

1.1.3. Steady-state visual evoked potentials (SSVEP)[4]

The neural bases of visual selective attention have been investigated in humans using a variety of techniques including neuroimaging of regional cerebral blood flow and metabolism and recordings of event-related electrical and magnetic activity patterns in the cerebral cortex. While studies using PET and fMRI have identified a number of anatomical brain areas that participate in attentional selection processes, recordings of ERPs and magnetic fields have more precisely revealed the time-course of sensory transmission and its modulation by attention (Corbetta, Miezin, Shulman, & Petersen, 1993; Heinze, Mangun, Burchert, Hinrichs, Scholz, Münte, et al., 1994). Using these methods to analyze mechanisms of visual spatial attention, it has been shown that stimuli at attended locations elicit enhanced neural responses in extrastriate visual cortex beginning at about 80 msec following stimulus onset (Hillyard, Mangun, Woldorff, & Luck, 1995; Mangun, Hopfinger, Kussmaul, Fletchert, & Heinze, in press). An alternative method, which allows studying attention to more continuously presented stimuli, is to record steady-state visual evoked potentials (SSVEP) to light sources that are flickering at a regular repetitive rate of 6 Hz or above. Recordings of the SSVEP are being used increasingly to investigate

[4] This section contains adapted parts of the articles: Müller, M.M., Teder, W., Hillyard,.S.: Magnetoencephalographic recording of steady-state visual evoked cortical activity. *Brain Topography*, 1997, 9, 163-168, and Müller, M.M., Picton T.W., Valdes-Sosa, P., Riera, J., Teder-Salejarvi, W., Hillyard, S.A.: Effects of spatial selective attention on the steady-state visual evoked potentials in the 20-28 Hz range. Submitted for publication.

normal and abnormal visual processing (Tobimatsu, Tomoda, & Kato, 1996) and cognitive processes including attention, memory, and decision making (Morgan, Hansen, & Hillyard, 1996; Silberstein, et al., 1995; Silberstein, Schier, Pipingas, Ciorciari, Wood, & Simpson, 1990; Wilson & O`Donnell, 1986).

The amplitude and phase characteristics of the SSVEP depend upon the frequency, intensity, and structure of the repetitive stimulus; an unstructured flickering stimulus reportedly elicits SSVEPs with amplitude maxima in separate low (5-12 Hz), medium (12-25 Hz) and high (30-50 Hz) frequency bands (Regan, 1989). In section 2.2, the first experiment was conducted to test whether SSVEPs can actually be elicited with a big variety of stimulation frequencies, since Regan (1989) never presented actual empirical data supporting his model.

Only a few studies have investigated the neural generators of the various types of SSVEPs. Investigations by Silberstein and associates, using spatial deblurring techniques (reviewed in Silberstein, 1995), have found that the SSVEP has a complex amplitude and phase topography across the posterior scalp with considerable intersubject variability. Several possible mechanisms were suggested to account for these results: multiple dipole generators in different cortical areas, interacting traveling waves produced by multiple cortical sources, and "limit cycle oscillations" of dispersive wave activity. Experiment 2 in section 2.2 employed magnetoencephalographic (MEG) recordings of steady state visual evoked fields (SSVEFs) to investigate whether discrete dipole generators may be identified in posterior cortical areas. Because of the well-known properties of MEG recordings, which emphasize tangential over radial sources and eliminate spatial smearing due to skull-scalp resistivity, it was anticipated that SSVEF recordings might help to clarify the neural generators of evoked steady-state activity. The principal aims of this study were to find out whether consistent localizations of equivalent current dipole (ECD) sources could be obtained across subjects for SSVEFs at three different stimulation frequencies (6.0, 11.9, and 15.2 Hz), and to see whether these ECD localizations varied systematically as a function of frequency.

Most electrophysiological studies of visual attention have recorded transient evoked potentials to individual stimuli presented at reasonably long

intervals (0.3-1.5 seconds) in order to allow the underlying neural generators to recover after each stimulus. This method can reveal the detailed time course of post-stimulus processing, but it is difficult to maintain a focused state of attention upon stimuli that are only presented transiently (Yantis and Jonides, 1990). Recently, it has been reported that the SSVEP is a sensitive index of visual-spatial selective attention in a task where subjects attended to a sequence of alphanumeric characters superimposed on a flickering background in one visual field while ignoring a concurrently presented sequence and flicker in the opposite field (Morgan, et al., 1996). It was found that the SSVEP to the flicker at the attended location (at either 8.6 or 12 Hz) was enlarged by almost a factor of two relative to its amplitude when the opposite location was attended. A follow-up study carried out with both SSVEP recordings and fMRI during this same task suggested that the attentional enhancement of flicker-evoked activity occurred primarily in ventral and lateral extrastriate cortex of the occipital lobe (Hillyard et al., in press).

Experiment 3 (see section 2.2) examined whether the SSVEP to a flicker in a higher frequency range (20-28 Hz) could be modulated by spatial-selective attention. These frequencies belong to the "medium frequency" band of SSVEP responsiveness identified by Regan (1989), which is likely to have different functional properties from the 8-12 Hz "low frequency" band studied previously. If the SSVEP were found to be attention-sensitive at 20-28Hz, this would provide a higher resolution measure of attentional focusing and shifting among continuously presented flickering sources.

Traditionally, research on visual attention has focused on the spatial properties of attentional processes (see Hillyard, et al., 1995, for an overviwe). This is also true with respect to the experiments proposed so far in the present work. However, attentional processes are not only defined by spatial characteristics. It is at least equally important to investigate the temporal characteristics. Until recently, the temporal characteristics of visual attention have only been investigated by means of target detection experiments. In these experiments, a rapid serial visual presentation was used and subjects were instructed to report the first stimuli they have identified following a target or probe stimulus. Broadbent and Broadbent (1987) were the first to report an interference of detecting dual targets in a rapid serial presentation of stimuli. They found that the identification of a

first target made it very difficult to detect a second target, when this second target was presented earlier than 400 ms after the first target. Weichselgartner and Sperling (1987) presented a stream of digits at a rate of approximately 10 Hz and instructed their subjects to identify a certain target digit and the three digits that immediately followed the target digit. On average, subjects reported the digit directly following the target, and the digits approximately 350 ms after the target digit. Based on their results, Weichselgartner and Sperling (1987) proposed a two stage model with two consecutive attentive processes: a first automatic process related to target detection which requires no effort or practice and is independent of task difficulty, and a second slow attentive process which is proposed to be a controlled process whose latency depend on factors like task difficulty, practice, expectation, and stimulus probability. Raymond, Shapiro and Arnell (1992) also found a deficit in reporting a probe which occurred between 180 and 450 ms after a target and referred to that period to as the "attentional blink".

The fourth experiment on SSVEP focused on the temporal characteristics of attentional processes. The high frequency stimulation technique of experiment 3 (see section 2.2) was employed (subjects were instructed to shift attention either to a left or right flickering LED bar) to investigate the cortical temporal features of attentional shifting in a spatial attention paradigm. It will be shown for the first time that the SSVEP serves as a powerful tool to investigate both, the spatial and the temporal characteristics of attention.

1.2. Induced gamma band activity[5]

How does the brain group different parts of an object into a coherent visual object representation? It is generally believed that neurons or neuronal assemblies which pertain to one object fire in rapid bursts (Hebb, 1949). However, we may well be aware of two different objects simultaneously. How can it be avoided that firing patterns which relate to a certain type of movement (processed inV1 and V5) or to a color (processed in V4, see Zeki, 1993) of one object mix with those which relate to another object? When multiple stimuli are processed in parallel, a functional separation of the spatially overlapping cell assemblies which pertain to the different stimuli is necessary in order to avoid false conjunctions. Theoretical considerations and experimental results in animals, presented below, suggest that synchronization of neuronal responses participating in the representation of the same stimulus would be a particularly useful mechanism to dynamically bind related responses for further joint processing (Malsburg & Schneider, 1986; Milner, 1974). This model can be summarized as follows (Engel, König, Kreiter, Gray, & Singer, 1991a):

(1) Assemblies are constituted by synchronization of oscillating neurons, i.e. the phase-information permits the distinction of assemblies and the selective binding of distributed features of an object.

(2) Even in the case of spatial interleave, the temporal coding mechanism permits the discrimination of two assemblies.

(3) Object representations are created in a flexible manner, which allows a given cell to "switch" rapidly from one assembly to another.

(4) The model predicts that neuronal response synchronization should occur in a stimulus-dependent manner. Figure 1.2.1 demonstrates the main principles.

---

[5] This section contains highly adapted versions of the articles: Müller, M.M., Bosch, J., Elbert, T., Kreiter, A., Valdes Sosa, M., Valdes Sosa P., Rockstroh, B.: Visually induced gamma band responses in human EEG - A link to animal studies. *Experimental Brain Research*, 1996, 112, 96-112, and Müller, M.M., Junghöfer, M., Elbert, T., Rockstroh, B.: Visually induced gamma band responses to coherent and incoherent motion: a replication study. *NeuroReport* , 1997, 2575-2579.

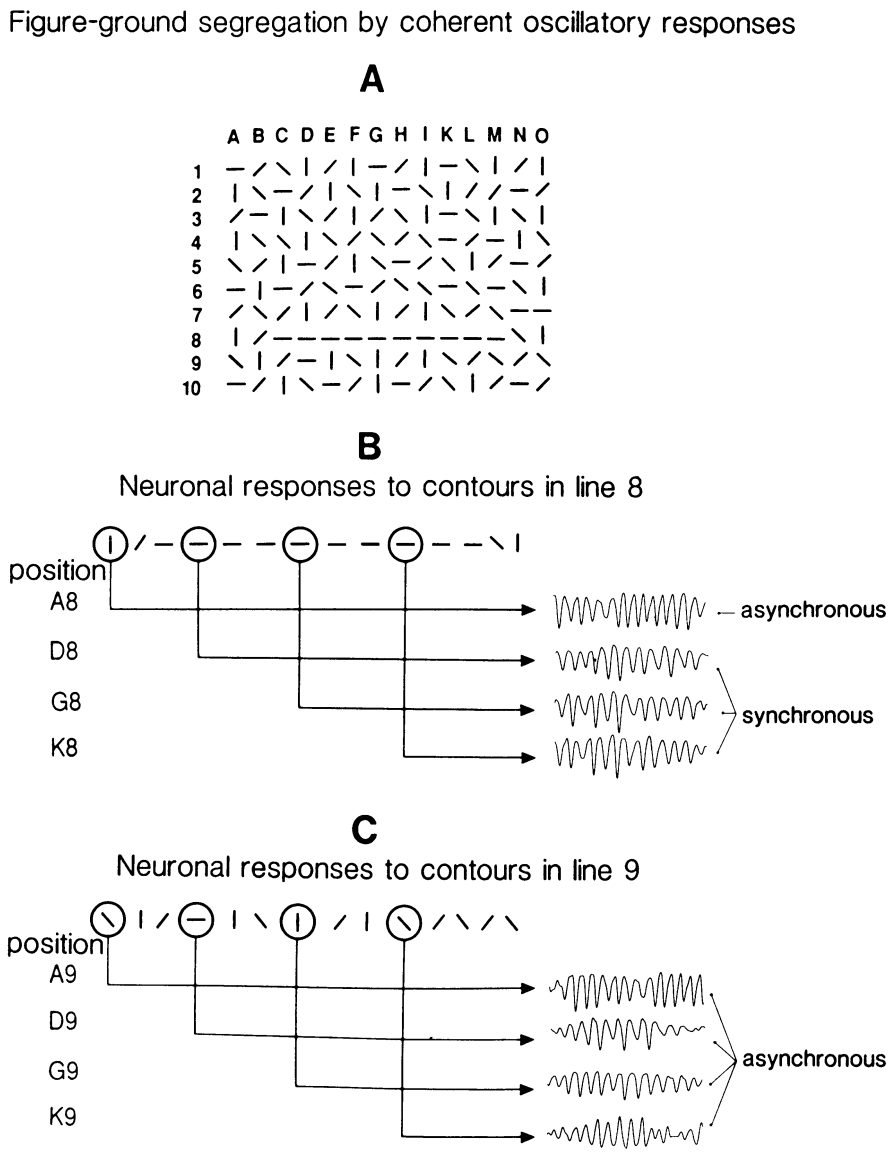

Figure 1.2.1. Schematic representation of figure-ground segregation by coherent oscillatory responses. (A) Example of a triangle embedded in a background. (B) Example of neuronal responses in line 8. The neurons responding to colinear contour elements (D8, G8 and K8) fire synchronously while the response of neurons at position A8 show no constant phase relation with responses to the base of the triangle. (C) Selected neuronal responses from line 9. The activity of the neurons show no stable phase relationship. (Singer, 1990)

However, very little attention was paid to Milner's and von der Malsburg's model until, in 1988, Eckhorn and colleagues (Eckhorn, Bauer, Jordan, Brosch, Kruse, Munk, et al., 1988) reported synchronized oscillatory neuronal activity in the gamma band range in cat visual cortex, which seemed to fit perfectly with Milner's and von der Malsburg's model. One year later Gray and co-workers also found such activity in cat visual cortex

(Gray, König, Engel, & Singer, 1989; Gray & Singer, 1989) by means of intracranial recordings. This activity was neither time nor phase locked to the stimulus (a long bar moving over the respective receptive fields) but was synchronized inter-columnar in Area 17 (Gray, et al., 1989) or between different cortical areas, such as A 17 and 18 (Eckhorn, et al., 1988; Engel, Kreiter, König, & Singer, 1991c)[6]. Both groups interpreted the functional relevance of this synchronized cortical activity as the mechanism by which the brain binds different features of an object or separated receptive field properties together.

In the following years, a series of experiments demonstrated synchronization in different brain areas (see Singer and Gray, 1995 for an overview) and even interhemispheric synchronization of induced gamma band activity in the visual cortex of anaesthetized cats (Engel, König, Kreiter, & Singer, 1991b). In the experiments conducted on anaesthetized cats, it was demonstrated that induced gamma band activity is related to the features of the stimuli. In the "conflicting stimulus paradigm" (Engel, et al., 1991a), the simultaneous presentation of stimuli with an orientation optimal to the propertyies of cells and orthogonal to the optimal orientation reduced the oscillatory modulation of the response (Engel, König, Gray, & Singer, 1990; Engel, et al., 1991a; Gray, Engel, König, & Singer, 1990). It has also been shown that long-range synchronization in area 17 of the anaesthetized cat reflects global stimulus properties (Gray & Singer, 1989). In this experiment, multiunit activity was recorded from two sites which preferred vertical orientations and were separated by 7 mm. The corresponding receptive fields were non-overlapping and colinearly arranged. This arrangement allowed three different stimulus conditions: (A) a long continuous light bar moving across both fields, (B) two independent light bars moving in the same direction, and (C) the same two bars moving in opposite directions. Figure 1.2.2 depicts the three stimulation conditions schematically.

---

[6] It should be mentioned, however, as early as 1975, Freeman described oscillatory field potentials recorded from the olfactory bulb of rabbits in a frequency range of 35-90 Hz which were linked to a previously learned odor Freeman, W. J. (1975). *Mass action in the nervous system.* New York: Academic Press.

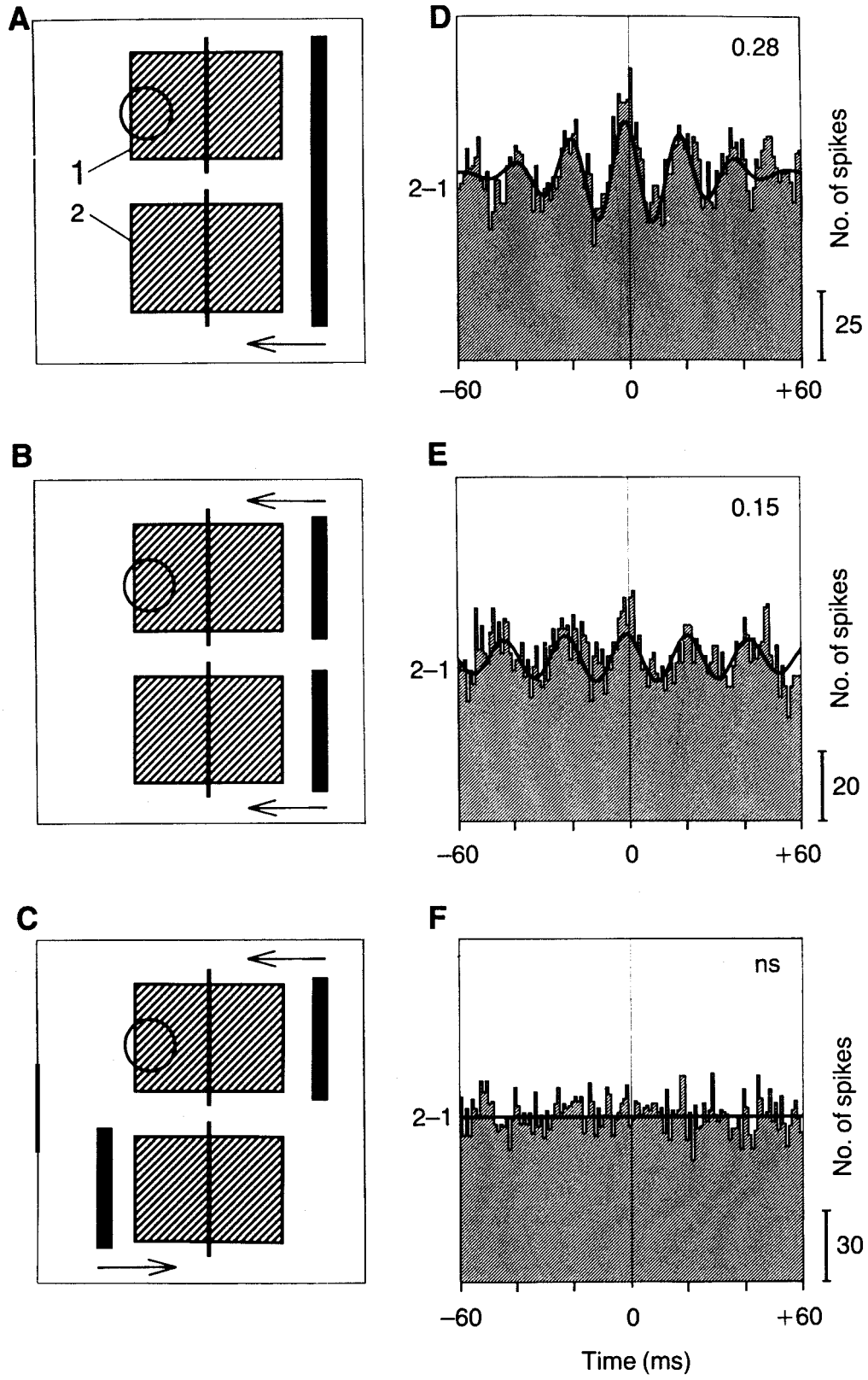

Figure 1.2.2. Schematic representation of the stimulus conditions of the "long bar" experiment (Gray & Singer, 1989) . Rectangles represent the receptive field, the line across the receptive field indicates the preferred orientation and the circle locates the center of the visual field. (Engel, König, Kreiter, Schillen, & Singer, 1992). See text for stimulus configuration.

The results showed, that the induced gamma band responses of the two receptive fields were synchronized, when the long bar was presented. In the case of the two independent bars, moving in the same direction (Figure 1.2.2, B), the synchronization across the two receptive fields became weaker and totally disappeared if the motion of the stimuli was incoherent (Figure 1.2.2, C). However, the neuronal activity in the respective receptive field was strongly synchronized.

Moving bars have frequently been used as stimuli to elicit gamma band oscillations in animal research. The presence of induced gamma band responses has been demonstrated in the visual cortex of anaesthetized cats (Eckhorn, et al., 1988; Eckhorn, et al., 1990; Eckhorn, Schanze, Brosch, Salem, & Bauer, 1992; Engel, et al., 1991a; Engel, et al., 1991b; Engel, et al., 1991c; Gray, et al., 1990; Gray, Engel, König, & Singer, 1992; Gray, et al., 1989),awake behaving monkeys (Kreiter, 1992; Kreiter & Singer, 1992), in the optic tectum of pigeons (Neuenschwander, Engel, König, Singer, & Varela, 1996; Neuenschwander & Varela, 1993), and in the dorsal cortex and the dorsal ventricular ridge of pond turtles (Prechtl, 1994). On the other hand, experiments on monkies measuring single-unit activity have also failed to find oscillations using moving light bars (Young, Tanaka, & Shigeru, 1992), dynamic random dot displays with a fraction of dots moving coherently (Bair, Koch, Newsome, & Britten, 1994) and static stimuli (Tovee & Rolls, 1992). These findings raised doubts as to whether gamma band oscillations are relevant for feature binding and higher cognitive processes in general, leading to the consideration that they simply represent an epiphenomenom without functional relevance (Kirschfeld, 1992). However, it may well be the case, that recordings at the cellular level, which have the disadvantage of a spatial sampling bias, may not see the synchronization of large populations of neurons. As a result, rhythmic activity is prominent at the level of field potentials, but is weak or not apparent at the level of single-unit activity (Young, et al., 1992; Singer & Gray, 1995).

Nonetheless, the mechanism which generates synchronous gamma band activity is not fully understood. It is possible that thalamocortical as well as cortico-cortical mechanisms play a role. It was shown that some cells of the intralaminar nuclei of the thalamus fire rhythmic bursts of extremely rapid spikes (up to 1000 Hz), with an interburst interval of 20 to 40 Hz (Steriade, McCormick, & Sejnowski, 1993). In a subsequent study, extra- and intracellular recordings from the thalamus and the cortex demonstrated that

thalamic oscillations in the gamma band range become synchronized with the oscillations in the cortex (Steriade, et al., 1996). A thalamocortical mechanism was not only hypothesized by Steriade and co-workers (Steriade, 1996; Steriade, et al., 1996; Steriade, Contreras, & Amzica, 1994; Steriade, Gloor, Llinás, Lopes da Silva, & Mesulam, 1990; Steriade, et al., 1993) but also by Llians and co-workers (Llinás & Ribary, 1993; Llinas, 1992; Llinas & Ribary, 1992; Ribary, Ioannides, Singh, Hasson, Bolton, Lado, et al., 1991). With respect to the cortico-cortical mechanisms, Gray & McCormick (1996) recently found cells in the superficial layers of visual cortex of the cat which fire with an extremely high intraburst firing rate (up to 600 Hz) and an interburst interval in the gamma frequency range. This "chattering", Gray and McCormick argued, might be the pacemaker for the widespread gamma oscillations since rapid bursts of action potentials are very effective in depolarizing other neurons. However, when viewing the evidence for both talamocortical and cortico-cortical mechanisms, it seems possible that gamma oscillations may be generated in both the thalamus and cortex. It has been suggested that the oscillations in the intralaminar nuclei are required to co-ordinate the oscillations between different cortical regions, as opposed to driving the cortical oscillations (Steriade, 1996).

Even more than intracranial recordings in animal experiments, noninvasive investigation of induced gamma band responses in humans is confronted with problems. First, *methodological problems:*

As opposed to previously reported *evoked* gamma band responses in the auditory modality (Galambos, 1992; Pantev, et al., 1993; Tiitinen, Sinkkonen, May, & Näätänen, 1994), detection of induced gamma band responses required examination of the individual traces since the oscillatory spindles are generally not phase- and time-locked to the stimulus (Eckhorn, Frien, Bauer, Woelbern, & Kehr, 1993; Eckhorn, et al., 1990; Engel, et al., 1991a; Engel, et al., 1991b; Engel, et al., 1991c; Gray, et al., 1989; Gray & Singer, 1989; König, Engel, & Singer, 1995; Kreiter & Singer, 1992) and are, thus, suppressed by conventional averaging across trials (Bauer, Brosch, & Eckhorn, 1995; Eckhorn, et al., 1990; Makeig, 1993). In addition, the duration of synchronous firing is rather short (100 to 200 ms in cats, Gray, et al., 1989), requiring short analysis windows. Figure 1.2.3 gives an illustration of the above mentioned.

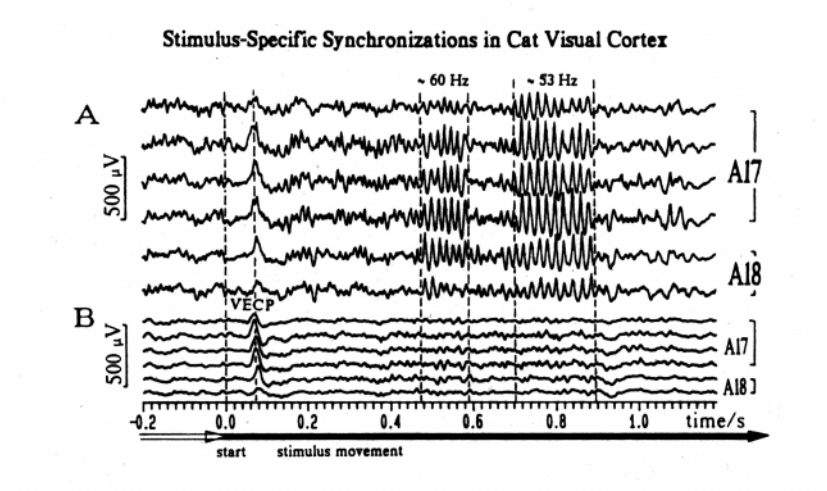

Figure 1.2.3. Induced gamma band activity in local field potentials of area 17 and 18 of the cat. The stimulus was a drifting grating. Movement started at t = 0. (A) Single sweep local field potentials. (B) Averages of 18 local field responses to identical stimuli. The oscillatory components (480-900 ms poststimulus) are averaged out. Averaging pronounces the visual evoked cortical potential (VECP). Derived from (Eckhorn, et al., 1990)

Therefore, conventional Fast Fourier Transformations seem to be inadequate to extract this signal which is not constant over time (Sinkkonen, Tiitinen, & Näätänen, 1995). Instead of composing the signals by means of an inadequate series of sine- and cosine functions and then restricting the arising problems by multiplication with a window function, Gabor (1946) suggested to directly built the window into functions of finite length. A finite signal is better represented by a sum of finite Gabor functions. Therefore, we performed a spectral analysis on the basis of Gabor transforms on a single trial basis (see 2.3.1).

Induced gamma band responses in humans had been reported in the visual cortex (Lutzenberger, Pulvermüller, Elbert, & Birbaumer, 1995; Tallon, Bertrand, Bouchet, & Pernier, 1995; Tallon-Baudry, Bertrand, Delpuech, & Pernier, 1996; Tallon-Baudry, Bertrand, Delpuech, & Pernier, 1997), in the auditory cortex (Jokeit & Makeig, 1994), in the sensorimotor cortex (Kristeva-Feige, Feige, Makeig, Ross, & Elbert, 1993) and during procession of words and pseudo words (Eulitz, Maess, Pantev, Friederici, Feige, & Elbert, 1996; Lutzenberger, Pulvermüller, & Birbaumer, 1994; Pulvermüller, Eulitz, Pantev, Mohr, Feige, Lutzenberger, et al., 1996; Pulvermüller, Lutzenberger, Preissl, & Bierbaumer, 1995). In most of these studies, power spectra were calculated by using FFTs with either short overlapping data windows or data

windows over the whole epoch[7]. In addition, window shapes differed across these studies, making it difficult to compare the results.

A second problem which is related with human gamma band studies in the visual modality is related to the *anatomy* of the visual cortex. Most parts of Area 17 (V1) in humans are located in the dorsal part of the calcarine fissure of the respective hemifield which may lead to a cancellation of opposing electrical dipoles under visual fullfield stimulation. Therefore, we presented the stimuli only in one visual hemifield.

Despite these methodological problems and discrepancies, some other questions were raised. One question was, whether the activity one can see in the gamma band does only reflect higher harmonics of the alpha band (Jürgens, Rösler, Hennighaus, & Heil, 1995). A second, more fundamental question was, whether one is able to detect this activity with surface electrodes since electrocorticogram recordings in two humans have shown that spatially correlated activity was restricted to a very small area in the somatosensory cortex (Menon, Freeman, Cutillo, Desmond, Ward, Bressler, et al., 1996). However, a closer inspection of the findings of Menon et al. (1996) gives rise to some questions about the interpretation of the results as provided by the authors and of the appropriateness of paradigm used in this investigation (Lutzenberger, Preissl, Birbaumer, & Pulvermüller, 1997).

Up to today, a series of hypothesis exists to explain why cell assemblies oscillate.

1. Synchronized oscillatory activity is the mechanism by which various brain regions form one percept and are, therefore, the key mechanism for feature binding (Gray, et al., 1989; Singer & Gray, 1995). The underlying physiological mechanism of how these oscillations are paced is not fully understood, but one possibility is that so-called "chattering cells" are the pacemakers for the widespread gamma oscillations on the cortical level (Gray et al., 1996). However, as has been discussed above, thalamocortical

[7] Only the studies by Tallon, et al. (1997) used a different approach, which is similar to the method which is used in the present work. Instead of using a moving window FFT, the French group used a wavelet algorithm. However, this algorithm has the disadvantage that analysis windows will be adapted to the frequency, i.e., the lower the frequency, the longer the analysis window. Below 20 Hz, the wavelet duration is very long (hundreds of ms) which results in a poor temporal resolution. Therefore a comparison of alpha- and gamma-band activity is not possible with the same time resolution.

mechanisms may also contribute to these phenomena (Steriade, et al., 1996; Llinas & Ribary, 1993).

2. According to Freeman (Freeman, 1992; Freeman, 1996; Freeman & Dijk, 1987; Freeman & Prisco, 1986), the stimulus itself might be coded in oscillations or, more precisely, as a nonlinear dynamic pattern which appears to be an oscillation to the observer. On the basis of intracortical recordings from the olfactory bulb of the rabbit, Freeman and Di Prisco (1986) concluded that after the presentation of a learned odor, the system switches from a spatially and temporally unpatterned chaotic state to global odor-specific state, which is characterized by a single near-limit attractor. In other words, the attractor governing the dynamic pattern is related to stimulus encoding; everything that is not coherent to this signal is dismissed as noise.

3. With respect to oscillations in the alpha range, it was hypothesized that these oscillations reflect idling in neural mass systems (Hari & Salmelin, 1997; Pfurtscheller, 1992; Pfurtscheller & Aranibar, 1979; Pfurtscheller, Flotzinger, & Kalcher, 1993; Pfurtscheller & Klimesch, 1992). These 10 Hz oscillations are found over the posterior parts of the brain (alpha), over the rolandic regions (mu) and the supra-temporal auditory cortex (tau). This idling state would allow the system to start more rapidly than by a "cold start" (Hari & Salmelin, 1997). In the somato-motor system, such oscillations can be measured not only in the alpha range but also in a frequency range around 20 Hz (Hari & Salmelin, 1997; Kristeva-Feige, et al., 1993; Pfurtscheller, Stancak, & Edlinger, 1997). Both the rolandic mu rhythm and the 20 Hz oscillations are dampened by limb movements and tactile stimulation.

4. Oscillations have no functional meaning but are simply a by-product of neuronal activity (Kirschfeld, 1992).

In the present work, a total of four experiments, presented in section 2.3, were conducted on induced gamma band responses. The main purpose was to investigate whether these cortical activities are related to the features of a stimulus (see hypothesis 1 and 2), whether they represent a different functional state as compared to the oscillations in the alpha range (hypothesis 3) and, finally, that they are not simply a by-product of neuronal activity (hypothesis 4).

In the first two experiments, it will be investigated whether visually induced gamma band responses can be extracted from the human EEG. As in the animal studies described above, the "long bar" paradigm from Gray et al. (1989) was used to test the feature dependence of induced GBRs from the stimulus. Induced GBRs were extracted by means of the Discrete Gabor Transform (DGT), an algorithm developed in co-operation with the Cuban Center of Neuroscience in Havana. Prior to the application to human EEG data, this algorithm was tested with data from intracortical recordings from monkey primary visual cortex to test whether this method is able to detect the short bursts of gamma band activity. In addition it was examined whether the results obtained in the gamma band can be explained in terms of higher harmonics of the alpha band. Differences in the temporal and spatial features between the two bands would strongly suggest, that the two bands represent two different functional cortical states e.g., idling versus working brain (hypothesis 3).

Contrary to results related to a simple stimulus like a moving bar, Vijn and co-workers (van Dijk, Vijn, & Spekreijse, 1994; Vijn, van Dijk, & Spekreijse, 1991; Vijn, van Dijk, & Spekreijse, 1992; Vijn, 1992) reported a GBR power *reduction* (up to 40 Hz) when a complex stimulus (a dartboard) is presented in motion as compared to a standing complex stimulus. This was consistently found in cats (van Dijk, et al., 1994), in local field potentials and surface recordings of the awake monkey (Vijn, et al., 1992; Vijn, 1992) and in the human EEG (Vijn, et al., 1991; Vijn, et al., 1992). The authors hypothesized two functionally different states in the visual cortex to explain for the suppression effect: the "scanning state" and the "detection state". During the "scanning state", the cortex is scanning the environment for relevant information. Since there is no information on which information is of relevance e.g. motion, color, luminance, this state requires a global analysis in which many spatially distributed neurons are involved. After a cue appeared, the visual cortex switches to the "detection state". A certain assembly loosens its connections with the broad environment, resulting in a drop in overall gamma band activity, and strengthens the connections with the neurons within the assembly. According to Vijn (1992), in the above mentioned animal studies the brain was in the "detection state".

The third experiment presented in section 2.3, was conducted to compare the induced gamma band activity of a complex moving stimulus with a complex standing stimulus to see if Vijn's findings can be replicated, which

would give strong support to the hypothesis that induced GBRs are related to the features of a stimulus (hypothesis 1 and 2) and have a functional meaning (against hypothesis 4).

The last experiment investigated the modulation of visually induced gamma band responses upon spatial visual attention. At the 25th annual meeting of the Society of Neuroscience, (Beauchamp & DeYoe, 1995) reported on an experiment in which they investigated the feature-specific attentional modulation of area MT by means of a fMRI study. They showed that area MT and V3 exhibited a consistent activation when subjects attended to the motion of moving stimuli, which was reduced up to 98% when subjects ignored the motion and attended to the luminance of the same stimuli. On the basis of this report and the finding with respect to the SSVEP of the present work, it was speculated that attending to a moving bar should enhance the cortical induced gamma band activity as compared to when the moving bar was ignored. In contrast to experiment 3, subjects were demanded to fulfill a target detection task and not just alertly attend to different stimuli. In experiment 4 (section 2.3) it will be shown, for the first time, that visually induced gamma band responses are altered by spatial attention, which lends additional support for the functional relevance of these responses (against hypothesis 4).

2. Experimental section

In the preceding section the relevant literature was reviewed and the rational behind the experiments was explained. The following sections describe a series of 11 experimental investigations divided into the three sections (1) auditory SSR, (2) visual SSR and (3) visually induced gamma band response. If the general methods, data recording and data analysis weresimilar in a series of experiments, these are described first, followed by the respective experiments and, finally the conclusions drawn from them. Each section ends with a general discussion of the experiments provided.

Section 2.1 describes the experiments pertaining to the auditory SSR. They investigate whether "external" stimuli (oddball stimuli which require stimulus evaluation and task performance) and "internal" stimuli (intention and preparation of a self-paced voluntary button press) interfere with the continuous processing of early auditory information.

Since very little is known about the SSR in the visual modality, the first two experiments in section 2.2 are on a more "basic" level. First, it will be studied whether there is a prominent stimulation frequency which elicits a visual SSR (as in the auditory modality) and whether the location of a single moving dipole varies as a function of stimulation frequency to evaluate similarities or differences to the auditory SSR. Second, the modulation of higher frequency visual SSRs by means of visual spatial attention will be investigated, and, third, the visual SSR will be used as a tool to investigate the temporal characteristics of spatial attentional processes on the cortical level.

On the basis of the literature, it seems quite likely that SSRs and induced gamma band responses not only represent different phenomena, but are also related to different cortical processes (see section 1). Section 2.3 deals with experiments pertaining to induced gamma band responses. It was tested whether induced gamma band responses can be obtained by means of EEG recordings and whether theses responses are reliably related to the stimulus features (as shown in the animal experiments, see 1.2). Should it be the case that GBRs are related to the computational operation of the cerebral cortex to link consistent relations among incoming signals, one would expect a modulation of these responses when a certain object is attended as compared to when the same object is ignored. On the basis of

the experiments on the visual SSR, it was predicted that the amplitude of the induced gamma band response is augmented in the attended condition as compared to the ignored condition. If this should be the case, the finding would lend strong support to the notion that induced GBRs are of functional relevance. A further aim of the studies provided in section 2.3 is to show that the findings can not be explained in terms of artifacts due to muscle activity or as higher harmonics of a lower frequency band (in particular the alpha band).

2.1. Auditory steady-state response and slow cortical potentials

To investigate the influence of attentional processes as reflected in slow cortical potentials upon auditory steady-state responses, first, two experiments investigated the modulation of auditory SSRs in an oddball paradigm, and, second, SSR perturbations related to slow potentials that develop prior to and following motor responses was examined[1]. In the first step, the general methods for the three experiments is described, followed by the experiments. The hypothesis of the experiment will be provided in the respective section.

2.1.1. General methods, data recording and data analysis of experiments 1 to 3

Subjects

In all three experiments, healthy, right-handed student volunteers received course credit or monetary compensation for participation. Forty-five male subjects (mean age 22.2 years) participated in Experiment 1, ten subjects (5 male, 5 female, mean age 26.3 years) in Experiment 2, which was comprised of two sessions, and seventeen subjects (7 male, 10 female, mean age 24.8 years) in Experiment 3. All subjects were naive with respect to the scientific goal of the studies.

Stimulation and electrophysiological recordings

A steady-state stimulus train (SSR) was created by presenting 5-ms pulses (Gaussian envelope of 1000 Hz, 65 dB SPL (A)) at a rate of 40 per second in Experiments 1 and 2, and 39.25 per second in Experiment 3, with a zero rise and fall time of the stimuli. The SSR was presented via earphones monaurally to the right ear in Experiments 1 and 2 and binaurally in

---

[1] This chapter is a slightly adapted version of the book chapter: "SSR-modulation during slow cortical potentials", by Müller, M.M., Rockstroh, B., Berg, P., Wagner, M., Elbert, T., Makeig, S. In: Pantev, C., Elbert, T. & Lütkenhöner, B. (Hrsg). *Oscillatory event related brain dynamics.* Nato ASI Series, Plenum Press, New York, 1994, and the articles: "Effects of voluntary movements on early auditory brain responses" by Makeig, S., Müller, M.M., Rockstroh, B., published in *Experimental Brain Research* , 1996, 110, 487-492 and "Modulation of auditory responses during oddball tasks." by Rockstroh, B., Müller, M., Heinz, A., Wagner, W., Elbert, T., published in *Biological Psychology* , 1996, 43, 41-56.

Experiment 3. During the experiment the subject sat in a partially electrically shielded, dimly lit and sound-attenuated subject chamber. After being prepared for the physiological recordings, the subject received written instructions informing him/her about the stimuli and the task. The instructions also included a request to avoid blinks and eye or head movements by adopting a relaxed position and fixating on a spot on the opposite wall.

EEG was recorded with Ag/AgCl-electrodes along the mid-sagittal line (Fz, Cz, Pz) in Experiments 1 and 2, and, in addition, from C3 and C4 in Experiment 3. Recordings were obtained with a DC-amplifier (MES, Munich) using a time constant of 5 seconds in Experiments 1 and 2, and DC (direct current) in Experiment 3. In all experiments, the reference electrode was affixed to the left earlobe. The vertical EOG was recorded using Ag/AgCL-electrodes centered about 1 cm above and below the left eye. Data were filtered with a low-pass filter at 100 Hz and were digitized at a rate of 400 Hz (Experiments 1 and 2) or 312.5 Hz (Experiment 3). In Experiment 3, the electromyogramm (EMG) was recorded by a pair of silver/silver-chloride electrodes placed on the forearm (musculus flexor pollicis longus). After amplification (gain 1000, time constant 0.025 sec) the EMG signal was rectified and integrated with a time constant of 20 ms. The integrated EMG was digitized at the same rate as the EEG recordings (312.5 Hz).

Data analysis

Prior to data analysis, artifacts were corrected using a computer program (Berg, 1986) that first classified blinks, muscle potentials, drifts or large DC-shifts on the basis of various templates. The influence of eye blinks on the EEG was then corrected using a regression analysis. The artifact correction procedure led to the rejection of five subjects in Experiment 1, two subjects in Experiment 2 and one subject in Experiment 3. For the remaining subjects, data analysis was based on 83.3% of the data in Experiment 1, 83.1% in Experiment 2, and 78.8 % in Experiment 3.

In order to separate SSR and slow potential responses, subject-averages were separately filtered with a 25-Hz high-pass filter (2nd order) and with a low-pass filter of 15-Hz (Experiments 1 and 2) or 8 Hz (Experiment 3). Perturbations in the SSR time-locked to experimental events were analyzed by complex demodulation. The process of complex demodulation extracts

the modulating signal from the carrier (in this case 40 Hz). The amplitude *A(t)* of the modulating signal corresponds to the peak amplitudes of the SSR. Its phase *Phase(t)* corresponds to the latency shifts of the peaks.

The functions

$$x_s(t) = EEG(t) * \sin\left(40[Hz] \cdot 2\pi \; t[s]\right)$$
$$x_c(t) = EEG(t) * \cos\left(40[Hz] \cdot 2\pi \; t[s]\right) \quad (1)$$

are first computed from the averaged EEG traces, *EEG(t)*. In eq. (1) it is assumed that the time is measured in seconds [s]. These functions were then low-pass filtered (high frequency cutoff 5 Hz, 24 dB/octave), a procedure which extracts activity in the 35-45 Hz range. The amplitude *A(t)* of the modulating signal can then be determined according to

$$A(t) = 2 * \sqrt{x_{sfilt}(t)^{\,2} + x_{cfilt}(t)^{\,2}} \quad (2)$$

The phase was determined according to

$$Phase(t) = \arctan\left(\frac{x_{sfilt}(t)}{x_{cfilt}(t)}\right) \quad (3)$$

(taking the signs of X into account, this yields values in the range ± 180 deg)

The amplitude of the resulting time series corresponds to the peak-to-baseline amplitude of the SSR; and its phase corresponds to the latency shifts of the SSR peaks relative to stimulus onsets. Effects of foreground stimuli and tasks were evaluated by analyses of variance. For within-subject comparison of recording sites, p-values were obtained after adjusting the degrees of freedom by the Greenhouse-Geisser-Epsilon. Means ± standard errors are presented.

2.1.2. Experiment 1

In the first study, an oddball task was superimposed on the series of 1000-Hz pulses by shifting their frequency for 100 ms at a constant interval of 1.5 sec. Of the total of 1200 frequency shift events, changes to 2000 Hz on 70% of the trials (840) constituted standard or non-target events, while changes to 500 Hz on 30% of the trials (360) constituted the target stimuli. Thus, the SSR shifted briefly every 1.5 sec to either higher or lower frequency tone pulses. Subjects were instructed to press a button with their dominant hand as quickly as possible following every target. It was hypothesized that perturbations of the SSR will not only occur due to physical changes of the stimulus (oddball targets and standards, Makeig & Galambos, 1989) but also parallel to the P300 (Makeig, 1994).

Results

Event-Related Potential

The oddball task elicited the expected ERP sequence of N100, P300. The N100 reached its peak amplitude 119 ms after standard, and 124 ms after target stimuli ($F(1,39)= 9.7$, $p < 0.01$). N100 amplitude was larger in response to targets than in response to standards (STIMULUS, $F(1,39) = 61.8$, $p < 0.01$), this difference being more pronounced at the frontal (-5.6 ± 2.1 μV) and central (-5.5 ± 2.0 μV) electrodes (STIMULUS x ELECTRODE, $F(2,78) = 22.8$, $p < 0.01$), where N100 amplitudes were generally larger than at Pz (ELECTRODE, $F(2,78) = 78.4$, $p < 0.01$). The P300 reached its peak amplitude on average after 349 ms and was largest at the parietal site (ELECTRODE, $F(2,78) = 80.1$, $p < 0.01$) in response to targets (STIMULUS x ELECTRODE, $F(2,78) = 78.2$, $p < 0.01$; STIMULUS, $F(1,39) = 97.7$, $p < 0.01$; see Figure 2.1.1).

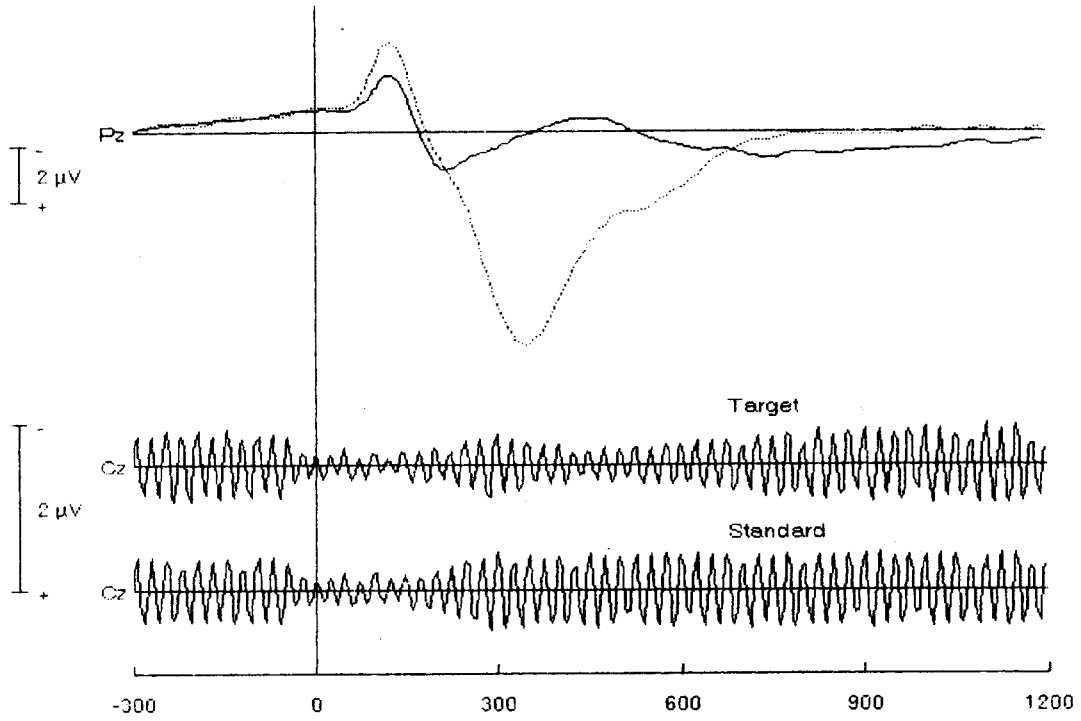

Figure 2.1.1. Top: Grand average of the parietal ERP to oddball stimuli (targets = dotted line, standards = solid line) during 300 ms prior to and 1200 ms following the stimuli. The vertical line marks the time point of oddball stimulus presentation. *Bottom:* Examples of SSR perturbations at the central electrode parallel to the ERP for target and standard oddball stimuli.

Steady-state response

Three additional subjects were excluded from the SSR analysis because their data did not show any measurable synchronization with the 40-Hz stimulus train. Reports are therefore based on 37 subjects. SSR-amplitudes were larger at frontal (0.51 ± 0.03 µV) and central (0.50 ± 0.03 µV) recording sites than at Pz (0.38 ± 0.02 µV, $F(2,72) = 63.1$, $p < 0.001$). A characteristic sequence of changes in SSR amplitude followed the oddball stimuli: first a reduction, R1, followed by an amplitude recovery , referred to as A1, and a second reduction, R2 (see Fig. 2.1.1 for an example, and Fig. 2.1.2 for the results of complex demodulation). Amplitude recovery or even an "overshoot" (A1) has been described by Makeig (1994) as a regular feature of the CERP. The peak latencies were 45 ± 5 ms for R1, 405.9 ± 15 ms for A1, and 413±16 ms for R2.

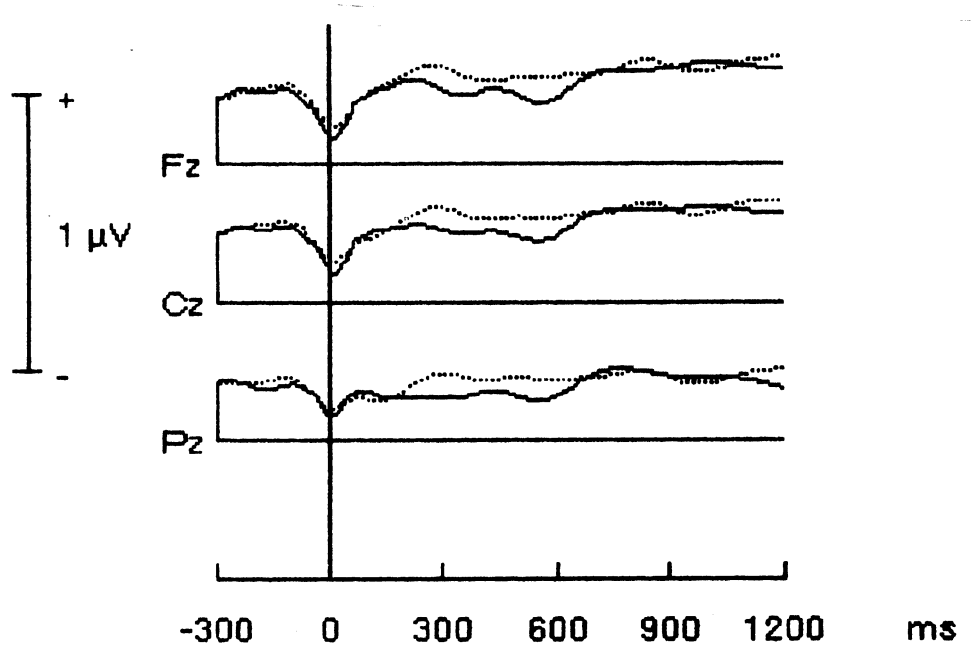

Figure 2.1.2. Modulation of SSR amplitude as determined by complex demodulation, plotted separately for the recording sites, and perturbations following targets (solid lines) and standards (dotted lines). Ordinate: Amplitude modulation in µV (minus indicating amplitude reduction).

A SSR amplitude reduction by 0.32 ± 0.02 µV at Fz and Cz but only by 0.23 ± 0.02 µV at Pz indicated that R1 was larger over the anterior than the posterior cortex (ELECTRODE, $F(2,76) = 66.2$, $p < 0.01$). Thus, SSR amplitude was reduced to 37% of baseline at Fz and to 36% at Cz, and to 39% of baseline values at Pz. This gradient of R1 was found irrespective of the stimulus meaning, i.e., for standards and targets. Amplitude recovery (A1) was more pronounced following standard than following target stimuli ($F(1,36) = 7.1$, $p < 0.05$) and was reached earlier at Fz and Cz than at Pz (390 ± 15 ms versus 434 ± 15 ms, $F(2,72) = 6.9$, $p < 0.01$). R2 was reduced to 57% of baseline values at Fz, to 60% at Cz, and to 66% at Pz, and was more pronounced following target than following standard stimuli (STIMULUS, $F(1,36) = 34.9$, $p < 0.01$). The differences between stimulus types were larger at Fz than at Cz and Pz (ELECTRODE x STIMULUS, $F(2,72) = 16.9$, $p < 0.01$).

Conclusion

The first study confirms earlier results: a CERP followed each stimulus, beginning within the first 100 ms, with a fronto-central predominance, and is followed by an augmentation in amplitude above baseline during the subsequent 300-400 ms. Furthermore, another perturbation of SSR-amplitude was observed following target stimuli only. This effect may be due to the attentional demands of the target detection task (see 2.1.5). A differentiation of SSR-amplitude by the present stimulus- and task-conditions began with the A1. It is tempting to associate the following second SSR-amplitude reduction with the target-evoked P300, as it became pronounced in the same latency range. However, every target-evoked P300 also elicited a motor response (button press). Thus, either the combination of the two or one of the factors alone could have influenced the SSR near 400 ms following target stimuli.

2.1.3. Experiment 2

Experiment 2 was designed to separate target-evoked P300 and motor response contributions of the previous experiment, by comparing SSR perturbations when subjects pressed a button to targets, in one condition, or silently counted the targets in another. Under the same experimental conditions as described in Experiment 1, ten subjects participated in two experimental sessions on successive days. In one session, their task was to respond with a motor response to every target (as in Experiment 1), whereas in the other session they were asked to silently count the number of targets. The order of these tasks was counterbalanced across subjects. Motivation to count was assured by asking the subject at irregular time intervals during the session for the number of targets counted so far. A frequency change to 500 Hz constituted the target. In order to evaluate effects of tone frequency on SSR modulation, two of the ten subjects participated in two further sessions, in which a frequency change to 2000 Hz constituted the targets.

Results

Event related potentials

As in Experiment 1, the oddball stimuli elicited the expected ERP including an N100 (mean peak latency 121.31 ± 2.5 ms, mean amplitude -4.82 ± 0.45 μV, frontal maximum, $F(2,14) = 50.5$, $p < 0.001$) and P300 (latency 325.35 ± 7.3 ms, amplitude 5.16 ± 0.5 μV, centro-parietal dominance, $F(2,14) = 140.3$, $p < 0.001$; see Fig. 2.1.3). While N100 did not differ between tasks or conditions, P300 was larger ($F(1,7) = 19.0$, $p < 0.01$) and peak amplitude was later ($F(1,7) = 33.7$, $p < 0.001$) after targets than after standards, in particular under conditions in which subjects indicated target detection by a motor response (STIMULUS x TASK; $F(1,7) = 7.3$, $p < 0.05$, STIMULUS x ELECTRODE; $F(2,14) = 28.6$, $p < 0.01$).

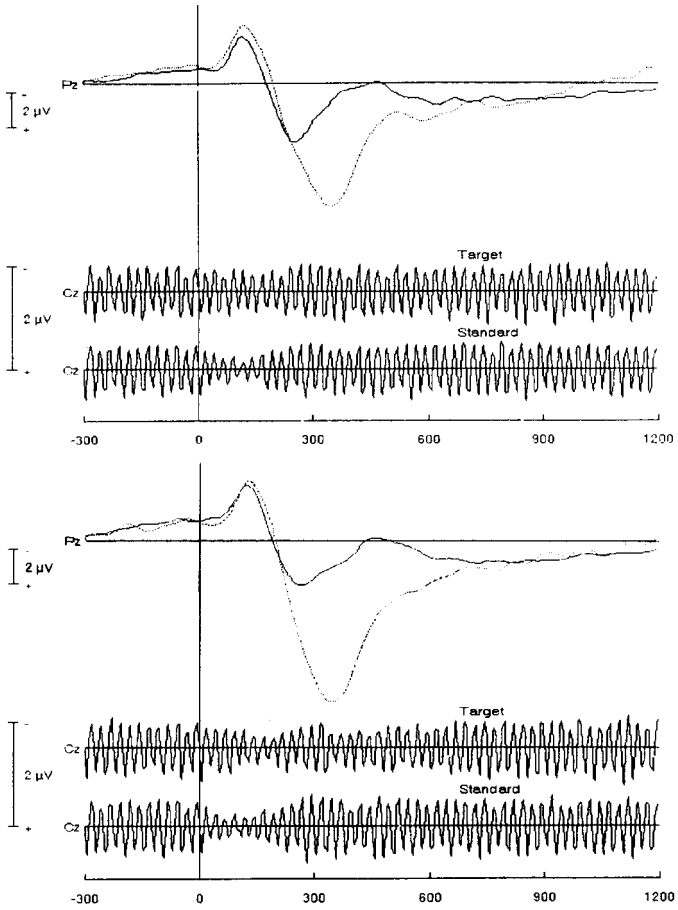

Figure 2.1.3. Grand averages of the parietal ERP (in μV, negativity up) to oddball stimuli (targets: dotted line, standards: solid line) during 300 ms prior to and 1.2 sec following the stimuli. *Top:* session with motor response required to targets. *Bottom:* session in which targets were to be counted. The vertical line marks the time point of oddball stimulus onset. Below each ERP, an example of SSR perturbations at the central electrode (averaged across subjects separately for targets and standards) is given.

Steady-state responses

As reported for the first study, the 40-Hz stimulus train drove an SSR (mean amplitudes 0.59 ± 0.03 μV at Fz, 0.55 ± 0.03 μV at Cz and 0.37 ± 0.02 μV at Pz, baseline-to-peak, $F(2,7) = 91.3$, $p < 0.001$). Figure 2.1.4 depicts the SSR amplitude and phase as obtained by complex demodulation for the count and botton press task.

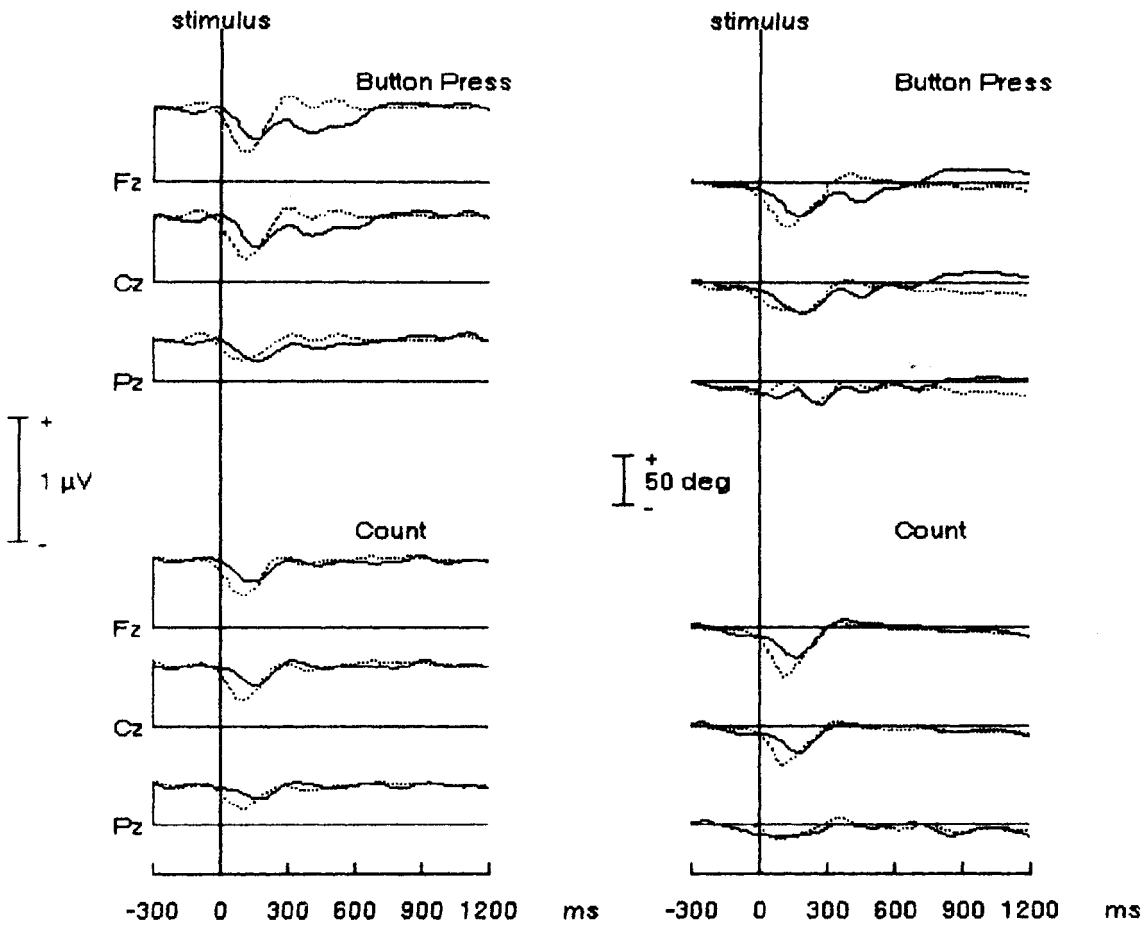

Figure 2.1.4. Modulation of SSR amplitude (left) and phase (right) as determined by complex demodulation, plotted separately for the recording sites, perturbations following targets (solid lines) and standards (dotted lines), and the sessions with a button press required to targets (top) and the session with targets to be counted. Ordinate: Amplitude modulation in μV (minus indicating amplitude reduction) or phase modulation in degrees (minus indicating phase advance relative to baseline). Time scale as in Fig. 2.1.3.

Oddball stimuli elicited an R1 with an average minimum at 97.6 ± 7 ms (see Fig. 2.1.4) to 52% of baseline level at Fz, to 51% at Cz and to 49% at Pz (no significant difference between sites). The peak latency of the R1 was 55 ms

later following target relative to standard stimuli ($F(1,7) = 10.9$, $p < 0.05$). The peak R1 amplitude was more pronounced following standards than targets (ELECTRODE x STIMULUS; $F(2,14) = 4.5$, $p < 0.05$). This effect has to be attributed to the tone frequency: When – in two subjects – the target stimulus was a higher frequency (2000 Hz), the relationship between amplitudes to targets and standards was reversed, i.e. the higher tones, irrespective of being targets or standards, counted or answered with a button press, induced SSR amplitude reductions of about 0.3 μV, whereas lower tones relative to the 1000-Hz stimulus train induced SSR amplitude reductions of about 0.1 μV. The *phase* component of the R1 was a phase advance (see Fig. 2.1.4) by 48 deg (or 3.3 ms) at Fz, 42 deg (or 2.9 ms) at Cz and 34 deg (or 2.4 ms) at Pz, peaking 126.8 ms after the oddball stimulus onset, with a pronounced fronto-parietal gradient ($F(2,14) = 4.8$, $p < 0.05$) which did not differ between stimulus conditions or tasks.

The SSR amplitude augmentation following the R1, occured in the latency range of 340 - 410 ms. In Experiment 1, this augmentation was refered to as A1. A1 was smaller following targets (2% of baseline values) and larger following standards (17% of baseline values) when subjects indicated target detection by button press; smaller differences (17% versus 16%) occurred when subjects silently counted the targets (TASK x STIMULUS, $F(1,7) = 5.4$, $p < 0.06$). Post-hoc comparisons confirmed the stimulus difference under conditions of button press ($t(7) = 2.8$, $p < 0.05$), and the larger A1 following counted targets ($t(7) = 2.4$, $p < .05$), while differences between stimulus types under counting conditions did not reach significance ($p = 0.5$). A slight *phase retard* of 11.5 deg (or 0.8 ± 0.01 ms) occurred later following targets (490 ± 17 ms) than following standards (410 ± 13 ms, $F(1,7) = 6.1$, $p < 0.05$), but was not affected by task.

Figure 2.1.4 also shows the presence of a R2 amplitude reduction. For mean SSR amplitude during the time interval 270 to 650 ms following oddball stimulus onset, a TASK x STIMULUS interaction indicates a more pronounced R2 when subjects pressed the button following targets (TASK x STIMULUS, $F(1,7) = 9.2$, $p < 0.05$). Post-hoc t-tests confirmed a significantly larger R2 following button press relative to counted targets ($t(7) = 3.2$, $p < 0.05$), and relative to standards of both types ($t(7) = 4.1$, $p < 0.05$), while R2 did not differ significantly between targets and standards under the counting condition. Following target stimuli, mean amplitude of the R2 trough was a reduction to 88% of baseline, the modulation being larger at Fz (reduction to

86%) than at Cz and Pz (reduction to 91%). Following standard stimuli there was no change in mean amplitude from the baseline level for any of the electrodes (ELECTRODE x STIMULUS; $F(2,14) = 8.4$, $p < 0.01$). The R2 was more pronounced at Fz (to 89%) than at Cz (to 93 %) and Pz (to 92%) for the button press condition, whereas there was no difference between electrode sites when subjects counted the targets (reduction to 96%, 98%, 94%, resp. , TASK x ELECTRODE, $F(2,14) = 7.8$, $p < 0.01$). Parallel to the R2, a *phase advance* was larger (17 deg or 1.2 ms) in response to targets than in response to standards (10 deg or 0.7 ms; $F(1,5) = 7.9$, $p < 0.05$), while no significant task effects could be found.

Subsequent to the R2, mean amplitude modulations (650-1450 ms) by stimulus types and tasks were reversed: Targets for which a button press was required produced a sustained amplitude augmentation of 5.8%, while an amplitude reduction by 4% of baseline was observed following standard stimuli. Counted targets, however, produced only a slight amplitude reduction, while no change relative to baseline levels followed standard stimuli ($F(1,7) = 5.5$, $p < 0.05$).

Conclusion

The results of this second study closely replicated the findings of Makeig (1994). The interaction of stimulus and task suggests that both motor responding and stimulus processing, with their related slow potentials, may contribute to the observed SSR perturbations. The R1 was equally pronounced at all recording sites (as percent reduction from baseline), suggesting that a common set of generators or equally effective modulation of all generators contributes to the response at all three sites. The R1 was sensitive to physical (tone) frequency but not to psychological (task-related) aspects of the stimuli. The subsequent CERP features (A1 and R2) revealed an impact of stimulus and task relevance. Rare targets in an oddball task absorb more attentional and cognitive resources (e.g. counting, pressing a response button) as compared to frequent standard tones. The new finding of experiment 1 and 2, however, is the demonstration that theses demands alter the processing of information in the primary auditory cortex.

2.1.4. Experiment 3

Experiment 3 was designed to explicitly examine SSR perturbations related to slow potentials that develop prior to and following motor responses. It might be speculated that the intention, preparation and processing of a self-paced motor response turns attention away from the stimulus train to the motor task. To the author's knowledge, SSR perturbations parallel to the development of a surface-negative Bereitschaftspotential (BP), the negative motor potential and the positive-going motor potential complex has not yet been studied. In order to elicit movement-related potentials, subjects were instructed to press a button with their dominant hand approximately every 10 seconds while the stimulus train was delivered. Prior to the experimental period, subjects were trained to estimate the time interval to avoid using a distracting strategy of silently counting to ten between every button press. A total of 250 button presses were collected per subject. Four additional subjects out of the remaining 16 subjects were found to have SSR signal-to-noise ratios too low to allow accurate measurement of SSR phase changes, and were omitted from the CERP analysis.

The course of the slow potential prior to and following the voluntary button presses was described by the following components (named according to Neshige, Lüders, & Shibasaki, 1988): mean potential during 1.5 - 0.5 sec prior to the button press, the Bereitschaftspotential (BP); mean potential during the last 500 ms prior to the button press, the negative slope (NS) of the BP; the negative peak surrounding the button press, the motor potential (MP). Post-response components were described by the maximum positive peak (positive motor potential, PMP), as well as mean potential during the 500 ms interval following the button press (motor potential complex, MPC); mean potential during the interval 0.5 - 2 sec following the button press, slow motor potential, MPS). SSR perturbations during similar time intervals were related to these scores.

Results

Event related potentials

The rectified grand average EMG for the 16 subjects is shown in Figure 2.1.5 along with the grand average button press evoked responses at the three central sites. As expected, these contain a prominent increase in surface-

negativity during the BP period, with a steeper negative slope (NS) appearing approximately 500 ms before the button press. Pre-movement negativity was larger at C3, contralateral to the movement, than at C4 ($t(15) = 5.1$, $p < 0.01$). The button press was followed by a positive deflection, the post-motor positivity (PMP), peaking at 191 ± 34 ms.

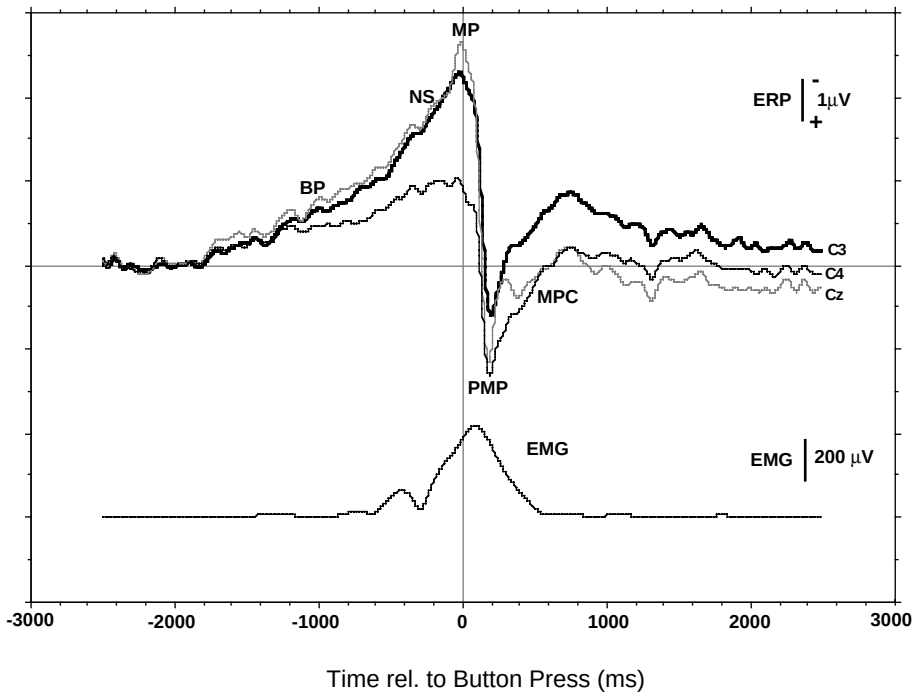

Figure 2.1.5. Grand mean evoked response (low pass filtered below 8 Hz) time locked to the moment of button press for 16 subjects at 3 central scalp channels. The vertical line marks the moment of the button press. The lower part of the figure shows the mean rectified EMG record. The ERP Bereitschaftspotential (BP), and pre-movement negative slope (NS), as well as the pre-motor (PM) and post-motor positivity (PMP) peaks are labeled in the ERP.

Steady-state response

Figure 2.1.6 shows mean baseline SSR amplitude and phase at the three central and two contralateral sites. SSR amplitude declined from Fz to Pz ($F(2,22) = 15.04$; $p = 0.001$), but did not differ at the two lateral sites. Baseline SSR phase increased by 116 deg from Fz to Pz (corresponding to an 8.2 ms relative delay), but did not differ at the three central sites ($F(2,22) = 3.19$; $p > 0.05$).

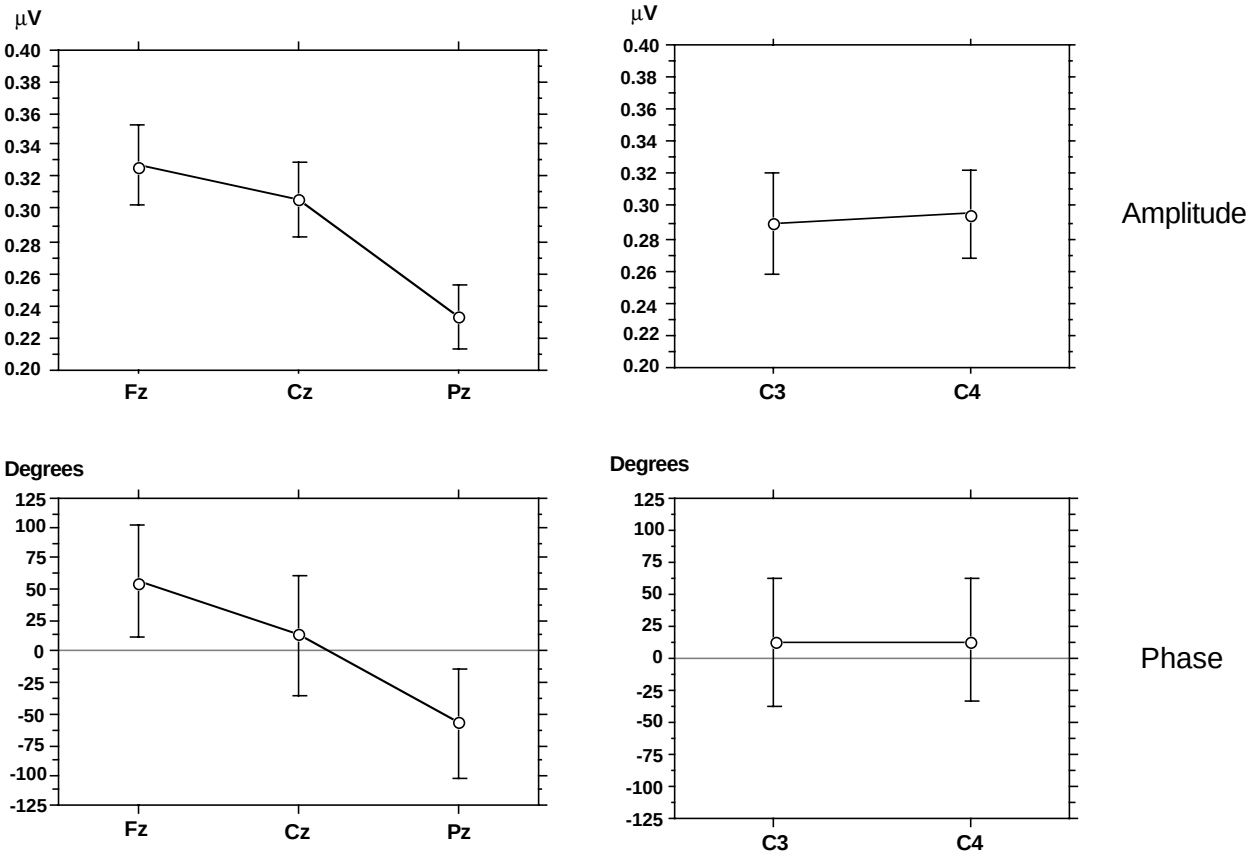

Figure 2.1.6. Mean baseline SSR amplitude and phase for 12 subjects at the three midline and two lateral scalp sites.

The Figure 2.1.7 shows the grand mean button press-induced CERP phase records at the five scalp sites, smoothed with a 5-Hz filter, and normalized by subtracting its phase baseline. The CERP phase responses at the five scalp sites did not differ significantly, suggesting they all measure the effects of a single SSR-modulating system.

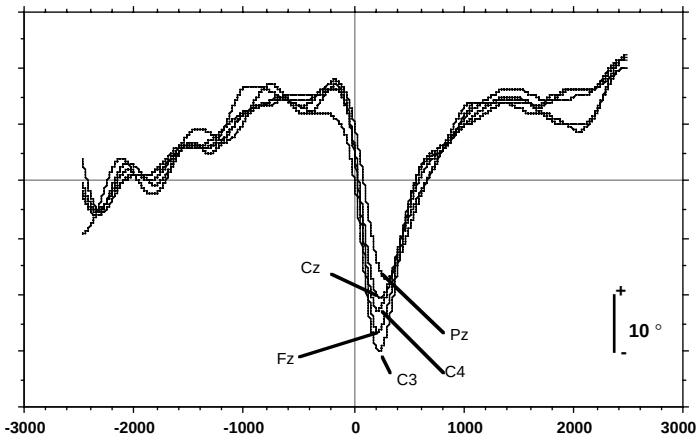

Figure 2.1.7. Grand mean baseline CERP phase for 12 subjects at the 5 scalp sites, each channel normalized to its baseline measure. *Note:* Time relative to botton press in ms.

Examination of the 5-Hz smoothed records confirmed that no significant changes in SSR amplitude occurred before the button press. Immediately after it, SSR amplitude dipped in 9 of the 12 subjects, reaching a minimum of 49% of baseline at 105 ± 27 ms ($F(1,15) = 47.9$, $p < 0.001$). Following this, amplitude increased, reaching a maximum near 550 ms at which the amplitude is slightly above baseline (significant at Fz only).

Before the button press, a definite *phase retard* evolved concurrent with the pre-movement BP, averaging 12 deg (or 0.85 ms) before, and 19 deg (or 1.35 ms) during the NS period at all recording sites. Beginning just before the button press, a significant phase advance ($F(1,11) = 8.84$, $p = 0.01$) developed that peaked during the onset of the post-motor positive slow potential (PMP). This advance peaked at 16 deg (or -1.1 ms), and was smaller at Pz giving rise to an overall interaction of electrode and phase components ($F(16,176) = 3.25$, $p < 0.001$). In the grand mean, the phase advance is followed by a sustained phase retard of 16.6 deg (or 1.2 ms) beginning near 900 ms in all 12 subjects.

For comparison with the ERP, the SSR records at all five scalp sites were averaged across subjects and converted to CERP amplitude and phase. Figure 2.1.8 superimposes this spatial grand mean on the ERP at the vertex (Cz). It can be seen that: (1) the BP negativity and the CERP phase retard begin together; (2) no notable CERP features accompany EMG onset; (3) the initial post-button press peaks in the three records differ in latencies, and (4) during the apparent amplitude maximum, SSR phase regains its immediate pre-movement baseline value, which is maintained to the end of the epoch.

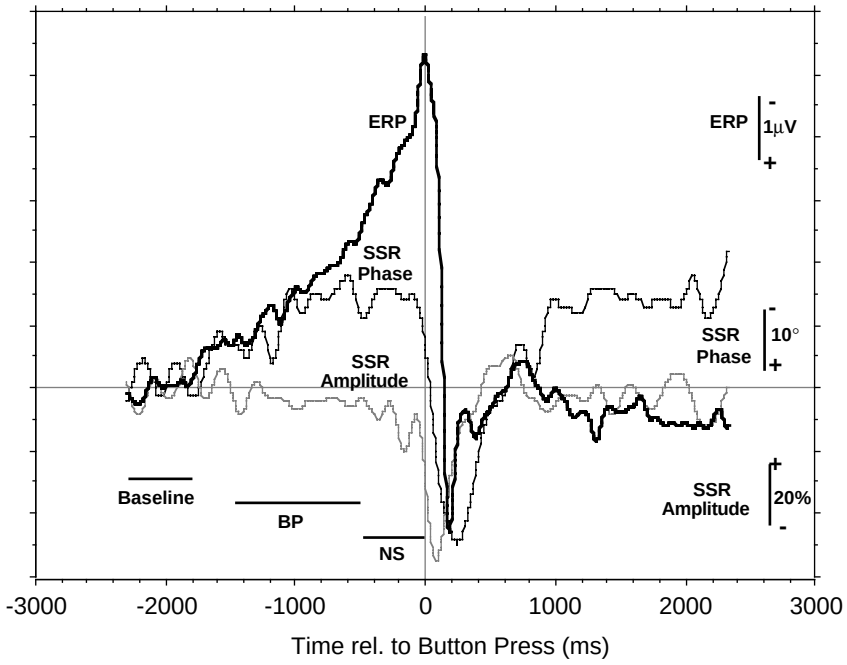

Figure 2.1.8. Grand mean CERP amplitude (thin trace) and phase (medium trace), averaged across the five recording sites and 12 subjects, superimposed on the grand mean botton-press ERP at Cz (bold trace).

Conclusion

In Experiment 3, SSR-amplitude was smaller than the SSR-amplitudes obtained in the preceding experiments. A major difference in the designs for the three experiments was that subjects had to pay attention to the continuous stimulus train in the first two experiments in order to detect changes in tone frequency, while no attention to the stimulus train was required in the last study. Possibly, the boring task of pressing a button for long periods of time may have distracted subjects from attending the stimulus train or may have induced drowsiness, a condition known to affect SSR amplitude (Galambos and Makeig, 1988). Despite some differences of SSRs in the auditory and visual modality (see section 1.1.3 and 2.2) a higher steady-state amplitude for attended as compared to unattended stimuli was also found in the visual modality which may be seen as a hint for common mechanisms with respect to attentional modulation. The voluntary movement clearly induced a CERP with features in many respects comparable to those described in the previous studies (amplitude reduction and phase advance). The reduction in SSR amplitude during the execution of a motor response is in line with the results of Böcker, Forget, and Brunia

(1993), who observed smaller amplitudes of the somatosensory evoked potential (SEP) to distinct somatosensory probes during the movement (250 ms after the motor response) as compared to SEPs to probes prior to the response or following the response at a later point in time. However, the SSR in this experiment is thought to be generated mainly in the auditory and not in the somatomotor cortex. While the size of the phase advance during the CERP is in line with the results obtained in Experiment 2, as well as results reported by Makeig (1994), the phase retard parallel to the development of the negative Bereitschaftspotential contrasts with findings of Rohrbaugh et al. (1990), who described a phase advance parallel to the negative slow wave following an auditory stimulus, which was attributed to an orienting response.

2.1.5. General summary and discussion of experiments 1 to 3

The series of experiments reported in this chapter clearly demonstrate perturbations of the auditory SSR following auditory stimuli, and, in particular, under conditions that require stimulus evaluation and motor performance, i.e. are related to attentional demands. Under these conditions, auditory stimuli also evoked slow potential shifts typically found in the oddball and in the voluntary response paradigm. As the author knows of only very few studies (other than Makeig, 1994 and Rohrbaugh et al., 1989, 1990) systematically exploring the relationship between SSR perturbations and slow potentials, the interpretation of the present results must remain speculative. In the present experiments, a CERP amplitude reduction and phase advance, relative to SSR baseline was consistently observed following a foreground stimulus, such as the oddball frequency shifts, but also following voluntary motor responses. This finding replicates results by Makeig (1993). However, varying the stimulus meaning (non-target and target events) provoked an additional SSR perturbation during the time period during which evaluation of and response to a meaningful stimulus is supposed to take place (P300). The SSR perturbation (R2) found when subjects indicated target detection by a motor response but not when targets were silently counted, suggests a major contribution of the processes related to motor responding to the observed SSR perturbation. It is possible that they contribute to processes of stimulus evaluation that are attributed to the P300. However, processes underlying the later SSR perturbation may be distinguished from those underlying the

R1. While the R1 was not sensitive to stimulus aspects (indicating standard or target stimuli), the subsequent CERP features revealed an impact of the task relevance of the target and the motor responding, or, in other words, they revealed an impact of attentional processes (see below). The results of Experiment 3 indicate that early processing of auditory information in the auditory cortex is altered before, during, and after voluntary movements. Experiment 3 is the first which demonstrates interactions between voluntary movements and auditory ERP componenets earlier than the N100.

The physiological mechanisms that produce the CERP perturbations are still not fully understood. Some facts strongly suggest that the reported evoked potentials related CERP features reflect changes in the auditory SSR:

1. The perturbations cannot be a consequence of the evoked potential (P300, Bereitschaftspotential) and the SSR-generator interacting on a physical level: The superposition of the volume currents generated by two distinct generators is a strictly linear phenomenon, i.e. if the ERP generators are added to a SSR generator, the result would exactly equal the sum of the two (Rockstroh, Elbert, Canavan, Lutzenberger, & Birbaumer, 1989).

2. The superposition of components with higher frequency, such as the evoked gamma-band response (Pantev, Makeig, Hoke, Galambos, Hampson, and Gallen, 1991), might mimic SSR modulation including a phase shift. However, these circa 40-Hz components appear in ERPs to isolated auditory stimuli only during the first 60-120 ms after stimulus onset (Makeig, 1990; Pantev, et al. 1991).

3. GBR peaks later than 50-60 ms are small or imperceptible at stimulus rates above 1 Hz (Makeig, 1990; Makeig, et al., 1995).

4. The best-fitting single-dipole source location for the magnetic SSR in the auditory cortex is different from that of the evoked gamma-band response (Pantev, et al., 1993; 1996).

In sum, the evidence from the studies suggest that “external” as well as “internal” stimuli (associated with the intention and preparation of a self-paced, voluntary button press) interfere with the continuous processing of early auditory information. Makeig (1994) links SSR perturbations to shifts

in attention. If processing of a foreground stimulus, as well as focusing on the execution of a cued or voluntary button press, demand attentional capacities as well as their neuronal substrates, similar perturbations might be expected for different tasks. This hypothesis is supported by the similarity of CERPs in the experiments with oddball stimuli and in the study including a voluntary response task, as well as by a phase retard during the preparation of the voluntary response. One might assume that during this interval, the subjects' attention was focused on the motor response and turned away from the rapid series of stimuli. However, direct tests of this assumption will require further research.

2.2. Steady-state visual evoked potentials (SSVEP)

The last section has provided some evidence that the auditory SSR, generated in the primary auditory cortex, is altered by attentional processes. The following section presents four experiments investigating the steady-state visual evoked potential (SSVEP). The first experiment was a pilot study to test whether SSVEPs can be elicited with a variety of stimulation frequencies, indicating fundamental differences to the auditory SSR. In the second study, a magnetoencephalographic recording was conducted to investigate whether the location of a single moving dipole varied systematically as a function of frequency. In experiment 3, the influence of spatial selective attention on high frequency SSVEPs was examined and, finally, in experiment 4, the high frequency SSVEPs were used to measure the time period for attentional shifting[1].

2.2.1. Experiment 1

Experiment 1 was conducted to test, whether or not SSVEPs can be elicited by a variety of stimulation frequencies.

Methods

Subjects

Three subjects (2 females, mean age 26 years) with normal or corrected-to-normal vision served as paid volunteer subjects after giving informed consent.

---

[1] This chapter contains the a slightly adapted versions of the following articles: Müller, M.M., Teder, W., Hillyard,.S.: Magnetoencephalographic recording of steady-state visual evoked cortical activity. *Brain Topography* , 1997, 9, 163-168, and Müller, M.M., Picton T.W., Valdes-Sosa, P., Riera, J., Teder-Salejarvi, W., Hillyard, S.A.: Effects of spatial selective attention on the steady-state visual evoked potentials in the 20-28 Hz range. Submitted for publication.

Stimuli and Design

While seated in a comfortable chair in a shielded recording chamber, subjects viewed a light-emitting diode (LED, luminance 2.5 cd/m^2) display presented against a background luminance of 0.25 cd/m^2. The display included two vertical rows of 5 red LEDs each; the individual LEDs were circular (subtending 0.5 degrees at a viewing distance of 58 cm) and the vertical rows (hereafter termed "bars") each subtended 3.45 x 0.5 degrees. The two bars were situated 5 degrees lateral to a central fixation point, one in the left visual field and one in the right visual field, centered on the horizontal meridian. Either the left or the right bar flickered for a period of 16 sec with one of the following frequencies: 6.0, 8.9, 11.9, 17.9, 26.3, 31.3, 35.7, 41.6, 45.5 or 50 Hz. The subject was required to maintain a fixed gaze on the central point and avoid blinks and eye movements during the flicker period.

Data Recording and Data Analysis

Brain electrical activity was recorded from 30 scalp electrodes mounted in an elastic cap. Electrode impedances were kept below 5kOhms. Standard 10-20 sites were Fz, F3, F4, F7, F8, Cz, C3, C4, Pz, P3, P4, 01, 02, T3, T4, T5, T6, and left mastoid. Non-standard sites included IPz, INz, IN3, IN4, P01, PO2, TO1, TO2, CP1, CP2, CT5 and CT6. The locations of these sites are given in spherical co-ordinates in (Clark & Hillyard, 1996) and are indicated schematically in Figure 2.2.1. Vertical eye movements and blinks were monitored with an electrode placed beneath the left eye.

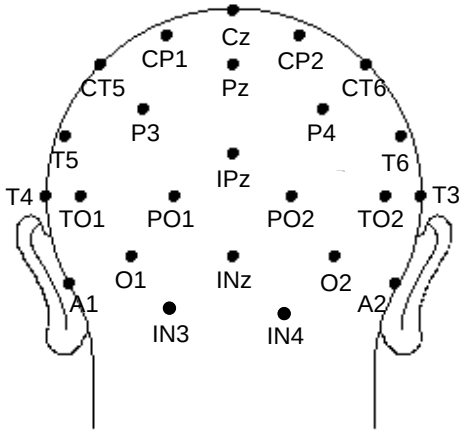

Figure 2.2.1. Schematic presentation of electrode sites.

The right mastoid served as a reference for all of the above channels. Lateral eye movements were monitored with a bipolar left-to-right outer canthus montage (horizontal EOG). This montage was identical in all EEG-experiments (experiments 1, 3 and 4). All channels were recorded with a bandpass of 0.3-300 Hz except for the horizontal EOG, for which the bandpass was 0.01-100 Hz. Signals in all channels were digitized at 1000 Hz and stored on disk for off-line analysis.

Individual trials were rejected from further analysis on the basis of blink or EMG artifacts in the scalp channels or lateral eye movements revealed in the horizontal EOG. The rejection criterion for horizontal EOG deflections was made increasingly stringent until the averaged deviation from baseline was less than 5 μV during the 16 sec period of attending, which corresponded approximately to a 0.5 degree shift in lateral gaze (Luck, Hillyard, Mouloua, Woldorff, Clark, & Hawkins, 1994). The SSVEPs to the concurrent left and right field flashes were averaged separately in the time domain using a moving window technique. The first step was to average the 15 sec epochs of EEG obtained on artifact-free trials separately for the left and right bar trials. For each of these averages, moving window averages were obtained to extract the respective SSVEPs. Beginning one second after flash onset, a moving 1000 msec epoch was synchronized to begin at each flash in the sequence at one of the frequencies, and these successive epochs were averaged together across the entire 15 sec epoch. Since this experiment was considered as pilot study, a statistical analysis of amplitude differences was not conducted.

Results

Figure 2.2.2 on the following page shows an example of unfiltered right bar SSVEPs for one subject averaged over electrodes T5, P3, TO1, PO1 and O1 for a period of 500 ms. SSVEPs can be elicited with all stimulation frequencies. Contrary to the auditory SSR, there is no specific frequency necessary in order to evoke SSVEPs. As stimulus intensity was constant for all frequencies, SSVEP amplitude decreases with higher stimulation frequencies.

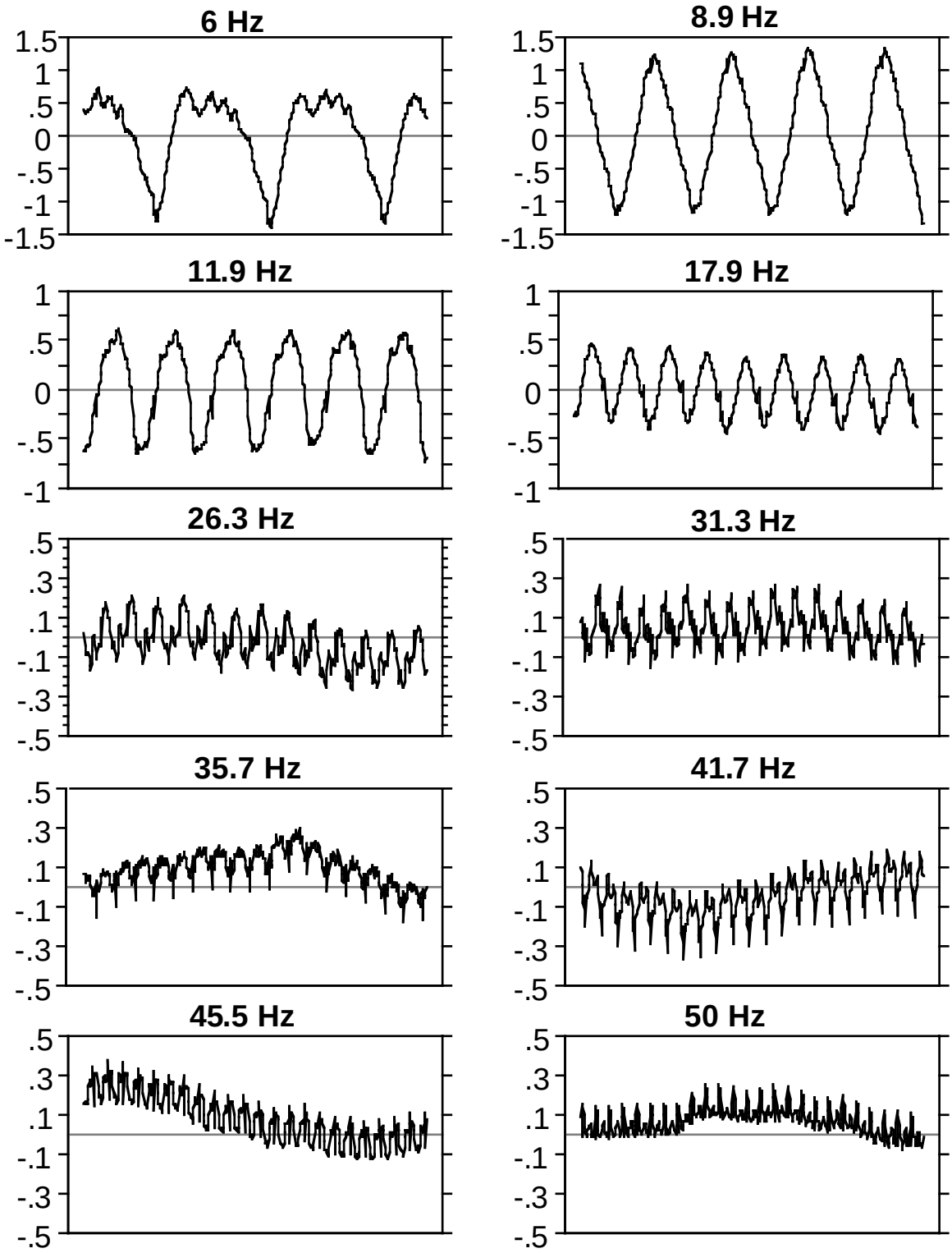

Figure 2.2.2. SSVEPs for different stimulation frequencies in μV for a period of 500 ms.

2.2.2. Experiment 2

Experiment 2 employed magnetoencephalographic (MEG) recordings of steady-state visual evoked fields (SSVEFs) to investigate whether discrete dipole generators may be identified in posterior cortical areas. Because of the well-known properties of MEG recordings, which emphasize tangential over radial sources and eliminate spatial smearing due to skull-scalp resistivity, it was anticipated that SSVEF recordings might help to clarify the neural generators of evoked steady-state activity. The principal aims of this study were to discover whether consistent localizations of equivalent current dipole (ECD) sources could be obtained across subjects for SSVEFs at three different stimulation frequencies (6.0, 11.9, and 15.2 Hz), and to see if these ECD localizations varied systematically as a function of frequency.

Methods

Subjects

SSVEFs were recorded from ten healthy adult volunteer subjects (four females) with normal or corrected-to-normal vision. Mean subject age was 32 (range 20-42) years. Subjects received monetary compensation for participating, and informed consent was obtained.

Stimulation

Flickering visual stimuli were generated by an array of six light-emitting diodes (LEDs) located outside the magnetically shielded recording chamber. The stimuli were delivered into the chamber via 3 mm fiber optic guides that were attached to each LED. The ends of the six guides viewed by the subject were each covered by a red diffusing lens and arranged into a vertical bar that subtended 0.5 x 4 degrees of visual angle. This bar was positioned on the horizontal meridian of the subject's binocular field of view, 5.0 degrees to the left of a central fixation point.

The six LEDs flickered synchronously with a 50/50 on/off cycle. Stimulus luminance was 1.5 cd/m^2 against a background of 0.05 cd/m^2. Three different flicker frequencies (6.0, 11.9 and 15.2 Hz) were presented in

separate blocks of trials in counterbalanced order. Each block consisted of a sequence of ten 16-second periods of stimulation separated by 4-second breaks, followed by a longer rest period. During stimulation, the subject lay prone with forehead and chin supported by a head rest that did not restrict his/her field of view. The subject was instructed to fixate on a central point while avoiding blinks or eye movements.

MEG Recording

SSVEFs to the flickering stimuli were recorded with a 37-channel biomagnetometer (Biomagnetic Technologies Inc., San Diego) with having sensors configured as first-order axial gradiometers with a baseline of 5 cm. The exact locations of the sensors relative to fiducial points on the subject's head (nasion and pre-auricular points) were determined by a sensor position indicator system, which also revealed whether head movements occurred during the recordings. MEG activity was recorded with a digitization rate of 1042 Hz and system bandpass of 1-200 Hz. SSVEFs were averaged on-line over consecutive epochs with having a duration of 4 cycles per stimulation frequency.

An initial screening session was carried out in order to ascertain the optimal sensory array position for recording the SSVEFs at each frequency. During screening the sensor array was positioned as close to the head as possible and centered on scalp site Oz (International 10-20 System). For subsequent recordings, the array was moved so as to be centered approximately on the zero line of the dipolar magnetic field distribution for each frequency. The final sensor array had an average position centered near scalp site P4 for the 6.0 and 11.9 Hz flicker and midway between site Pz and Oz for the 15.2 Hz flicker. Averaged SSVEFs were then obtained over 1000 epochs for 6.0 Hz, 2000 epochs for 11.9 Hz, and 2500 epochs for 15.2 Hz for each subject.

Dipole Source Analysis

The averaged waveforms were digitally filtered at 1-18 Hz for the 6.0 Hz SSVEF and at 1-30 Hz for the 11.9 and 15.2 Hz SSVEFs using first-order Butterworth filters (6 dB/octave). The waveforms were filtered twice (forward and backward) in order to avoid phase shifts, resulting in an effective roll-off of 12 dB/octave.

Single equivalent current dipoles (ECDs) were fit to the field distributions of the filtered SSVEF waveforms from each subject using a spherical head model based on individual head shape (Sarvas, 1987). This dipole localization algorithm provides a best-fit ECD for a single time point based on the spatial distribution of magnetic field strength. The origin of the head-based co-ordinate system was the midpoint between the left and right preauricular points, as determined by the sensor position indicator. This line represented the medio-lateral or y-axis with positive values toward the left. The anterior-posterior or x-axis ran from the origin to the nasion perpendicular to the y-axis, with positive values towards the nasion. The inferior-superior or z-axis was perpendicular to the other two axes and ran from the origin towards the vertex with positive values above the origin.

Dipole locations and moments were calculated for 5 adjacent sampling points of the SSVEF waveform at the peak for which the root-mean-square (RMS) field amplitude over all 37 channels was maximal. For the 6.0 and 11.9 Hz SSVEFs, the dipoles calculated for each subject showed a correlation and goodness of fit of 0.95 or greater between the dipole's forward solution and the observed field distribution. For the 15.2 Hz response, all dipoles had a goodness of fit exceeding 0.90 except in one subject, who was excluded from the statistical analysis. A single ECD was then calculated for each subjects's averaged waveform at each frequency. The co-ordinates of this ECD were taken as the median values of the co-ordinates of the 5 individual ECDs.

For three subjects, MRI-scans (Signa GE, 1.5 T) were obtained so that ECD localizations could be visualized with respect to cortical anatomy. The nasion and pre-auricular points were identified on the MRI sections so that the x,y,z co-ordinates of the ECDs could be co-registered with the appropriate MRI sections. This co-registration method has a maximum error of 4 mm.

Statistical Analysis

In order to compare the localizations and amplitudes of the ECDs calculated for the SSVEFs at each of the three stimulation frequencies, one-way analyses of variance were carried out on the x,y, and z co-ordinate values, as well as on the dipole moments and RMS peak amplitudes averaged over all

37 sensors. Reported p-values were adjusted by the Greenhouse-Geisser correction where necessary. Post hoc paired t-tests of specific comparisons of significant ANOVA effects were carried out. Means and standard errors are presented.

Results

Figure 2.2.3 illustrates typical SSVEF waveforms from one subject at one recording site in response to the 6.0, 11.9 and 15.2 Hz stimuli. For each stimulation frequency, the responses were generally sinusoidal in form, with the largest amplitudes produced by the 6.0 Hz flicker. Topographical contour plots of the magnetic field distributions at the peaks and troughs of the waveforms at each frequency are shown in Figure 2.2.4 for a representative subject. In all subjects but one a clear dipolar field organization could be identified over the posterior scalp for the SSVEFs at each frequency.

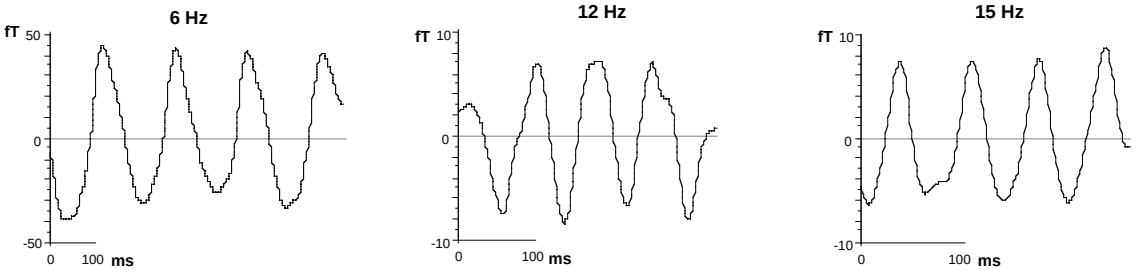

Figure 2.2.3. SSVEFs from one subject in response to the three stimulus frequencies recorded from one sensor location.

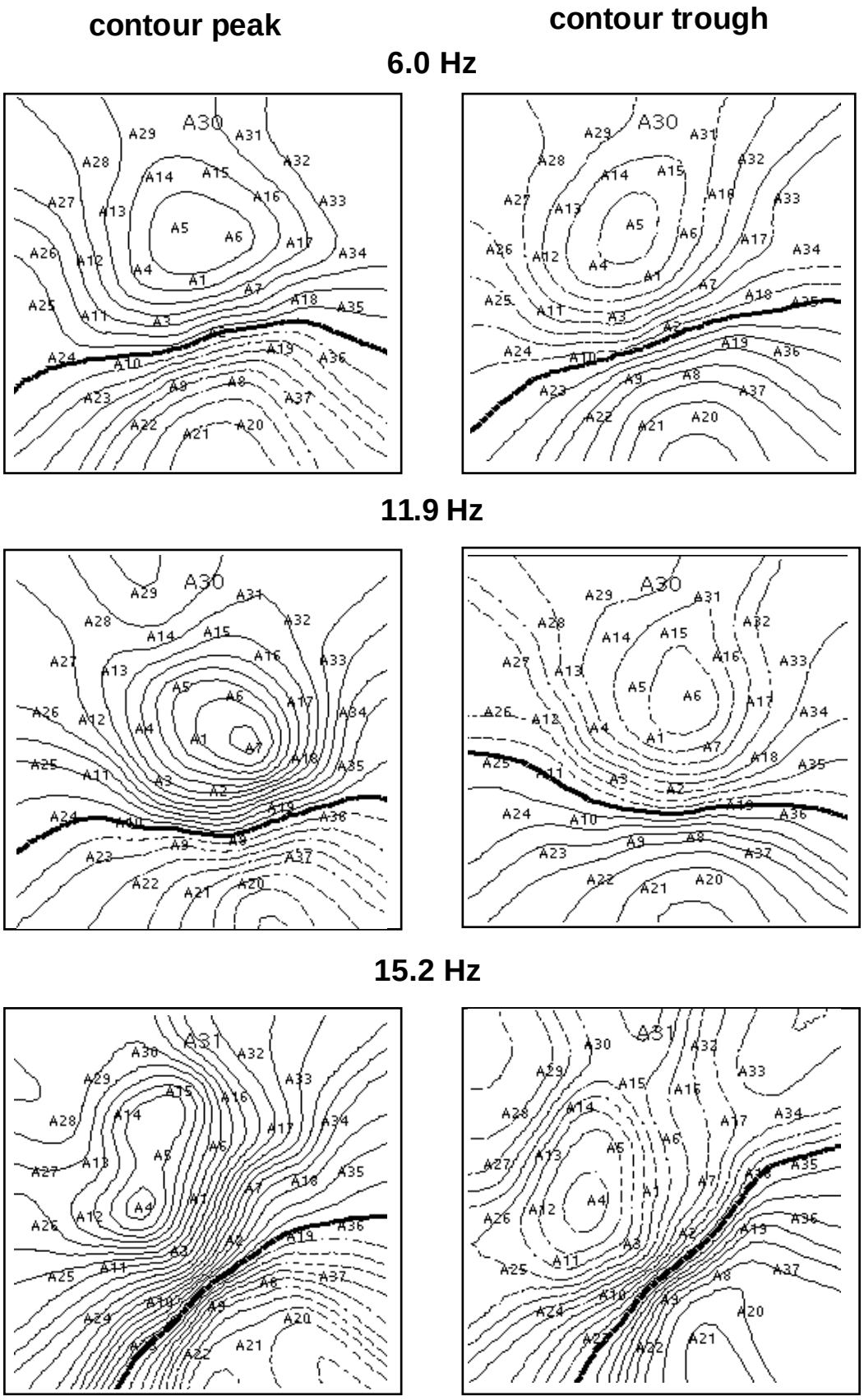

Figure 2.2.4. Magnetic field contour maps of one subject for peaks (left) and troughs (right) of averaged waveforms at the three stimulation frequencies. Isocontour lines are separated by 5 fT for the 6.0 Hz, by 2 fT for the 11.9 Hz, and 1 fT for the 15.2 Hz response.

Differences in SSVEF magnitude as a function of stimulation frequency were quantified both in terms of dipole moment and peak RMS amplitude across the sensory array (Figure 2.2.5). A significant effect of frequency on dipole moment ($F(2,16) = 5.96$, $p < 0.05$) was mainly due to differences between the 6.0 Hz and 11.9 Hz ($t(8) = 3.35$, $p < 0.05$) and between the 6.0 Hz and 15.2 Hz ($t(8) = 2.82$, $p < 0.05$) responses. A similar effect of frequency was seen on the RMS measure ($F(2,16) = 40.13$, $p < 0.001$), with the 6.0 Hz amplitude being larger than either the 11.9 Hz ($t(8) = 5.84$, $p< 0.001$) or the 15.2 Hz ($t(8) = 8.48$, $p < 0.001$) amplitudes.

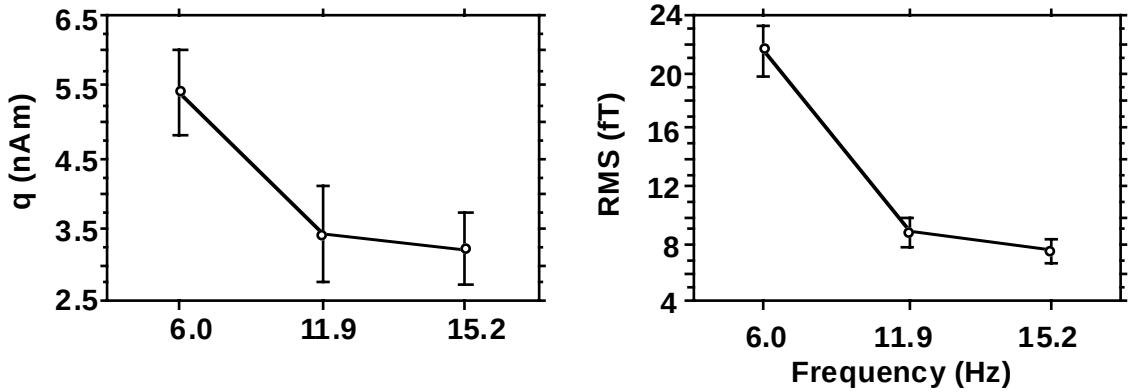

Figure 2.2.5. Mean dipole moment values (left) and RMS field amplitudes (right) over all subjects (± standard errors) for the three stimulation frequencies (in Hz).

The mean values of the x,y,z co-ordinates for the best-fit ECDs at the three stimulation frequencies are given in Table 2.2.1 and illustrated in Figure 2.2.6. The coordinates from each of the 10 subjects are plotted in Figure 2.2.7 to make the individual variability apparent.

	x (ant.-post)	y (med.-lat)	z (inf.-sup.)
6.0 Hz	-3.99	-1.60	7.12
	(0.36)	(0.19)	(0.33)
11.5 Hz	-3.48	-1.48	6.40
	(0.44)	(0.26)	(0.38)
15.2 Hz	-2.98	-0.60	6.38
	(0.38)	(0.22)	(0.56)

Table 2.2.1. Mean values in cm (± standard error) of x,y and z co-ordinates of ECDs calculated for SSVEPs at the three stimulation frequencies.

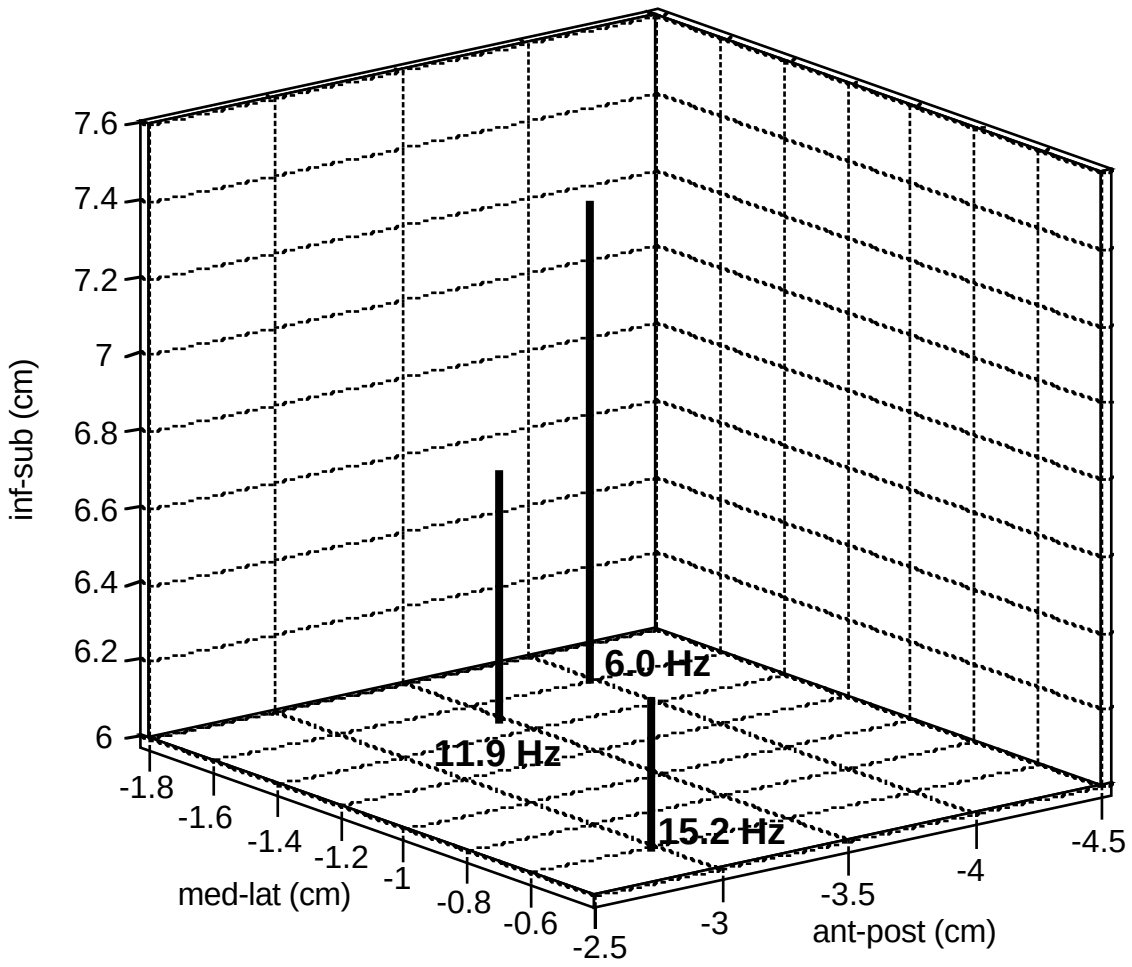

Figure 2.2.6. Mean locations of ECDs for the 6.0, 11.9 and 15.2 Hz SSVEFs over all subjects. The co-ordinate system of the source locations is described in the Methods section.

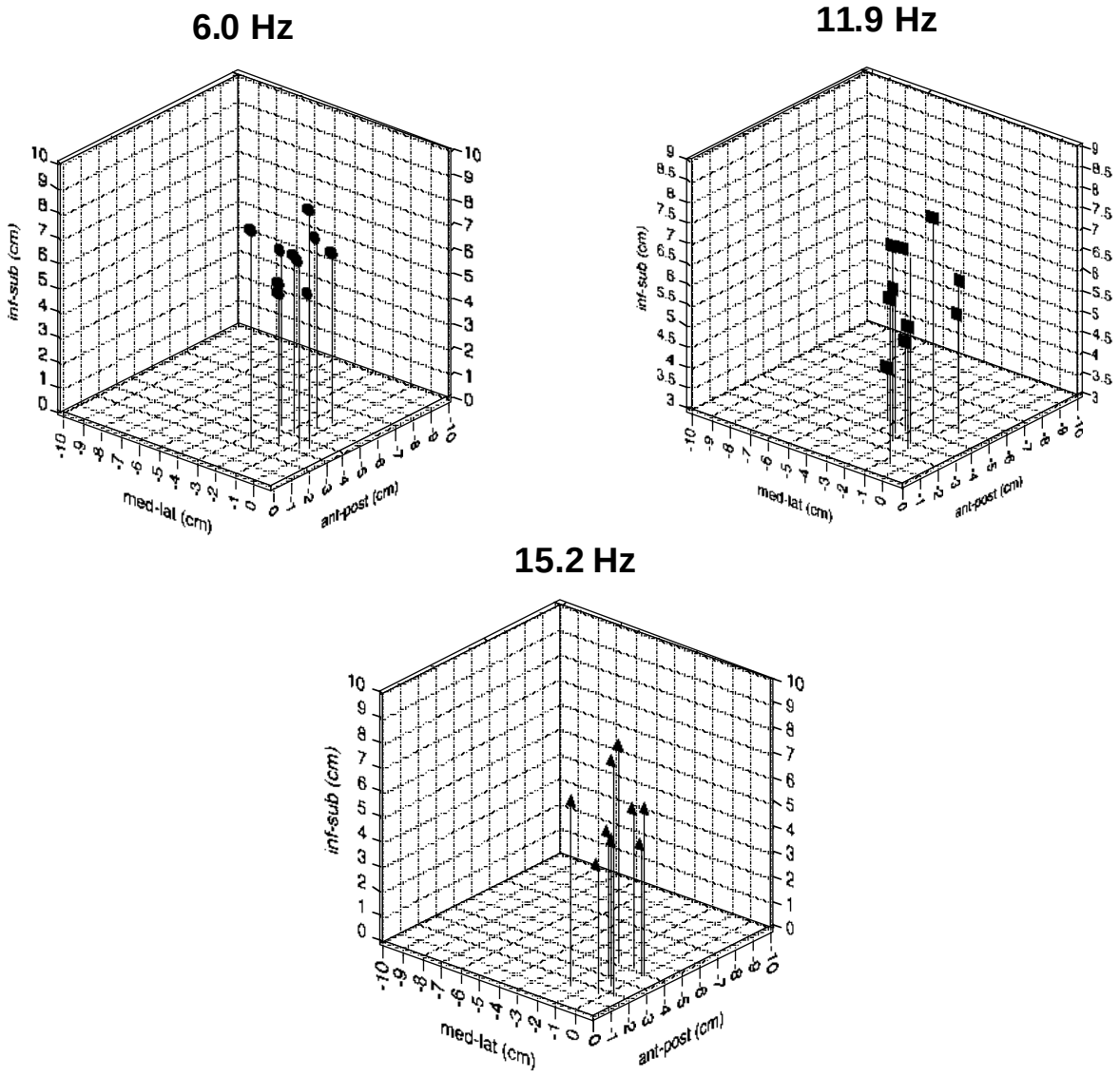

Figure 2.2.7. Locations of ECDs for each of the subjects for the 6.0, 11.9, and 15.2 Hz. SSVEFs over all subjects. The co-ordinate system of the source locations is described in the Methods section. Note: For the 15.2 Hz SSVEF only nine subjects were included in the analysis.

The mean location of the ECD for the 15.2 Hz response was situated medially and anteriorly with respect to the ECDs at the lower frequencies. These differences in dipole localization were reflected in significant effects of stimulus frequency along the medio-lateral (y) ($F(2,16) = 8.96$, $p < 0.05$) and anterior-posterior (x) ($F(2,16) = 5.63$, $p < 0.05$) axes, but not along the inferior-superior (z) axis ($F(2,16) = 2.37$, $p < 0.12$). Specific comparisons indicated that the ECD for the 15.2 Hz response was situated medially ($t(8) = 4.13$, $p < 0.01$) and anteriorly ($t(8) = 3.89$, $p < 0.01$) with respect to the 6.0 Hz ECD and medially with respect to the 11.9 Hz ECD ($t(8) = 2.55$, $p < 0.05$). Figure 2.2.8 shows the ECDs for each of the three stimulation frequencies

superimposed upon MRI sections in a representative subject whose ECD locations were closest to the group means.

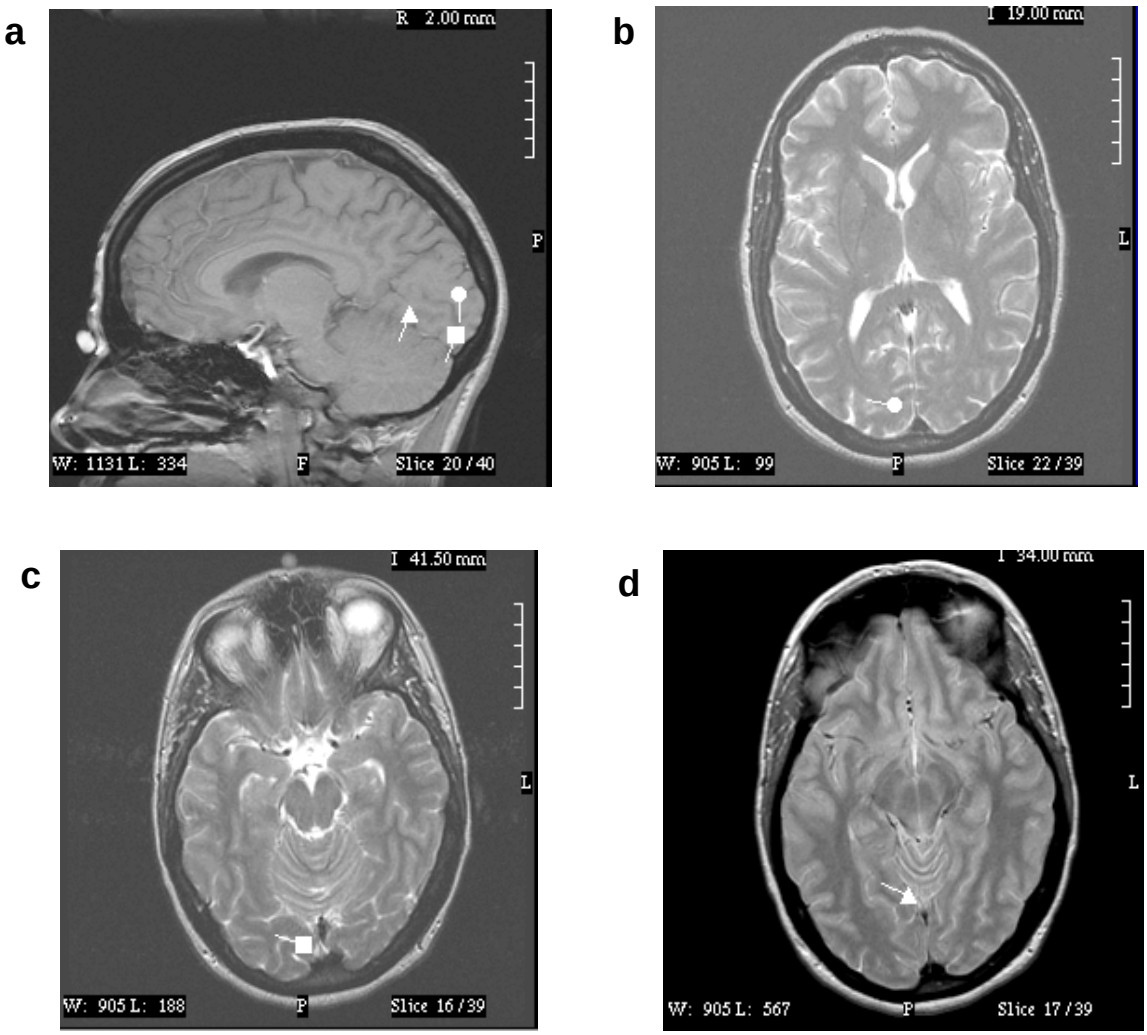

Figure 2.2.8. Superimposition of the calculated ECD locations for one subject upon corresponding sagittal (a) and axial (b-c) MRI sections. Circles indicate position of ECD for the 6.0 Hz response, squares the 11.9 Hz response, and triangles the 15.2 Hz response.

The ECDs for the 6.0 and 11.9 Hz responses were localized in the posterior occipital cortex near the calcarine fissure. The ECD for the 15.2 Hz response was situated anteriorly in the lingual gyrus, ventral to the calcarine fissure. The 6.0 Hz dipole was situated more dorsally than the dipoles for the higher frequencies. This was also the case in the two additional subjects from whom we obtained MRI scans, but as noted above, the inferior-superior differences as a function of frequency were not significant overall.

Conclusion

SSVEF topographies were found to have a dipolar form over the posterior scalp that could be well-modeled by a single ECD in every subject for the 6.0 and 11.9 Hz frequencies, and, in all but one subject, for 15.2 Hz. The localizations of the ECDs at each frequency were reasonably consistent across subjects, with standard errors ranging between 0.2-0.6 cm for the x,y, and z co-ordinates. The average position of the ECD for the 15.2 Hz response was found to be anterior and medial with respect to the ECDs for the lower frequency responses. Superimposition of dipole locations on appropriate MRI sections in a representative subject indicated that the 6.0 and 11.2 Hz ECDs were situated in posterior occipital cortex in the vicinity of the calcarine fissure (areas 17/18), whereas the ECD calculated for the 15.2 Hz response was positioned more anteriorly and ventromedially in the occipital cortex of the lingual gyrus. The ECDs at different frequencies also differed in their dipole moments, with the 6.0 Hz moment being larger than the 11.9 and 15.2 Hz moments; this may reflect a greater number of neural elements contributing to the lower frequency response (Williamson & Kaufman 1990; Elbert, Pantev, Wienbruch, Rockstroh, & Taub, 1995). The findings of experiment 2 give raise to the question of how the location of the ECDs will be distributed when stimulating with more and higher frequencies (see section 2.2.5 for a discussion).

2.2.3. Experiment 3

Recently it was shown that an irrelevant background steady-state stimulus, flickering with 8.6 Hz in the left and 12 Hz in the right visual hemifield, produced a SSVEP amplitude augmentation when attended as compared to the unattended condition (Morgan, et al., 1996). Experiment 3 was conducted to investigate whether higher frequency SSVEPs can also be modulated by spatial selective attention. On the basis of the findings of the Morgan et al. study an amplitude augmentation of SSVEPs was expected while the stimulus train is attended.

Methods

Subjects

Eleven healthy right-handed adults (5 female) with normal or corrected-to-normal vision served as paid volunteer subjects after giving informed consent. Their mean age was 22.9 (range 18 to 36) years.

Stimuli and Design

Two vertical rows ("bars") of 5 bicolor (red, green) LEDs each, were situated 5 degrees lateral to a central fixation point, one in the left visual field and one in the right visual field, centered on the horizontal meridian. Each bar subtended 3.45 x 0.5 degrees at a viewing distance of 58 cm.

Each trial began with the simultaneous onset of flickering of the two bars. All 5 LEDs in the left-field bar flickered synchronously at 20.8 Hz, and all 5 LEDs in the right bar flickered synchronously at 27.8 Hz. The two different stimulation frequencies were chosen for a better differentiation between effects in the respective hemifield. The on-off duty cycles were 50/50 for both frequencies, and the "on" luminance was 2.5 cd/m^2 against a background luminance of 0.25 cd/m^2. An attention-directing cue appeared 1296 msec after flicker onset. This consisted of a small LED situated 0.4 degrees to the left or to the right of the fixation point, which indicated which of the bars was to be attended on that trial. Both the cue and the flickering bars were then kept on for a 10 sec period, during which the subject attempted to detect color-change targets in the flickering bar on the side indicated by the cue. During task performance, the subject was required to maintain gaze fixation on the central point.

For most of the 10 sec period, the LEDs flickered in red. At randomly chosen intervals of 576, 720, or 884 msec (onset to onset), two of the LEDs in one of the bars changed from red to green for 144 msec. These color changes could occur in the right or left bar with equal probability. Also, the two changing LEDs could be located either at the top and middle, the bottom and middle, or the top and bottom, again equiprobably. The 144 msec color change in the top and bottom LEDs on the attended side was defined as the target to which the subject responded as quickly as possible by pressing a button. The responding hand was changed half way through the experiment, and the

sequence of hand usage was counterbalanced across subjects. Figure 2.2.8 illustrates the display and the task.

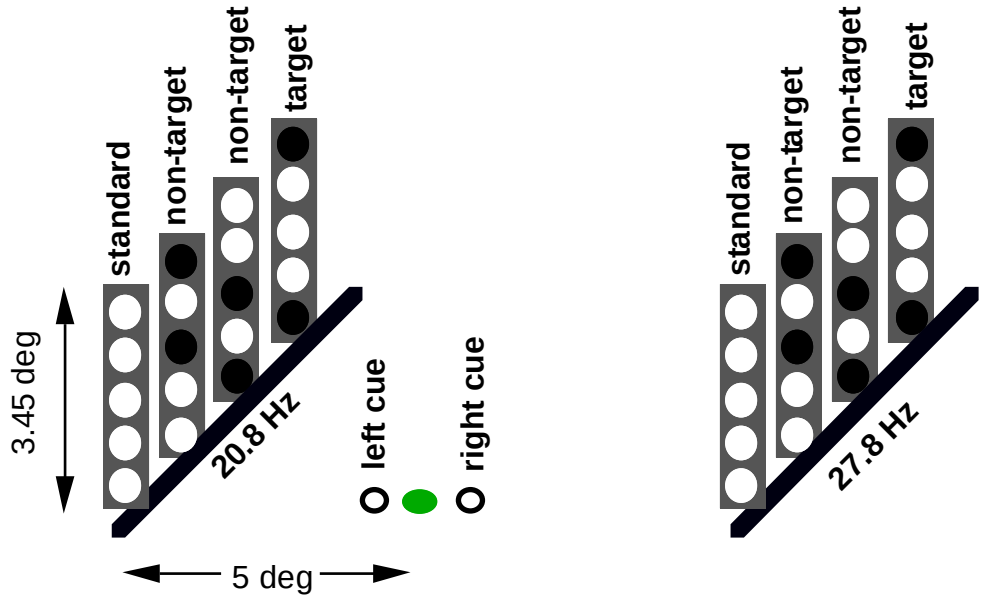

Figure 2.2.8. Illustration of the display and the task of the SSVEP spatial selective attention experiment.

The experiment consisted of 200 individual trials, each of 11,296 ms duration, presented in blocks of 10 trials each. Inter-trial intervals were 10-15 s long, with longer rest periods after each block. Behavioral performance was monitored on-line, and subjects received feedback on the percent correct target detections after each block.

SSVEP Recording

Brain electrical activity and EOG recordings were recorded in a manner identical to experiment 1 (see Figure 2.2.1 and 2.2.8). Electrode impedances were kept below 5kOhms. All channels were recorded with a bandpass of 0.3-300 Hz, except for the horizontal EOG, where the bandpass was 0.01-100 Hz. Signals in all channels were digitized at 1000 Hz and stored on disk for off-line analysis.

SSVEP Analysis

Individual trials were rejected from further analysis on the basis of blink or EMG artifacts in the scalp channels or lateral eye movements revealed in

the horizontal EOG. The rejection criterion for horizontal EOG deflections was identical to experiment 1, i.e., the averaged deviation from baseline was less than 5 μV (0.5 degree shift in lateral gaze) during the 10 sec period. One subject was totally excluded from further analysis due to too many artifacts. For the remaining 10 subjects, the mean rejection rate was 29% of attend-right trials and 27% of attend-left trials.

The SSVEPs to the concurrent left and right field flashes were averaged separately in the time domain using a moving window technique. The first step was to average the 11,296 ms epochs of EEG obtained on artifact-free trials for the cue-left and cue-right trials separately. For each of these averages two moving window averages were obtained to extract the 20.8 and 27.8 Hz SSVEPs. Beginning with cue onset, a moving 1200 ms epoch was synchronized to begin at each flash in the sequence at one of the frequencies. These successive epochs were then averaged across the entire 10 sec post cue epoch. The moving window averaging was then carried out for the other frequency, resulting in a total of four averaged SSVEP waveforms (attend left/right, 20.8/27.8 Hz) for each electrode site. These averages were then algebraically re-referenced to averaged mastoids by subtending 1/2 of the averaged signal recorded from the left mastoid from the averaged signals at each scalp site.

To obtain amplitude and phase values of SSVEP activity in the frequency domain, each re-referenced waveform was subjected to a Fast Fourier Transform (FFT) at the appropriate frequency. To minimize "spectral leakage", the FFTs for the 20.8 Hz responses were calculated over 1152 ms epochs (24 cycles) and for the 28.8 Hz responses over 1188 ms epochs (33 cycles). These epochs were expanded to 2048-point data arrays using spline-fitting routines Press, Teukolsky, Vetterling, & Flannery, 1992), and FFTs were performed on these arrays. SSVEP amplitudes were calculated in microvolts as the square root of the sum of the sequences of the real and imaginary components.

Statistical Analysis

SSVEP amplitudes and phases were subjected to repeated-measure analyses of variance with factors STIMULUS SIDE (left versus right), ATTENTION (attended versus unattended side), HEMISPHERE of recording (ipsilateral versus contralateral to the stimulus side) and SCALP SITE within

hemisphere (F7/8, F3/4, C3/4, CT5/6, CP1/2, T5/6, P3/4, TO1/2, PO1/2, IN3/4, O1/2). Reported p-values were adjusted by the Huynh-Feldt-epsilon procedure were necessary. Post hoc tests were carried out using paired t-tests adjusted by the Bonferroni-Dunn criterion. Means and standard errors are presented.

Isocontour maps of voltage were calculated for the SSVEP amplitude values using the spherical spline algorithm of Perrin, Pernier, Bertrand, and Echallier (1989). For comparing SSVEP scalp distributions between attention conditions, the amplitude values were normalized using with a procedure described by McCarthy and Wood (1985) and subjected to analysis of variance with the factors listed above. Additional comparisons of scalp distributions were carried out for the normalized amplitude values averaged over anterior (F7/8, F3/4, T3/4, C3/4, CT5/6, CP1/2) and posterior (T5/6, P3/4, TO1/2, PO1/2, IN3/4, O1/2) electrode sites.

Results

As indicated by the behavioral data, it seemed that subjects found the color-shift targets easier to detect for the right flickering bar (27.8 Hz) than for the left bar (20.8 Hz). Correct detections averaged 76 ± 4.7% for the right targets and 59 ±5.4% for the left targets ($t(9) = 6.04$, $p < 0.001$); corresponding reaction times for correct detections were 428 ± 22 ms (right) and 481 ± 15 ms (left) ($t(9) = 4.32$, $p < 0.01$).

For both left and right field flickering stimuli, the SSVEP showed substantial amplitude increases when attention was directed towards that stimulus as compared to when the stimulus in the opposite field was attended. Averaged SSVEP waveforms from a representative subject are shown in Figures 2.2.9 and 2.2.10. Mean SSVEP amplitudes over all subjects (calculated in the frequency domain) are given in Figures 2.2.11 and 2.2.12.

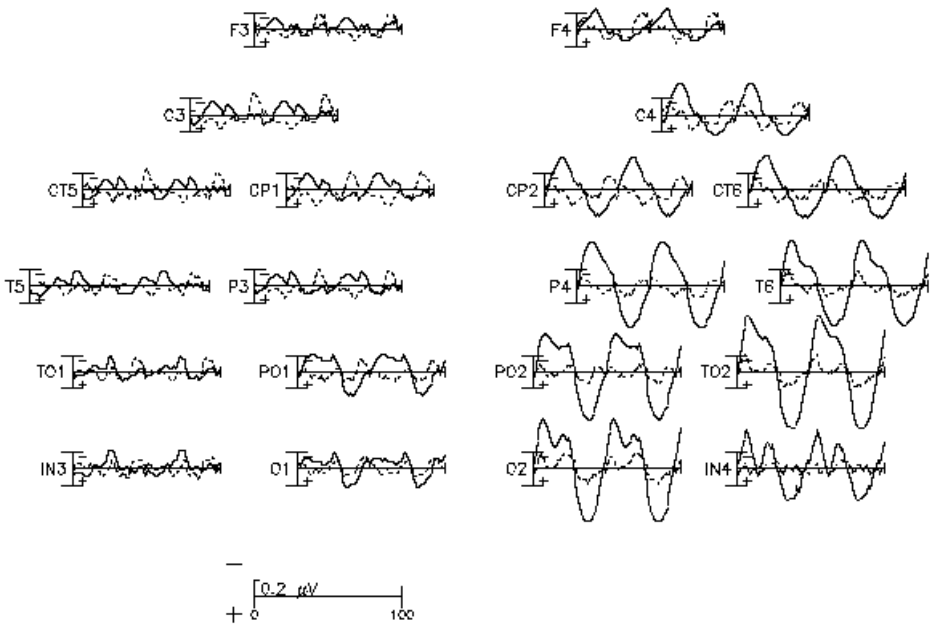

Figure 2.2.9. SSVEP waveforms from subject J.O., averaged using a moving window technique, in response to the flickering bar in the left visual field (20.8 Hz). The "attended" waveforms (solid lines) were recorded on trials when the left field stimuli were attended and the "unattended" waveforms (dotted lines) on trials when the right field stimuli were attended. Waveforms from 20 of the 30 scalp sites are shown, referenced to the algebraic average of the left and right mastoids.

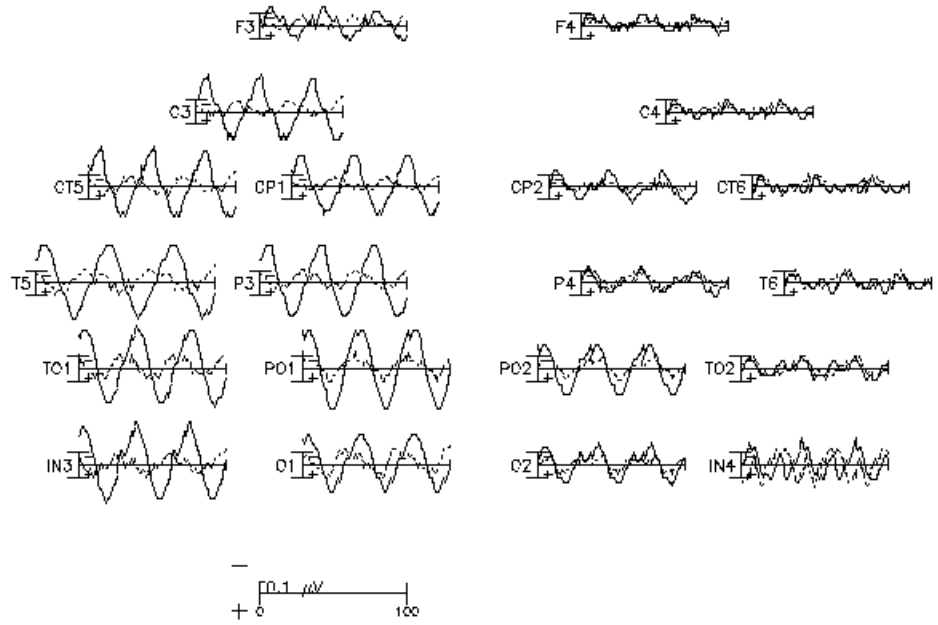

Figure 2.2.10. Same as Figure 2.2.9 for SSVEPs in response to the flickering bar in the right visual field (27.8 Hz).

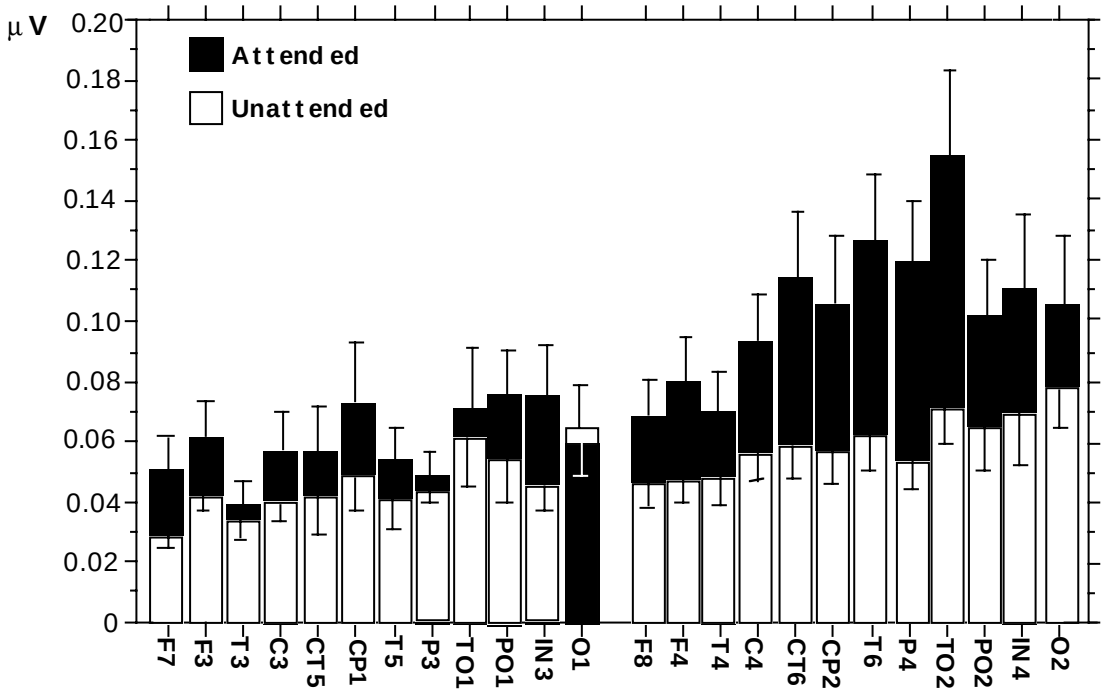

Figure 2.2.11. Mean SSVEP amplitudes over all subjects (with standard errors) at each scalp site in response to left field (20.8 Hz) stimuli. Amplitudes were calculated on the basis of FFTs at the driving stimulus frequency. Total bar height is attended amplitude (i.e., during attend-left condition) and white bar height is unattended amplitude (attend-right condition). Thus, the dark portion of bar equals increment in amplitude with attention. At site 01, however, the unattended amplitude was greater than the attended.

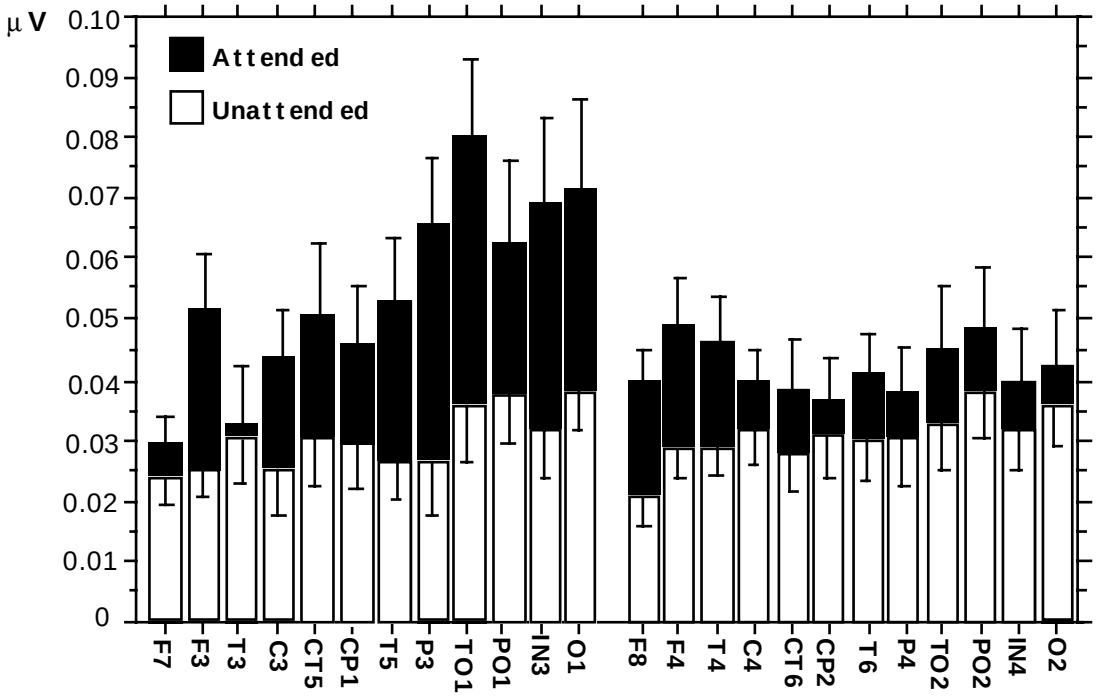

Figure 2.2.12. Same as Figure 2.2.11 for SSVEPs to right field (27.8 Hz) stimuli.

Although the overall SSVEP amplitudes were larger for the 20.8 Hz flicker than the 27.8 Hz flicker (STIMULUS SIDE, $F(1,9) = 27.9$, $p < 0.001$), the proportional enlargement of SSVEP amplitude with attention was similar for both frequencies and amounted to an approximate doubling of SSVEP amplitude over the posterior scalp contralateral to the side of the stimulus.

Statistical analysis showed a significant overall increase in SSVEP amplitude with attention ($F(1,9) = 14.9$, $p < 0.005$), and this increase was greater for the hemisphere contralateral to the field of stimulation (ATTENTION x HEMISPHERE, $F(1,9) = 5.31$, $p < 0.05$), more so for posterior than anterior electrode sites (ATTENTION x HEMISPHERE x SCALP SITE, $F(11,99) = 3.03$, $p < 0.05$ with Huynh-Feldt correction). The attention effects at individual scalp sites were evaluated by t-tests with Bonferroni-Dunn adjustment. For the left stimulus, significant SSVEP enhancement was found at sites C4, CT6, CP2, T6, P4 and TO2 (all ps < 0.05), and for the right stimulus the enhancement was significant at sites F3, C3, CT5, PO1, and O1 (all ps < 0.05) and at T5, P3, TO1, as well as IN3 (all ps < 0.01).

As can be seen in Figures 2.2.9 and 2.2.10, there were attention effects on SSVEP phase as well as amplitude. Due to inter-individual variability, however, phase changes were not significant and will not be considered further in this report.

The scalp distributions of the attended and unattended SSVEP amplitudes averaged over all subjects are shown in Figure 2.2.12.

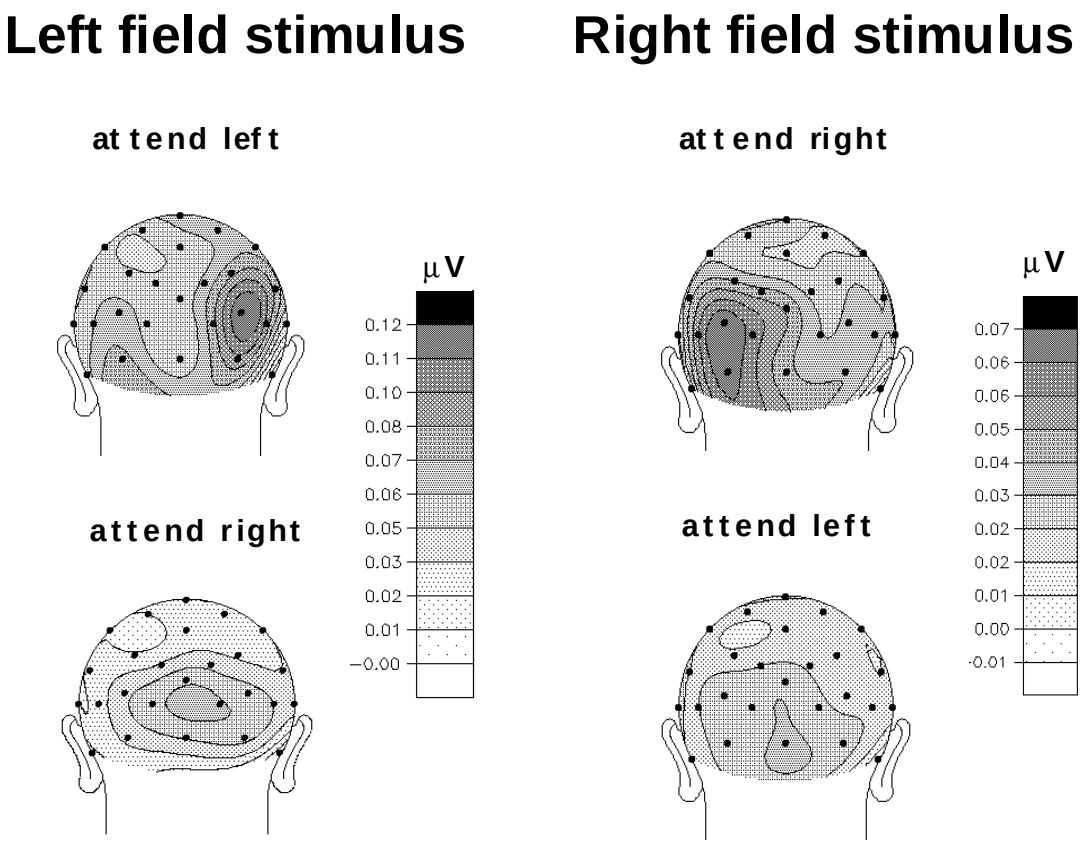

Figure 2.2.12. Grand-average scalp distributions of SSVEP amplitudes to left and right field stimuli. Amplitudes were calculated from FFTs at each scalp site in each subject and averaged over all subjects.

For both frequencies of stimulation, the unattended SSVEPs were largest around midline posterior scalp sites, whereas the attended SSVEPs showed a more focal distribution over the contralateral posterior scalp. This distributional difference was reflected in a significant ATTENTION x HEMISPHERE x SCALP SITE interaction ($F(11,99) = 3.64$, $p < 0.01$ with Huynh-Feldt correction) in the ANOVA of scalp amplitudes normalized by the procedure of McCarthy and Wood (1985).

The difference between attended and unattended scalp distributions was evaluated further by specific comparisons in which the normalized amplitudes were averaged in groups of 6 anterior and 6 posterior sites for each hemisphere (see Methods). At the contralateral posterior sites, the SSVEP amplitudes were larger in response to attended than unattended stimuli ($t(9) = 2.32$, $p < 0.05$), but no such attention effect was seen for the anterior sites ($t(9) = 0.29$, n.s.). In addition, at the posterior sites, the contralateral amplitudes were much larger than ipsilateral amplitudes in

response to the attended stimulus ($t(9) = 6.72$, $p < 0.001$), but not in response to the unattended stimulus ($t(9) = 1.36$, n.s.).

As shown in Figure 2.2.12, these attention-related changes in SSVEP voltage distribution were very similar for the right and left field stimuli (STIMULUS SIDE x ATTENTION x HEMISPHERE x SCALP SITE, $F(11,99) = 1.35$, n.s.).

Conclusion

The high frequency SSVEP was modulated by spatial selective attention. This holds for both the 20.8 and 27.8 Hz SSVEP. Although the amplitude for the 20.8 Hz SSVEP was larger as compared to the 27.8 Hz SSVEP, the proportional increase of SSVEP amplitude with attention was similar for both frequencies and amounted to an approximate doubling of SSVEP amplitude over the posterior scalp contralateral to the side of the stimulus. These topographical features were confirmed by testing the topography by means of normalized amplitudes. On the basis of the amplitude topography it seems obvious that the main source of the higher frequency SSVEPs are not in the primary visual cortex but in extrastriatal locations, which was also confirmed by an additional analysis (see section 3).

2.2.4. Experiment 4

In experiment 4, the high frequency SSVEP was used to measure the time course of the attentional shifting. On the basis of the results of experiment 3, which concluded that attending to a flickering bar produces almost a doubling in amplitude as compared to not attending to the same bar, we hypothesized that the time between the cue, indicating to which side the subject has to attend to, and the first time point of a significant SSVEP amplitude increase as compared to baseline might serve as a good marker of how long it takes for the brain to shift from one task to another. In addition, we measured the behavioral response (percentage of correct responses) as an additional marker for the time point at which subjects reach their maximum performance level. On the basis of the findings with regard to the attentional blink (see section 1.1.3) a correlation between behavioral performance and SSVEP amplitude increase was expected.

Methods

Subjects

In order to find subjects which show a clear SSVEP, we first screened 15 subjects. Of these 15, 10 subjects (three females; mean age 22 years) showed a clear SSVEP and were therefore asked to participate in the study. All subjects had normal or corrected-to-normal vision and were paid for participation after informed consent was obtained.

Stimuli and Design

Stimuli and task were identical to experiment 3 except for three differences in the design. First, to obtain more trials for analysis time locked to the attention direction cue, the task period was shortened to 3 s. Therefore, 250 trials were presented for each condition (attend left, right) in about the same time period for the whole experiment as for experiment 3. Second, targets and non-targets were presented with a stimulus onset asynchrony (SOA) of 400 to 700 ms (onset to onset) to assure that targets were presented with an equal probability over all trials in the whole three seconds task period in order to allow for the comparison between EEG and behavioral measures. Third, the experiment was divided into blocks of 25 trials each (resulting in 20 blocks) with subjects receiving an additional 50 cents reward if they detected at least 80% of the targets in one block in order to maintain motivation to detect targets. As in experiment 3, the responding hand was changed half way through the experiment, and the sequence of hand usage was counterbalanced across subjects.

SSVEP Recording

Brain electrical activity was recorded in a manner identical to experiment 1 and 4 (see Figure 2.2.1 and 2.2.8) with the exception that sampling rate was 250 Hz and channels were recorded with a bandpass of 0.3-100 Hz except for the horizontal EOG where the bandpass was 0.01-100 Hz.

SSVEP Analysis

As in the previous experiments, trials with blinks, EMG artifacts and lateral eye movements exceeding 0.5 deg of lateral shift were excluded from further

analysis. This lead to the exclusion of one subject. For the remaining 9 subjects, the mean rejection rate of attend-right trials and attend-left trials was 13.5% and 13.9%, respectively.

Trials for each condition were averaged time locked to the attention cue onset for an epoch exceeding 1000 ms before and 3000 ms after cue onset. Time domain averages were then algebracially re-referenced to averaged mastoids and transformed into the frequency domain by means of a sliding window Fast Fourrier Transform (FFT), restricted to the stimulus frequency with a window lenght of ten cycles. This resulted in a window lenght of 480 ms for the left and 360 ms for the right bar. The respective imaginary and real components were stored at the leading edge of the sliding window and amplitudes were calculated in microvolts as the square root of the sum of the squared real and imaginary components. FFT-windows were slid from data point to the next data point, to obtain the time course of amplitude in the frequency domain. Due to the window length of 480 ms for the 20.8 Hz response, the analysis epoch was defined as 1000 ms prior to cue onset until 2500 ms after cue onset for both (left/right) responses.

Behavioral Data Analysis

A correct response was defined as a botton press in a time period of 200 to 1200 ms after target onset. Due to the duration of 144 ms for targets and non-targets, the best time resolution for which all time bins had a target was 144 ms. Therefore the percentage of correct responses to targets was calculated for 144 ms time bins over a period starting at cue-onset to 2448 ms after cue-onset, resulting in 17 windows[2]. In addition, the overall percentage of correct responses and the overall reaction time was calculated for left and right targets, respectively.

Statistical Analysis

For statistical analysis, the electrode pair with the most pronounced SSVEP was chosen. As in experiment 3, electrodes TO1, TO2 exhibited the largest

[2] To avoid overlap the first time bin was defined as 0 to 143 ms after cue-onset, the second from 144 to 287 ms, etc.. We also tested the distribution of correct responses with respect to the 144 ms windows. We found no difference since an overlap could only occurre if a target occured at exactly the common time point e.g. at time point 144 ms, 288 ms and so one. This was obviously never the case.

SSVEP amplitudes (see Figure 2.2.11 and 2.2.12). To demonstrate the relationship between cortical and behavioral responses, the time course of the baseline corrected SSVEP amplitude of electrodes TO2 and TO1 was then divided into 144 ms bins, beginning at 432 ms prior to attention-cue onset. The 144 ms time bin in the frequency domain corresponds to an epoch of 624 ms for TO1 (left bar) and 504 ms for TO2 (right bar) in the time domain. The baseline was calculated as the mean frequency domain amplitude from 1000 to 500 ms before attention-cue onset.

Since the main purpose of the present study was to find the time point at which the amplitude of the attended condition significantly exceeds the baseline level, the first three 144 ms time bins were further divided into 48 ms pieces to obtain a finer time resolution for the cortical data. The mean amplitude of each 48 ms piece was subject to a one-group t-test. The remaining 144 ms time bins (432-2448 ms) were then subject to a 3 factor repeated measurement ANOVA (T02/TO1 x TIME BIN x ATTENTION). Reported p-values were adjusted by the Huynh-Feldt-epsilon procedure were necessary.

With respect to the behavioral data, mean reaction time and overall percentage of correct responses were tested by paired t-tests. To identify the time bin at which subjects have reached their maximum performance level (i.e. no significant increase of percentage of correct responses from one time bin to the next), the time bins were tested by means of paired t-tests for left and right targets, respectively. To test the relation between behavioral and cortical data, the time bin in which a subject reached maximum performance was correlated with the peak amplitude of the SSVEP. Correlation coefficients underwent a z-transformation for statistical analysis. Means and standard errors are presented for both EEG and behavioral data.

Results

In the top panel of Figure 2.2.13 an example of an averaged evoked response time locked to the attention-cue onset for a single subject for the attend right condition is presented. The expanded time scale depicts the SSVEP for the attended (bold) and unattended (thin line) condition in the time window of 1500 to 2500 ms after cue onset. The lower panel depicts the baseline corrected time course of the SSVEP amplitude in the frequency domain for the attended and unattended condition (same subject).

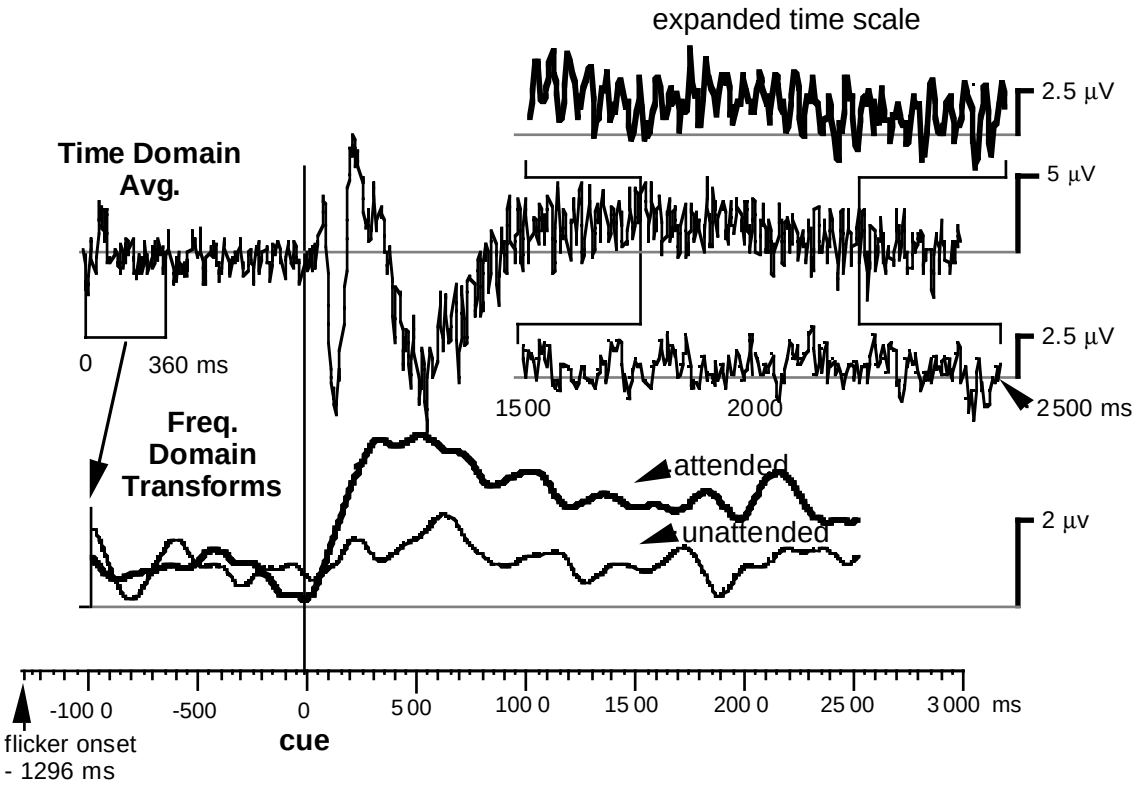

Figure 2.2.13. Top panel: Example of an averaged evoked response time locked to the attention-cue onset for a single subject for the attend right condition. The expanded time scale shows the SSVEP for the attended (bold) and unattended (thin line) condition. *Note:* Positive values are plotted upwards. *Lower panel:* Baseline corrected time course of the SSVEP in the frequency domain for the same subject for the attended (bold) and unattended (thin line) condition.

In the top panel, Figure 2.2.14 presents the baseline corrected grand mean amplitude time course for TO2 (left bar) and the percentage of correct responses to left targets in 17 time windows 144 ms each (lower panel). In Figure 2.2.15 the same is shown for TO1 (right bar).

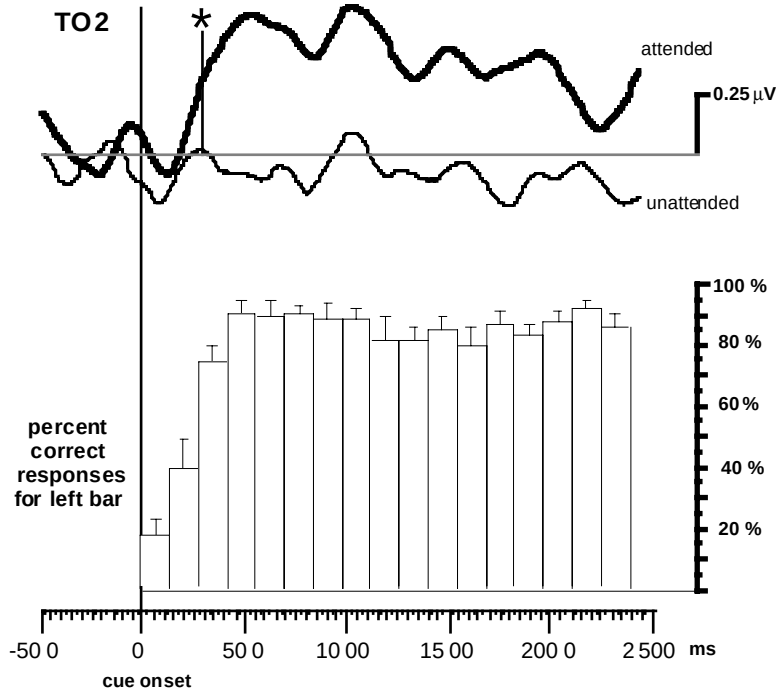

Figure 2.2.14. Top panel: Baseline corrected grand mean time course of SSVEP amplitude in the frequency domain for TO2. The vertical line marks the time point from which the attended amplitude differs significantly from baseline values. *Lower panel:* Percentage of correct responses for left targets in 144 ms time bins.

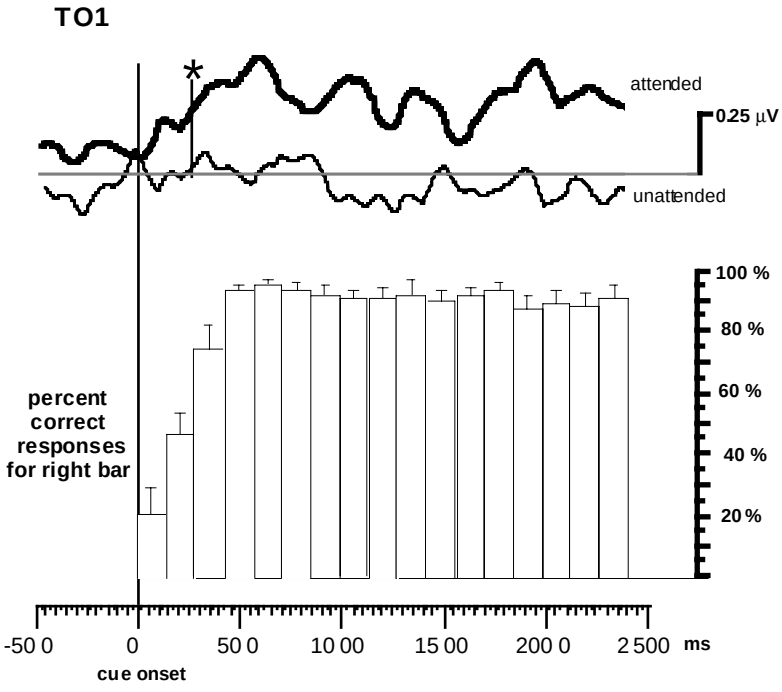

Figure 2.2.15. Same as Figure 2.2.14 for TO1 (right bar).

As apparent from Figures 2.2.14 and 2.2.15, the 20.8 Hz SSVEP again had a larger amplitude than the 27.8 Hz SSVEP. The grand mean slope of the TO1 response in the attended condition was less steep than the TO2 response. However, for the 20.8 and the 27.8 Hz stimulus, the attended condition resulted in a marked higher amplitude than the unattended condition, and, in the time course, the unattended condition maintained approximately baseline level. The first 48 ms time bin for TO2 (attending to the left stimulus), which differed significantly from baseline, was the 288-356 ms time bin ($t(8)= 2.65$, $p < 0.05$), which corresponds to 288-836 ms in the time domain. This time point is marked by the vertical line in Figure 2.2.14, panel (A). With respect to TO1 (attending to the right stimulus), the first significant time bin was the 240-288 ms bin($t(8)= 2.33$, $p < 0.05$), which corresponds to 240-648 ms in the time domain. This time point is marked by the vertical line in Figure 2.2.15, panel (A). For both electrodes, the following 48 ms time bins (up to time bin 432 ms) revealed a significant amplitude augmentation as compared to baseline. For the remaining time bins (432 to 2448 ms), a highly significant ATTENTION main effect ($F(1,8) = 41.85$, $p = 0.0002$) was found.

With respect to the behavioral data, the test of mean reaction times revealed significantly slower reaction times for left targets ($M = 455.1 \pm 14.7$ ms) than for right targets ($M = 438.3 \pm 12$ ms; $t(8) = 2.9$, $p < 0.02$). The difference between left and right targets was also maintained with respect to overall correct responses. On the left side, subjects had significantly less correct responses ($M = 78.2 \pm 2.9\%$) than on the right stimulation side ($M = 84.3 \pm 3\%$; $t(8) = 2.8$, $p < 0.03$).

For the left and right bar, the percentage of correct responses increased significantly until 432 ms after cue onset (Figure 2.2.14, 2.2.15, panel (B)). For the left bar, the average increase of correct responses from the first (0-144 ms) to the second time bin (144-288 ms) was 21.5% ($t(8) = 3.36$, $p = 0.009$), from the second to the third (288-432 ms) 34.8% ($t(8) = 4.53$, $p = 0.002$), and from the third to the fourth (432-576 ms) 16.6% ($t(8) = 6.72$, $p = 0.0001$). For the right bar, the average increase of correct responses from the first to the second time bin was 26.3% ($t(8) = 4.44$, $p = 0.002$), from the second to the third 29.2% ($t(8) = 4.2$, $p = 0.003$), and from the third to the fourth 17.9% ($t(8) = 2.92$, $p = 0.02$). Thus, after 432 ms subjects reached their best performance for left and right targets with only marginal fluctuations for the remaining task period. However, subjects differed in the slope of reaching their maximum

performance level at time bin 432-572 ms which was also related to the latency of SSVEP-amplitude maximum. The correlation between the latency of the peak of SSVEP-amplitude and the time bin for best performance was highly significant for the left ($r = 0.78$, $z = 2.5$, $p = 0.01$) and the right bar ($r = 0.80$, $z = 2.7$, $p = 0.008$).

A grouping into 4 fast and 4 slow responding subjects on the basis of the performance data provided also a different time course of the SSVEP amplitude between these two groups. Figure 2.2.16 depicts the first 1576 ms of the SSVEP-amplitude and the respective time bins for the behavioral data for fast and slow reacting subjects as defined by the steepness of the slope of the time needed to reach maximal performance. Figure 2.2.17 depicts the same for the right bar.

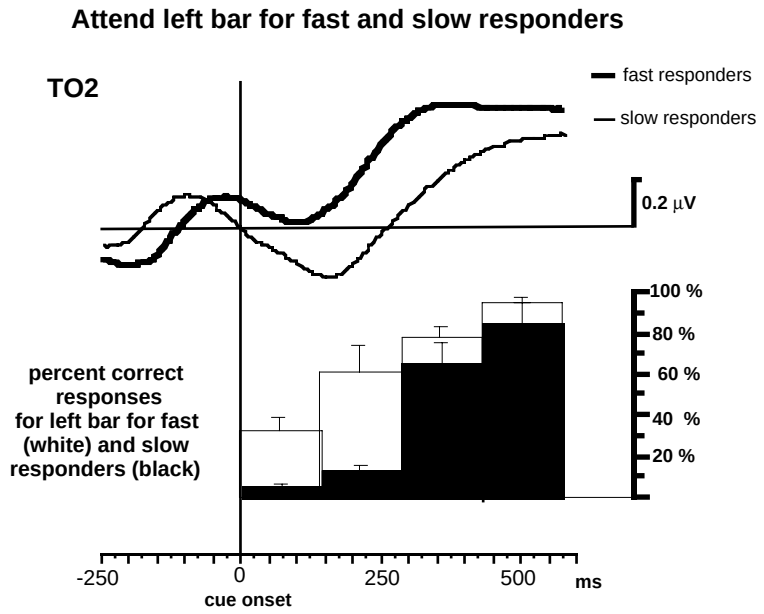

Figure 2.2.16. Time course of SSVEP-amplitude for electrode TO2 for four fast (bold line) and four slow reacting subjects (thin line). The white bars represent the average percentage (+ standard error) of correct responses for the left bar for fast subjects for the respective 144 ms bin. The black bars show the same for the slow reacting subjects.

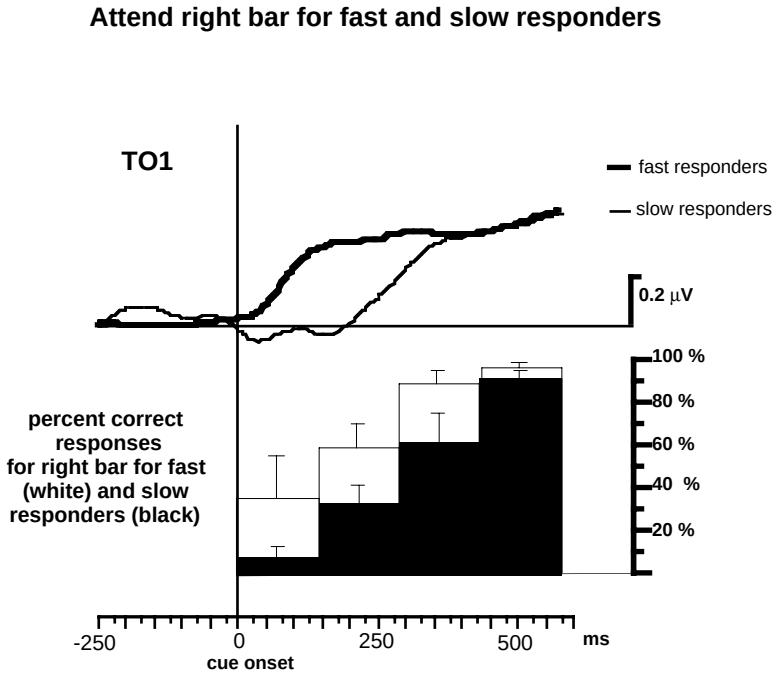

Figure 2.2.17. Same as Figure 2.2.16 for right bar targets.

As can be seen in Figure 2.2.16 and 2.2.17, on the average the peak of SSVEP-amplitude was earlier for fast as compared to slow responding subjects, which was the case for the left (327 ms vs. 522 ms, $(t(6) = 2.65, p < 0.05)$ and right stimulation side (182 ms vs. 451 ms, $t(6) = 3.21$, $p < 0.05$; time points refer to frequency domain data).

Conclusion

Experiment 4 demonstrates that the SSVEP can serve as a useful tool to investigate the *temporal* characteristics of visual spatial attention. The course of SSVEP-amplitude increase was highly correlated with the behavioral performance data. Fast reacting subjects reached a particular performance level one time bin before the slow reacting subjects, which was roughly the delay of the SSVEP-amplitude point of inflexion. In addition, fast responding subjects had a shorter latency of the peak of the SSVEP-amplitude for the attended condition. Thus, the current approach has shown that the time the brain needs to shift from one task to another can be measured by means of EEG. These results also indicate that the shifting time can not be seen as a time constant in the brain. It is more likely that this time is dependent on processes like attention, difficulty of task and, probably, individual experience with a task (see also section 3).

2.2.5. General summary and discussion of experiments 1 to 4

Unlike auditory SSRs, visual SSRs can be elicited over a broad range of frequencies, indicating a fundamental difference to the auditory SSR. In the current work, stimulation frequencies up to 50 Hz were tested (6.0, 8.9, 11.9, 17.9, 26.3, 31.3, 35.7, 41.6, 45.5, and50 Hz), which elicited a clear SSVEP.

Regan (1989) separated the SSVEPs into three frequency bands with amplitude maxima in the low (5-12 Hz), medium (12-25 Hz) and high (30-50 Hz) frequency band. Only a few studies, however, have investigated the neural generators of the various types of SSVEPs. In experiment 2, it was, therefore, investigated whether consistent localizations of equivalent current dipole sources could be obtained across subjects for SSVEFs at three different stimulation frequencies (6.0, 11.9, and 15.2 Hz), and to see whether these ECD localizations varied systematically as a function of frequency.

The ECDs were reasonably consistent across subjects and the average 15.2 Hz response was found in the occipital cortex of the lingual gyrus, which was more anteriorly and ventromedially as compared to the 6.0 Hz and 11.9 Hz ECD, which were situated in the posterior occipital cortex in the vicinity of the calcarine fissure. The observed differences in localization among the ECDs at different frequencies suggest a differential activation of anatomically separate components of the visual pathways. These differences may correspond to the separate frequency bands of the SSVEP that Regan (1989) has identified. The 6.0 and 11.9 Hz responses would clearly belong to Regan's low-frequency band, whereas the 15.2 Hz response would fall more within the medium-frequency band. It also seems likely that high frequency flickers would preferentially activate the magnocellular (M) visual pathways, whereas lower frequencies would produce relatively greater activity in parvocellular (P) pathways (Silberstein, 1995), because cells of the M pathway respond in contrast to cells of the P pathway faster and more transiently (Livingstone & Hubel, 1988). Anatomical differences between the M and P cell projections might then contribute to differences in the SSVEF dipole moments and localizations.

The present MEG recordings undoubtedly provide a simplified and incomplete picture of the neural generators of steady-state visual evoked

activity. Although a single ECD model almost invariably provided an excellent fit to the limited portion of the posterior SSVEF topography that was recorded by the 37-sensor array, there is good evidence that multiple sources are generally activated by repetitive flickering stimuli (Silberstein, 1995). Accordingly, it seems likely that our posterior MEG recordings only registered a subset of tangentially oriented sources that were most strongly activated by a given stimulus frequency. The goodness of fit achieved by the single ECD model, however, suggests that a single dipolar source dominated the SSVEF topography in nearly every case. The ability of MEG recordings to reveal consistent, frequency-selective SSVEF sources suggests a wider application of these methods in studies of normal and abnormal visual system functioning.

In experiment 3, it was demonstrated that the SSVEP to flicker in the frequency range 20-28 Hz (Regan's "medium frequency" band) is highly sensitive to spatially focused attention. When attention was directed to a LED display flickering at either 20.8 or 27.8 Hz in one visual field, the SSVEP driven by the attended flicker was substantially increased in amplitude (by about a factor of two at posterior, contralateral scalp sites) compared to when the display in the opposite field was attended. This attention-related increase was similar in magnitude (percentage wise) and in scalp topography for the 20.8 and 27.8 Hz responses, although the baseline amplitudes were considerably smaller at the higher frequency.

The present data extend previous observations of spatial attention effects on SSVEPs to low frequency (8.6/12 Hz) flicker (Morgan, et al., 1996; Hillyard, et al., in press). These previous studies differed substantially, however, in design as well as in flicker frequency from the present experiment. Whereas the flickering stimuli themselves were task-relevant and attended in the present study, in the preceding studies the 8.6/12 Hz flicker was an irrelevant background upon which the task-relevant stimuli (alphanumeric characters) were superimposed. The fact that similar attentional modulations (amplitude increases of 70-110%) were observed under these diverse conditions suggests that the SSVEP may serve as a general index of the spatial focusing of attention regardless of whether the flickering stimulus is task-relevant.

The scalp distribution of the attention-related increases in the 20.8 and 27.8 Hz SSVEP showed a narrow focus over the occipito-parietal scalp contralateral to the visual field of stimulation. This contrasts with the more broadly distributed SSVEP attention effect reported for 8.6/12 Hz flicker (Morgan, et al., 1996; Hillyard, et al., in press), which was less strongly contralateral and larger overall at right hemisphere recording sites. Dipole modeling of the 8.6 and 12 Hz SSVEP distributions along with observations of fMRI activation patterns suggest that the attentional modulation of this low-frequency flicker-evoked activity was occurring in ventral and lateral extrastriate visual areas in occipital and occipto-temporal cortex (Hillyard, et al., in press).

The finding that the SSVEP to 20-28 Hz stimuli can be modulated by attention opened the possibility of using this modulation to track the time course of attentional shifts between flickering sources, which was investigated in experiment 4. As has discussed in the "Introduction" section (see 1.1.3), the temporal characteristics of visual attention have only been investigated by means of reaction time and target detection experiments. The so-called "attentional blink" (Raymond, Shapiro, & Arnell, 1992) was dependent on the difficulty to detect a second probe after a target and not on the difficulty to detect the first target. The time span of the attentional blink varied between 350 and 600 ms (Broadbent & Broadbent, 1987; Raymond, et al., 1992; Shapiro, Raymond, & Arnell, 1994; Weichselgartner & Sperling, 1987). Consistent to previous findings, the latency of best accuracy in target detection of experiment 4 was in the 432 to 572 ms time bin.

Shapiro, Caldwell, and Sorensen (1997) recently demonstrated once again that the attentional blink is not related to the difficulty to target detection (Shapiro, et al., 1994), which would relate to process one in the Weichselgartner and Sperling (1987) model (see 1.1.3), but varies dramatically with the difficulty to detect a stimulus following the target. In these experiments, the second target probe was either the subjects own name, another name, or a specified noun from a stream of distractor nouns. Subjects exhibited almost no attentional blink when the second probe was their own name, but the authors found the usual attentional blink, when another name or a noun was used as the second probe (Shapiro, Caldwell, & Sorensen, 1997) .

In experiment 4 of this section, the first significant difference between SSVEP baseline and augmented amplitude after the attention shifting cue occurred no earlier than 288 ms and 240 ms for the left and right bars, respectively. After that time point, the SSVEP amplitude still increased. The time point of the first significant effect in SSVEP amplitude was the time bin in which subjects detected at least approximately 50% of the targets correctly. This parallels the findings of (Shapiro, et al., 1997) who also found a performance of 50% for second probe detection (noun or not-subjects-name) at around 300 ms after target onset. In the present experiment, the reaction times for left bar targets were significantly slower and the percentage of correct responses were significantly lower as compared to the right bar targets, indicating that left bar targets were more difficult to detect. This might account for the later time point of a significant increase of SSVEP amplitude for the left than the right bar. This interpretation is also supported by the finding that fast and slow reacting subjects showed a marked difference in the latency of the SSVEP amplitude maximum for the attended bar. Again, this point was related to a certain performance level, as has been shown by a significant correlation between SSVEP and behavioral data. Thus, the possibility of measuring the temporal characteristics by means of SSVEPs opens a whole field for new research strategies to get a better understanding of attentional processes in general.

2.3. Visually induced Gamma band responses (GBR)

This section focuses on experiments which investigate visually induced gamma band responses in the human brain. As outlined in section 1, induced GBRs are discussed as a physiological correlate of the binding mechanism. In the first experiment, the Discrete Gabor Transform (DGT) algorithm was tested with intracortical recordings from the monkey visual cortex to see whether this algorithm is able to detect the short bursts of gamma band activity which are not time- and phase-locked to the stimulus. Next, an EEG recording was obtained using identical stimuli to that used in the first animal experiments, which demonstrated that induced GBRs are related to the features of the stimuli (see "Introduction" section). The major aim in experiment 1 was to mimic the animal model in order to determine if induced GBRs in the EEG exhibit the same features. Experiment 2 was conducted to test the replicability of the findings and to determine if gamma- and alpha band activity are related to each other. In the third experiment, a complex moving stimulus was used to compare the gamma band response to a complex standing stimulus. On the basis of the model of Vijn (1991, see section 1.2) it was hypothesized that motion of a complex stimulus is related to a reduction of gamma band spectral power as compared to the standing complex stimulus. And, finally, in experiment 4, the modulation of visually induced GBRs by means of spatial selective attention was investigated to give support to the notion that visually induced gamma band responses have a functional meaning[1]. The following section first describes the Discrete Gabor Transform, the frequency analysis which was used for all experiments, followed by the four experiments.

---

[1] In this section experiment 1 and 2 are slightly adapted versions of the articles: Müller, M.M., Bosch, J., Elbert, T., Kreiter, A., Valdes Sosa, M., Valdes Sosa P., Rockstroh, B.: Visually induced gamma band responses in human EEG - A link to animal studies. *Experimental Brain Research*, 1996, 112, 96-112, and Müller, M.M., Junghöfer, M., Elbert, T., Rockstroh, B.: Visually induced gamma band responses to coherent and incoherent motion: a replication study. *NeuroReport* , 1997, 8, 2575-2579.

2.3.1. General data analysis of experiments 1 to 4

Frequency analysis

The frequency analysis in experiments 1 to 4 was obtained by using an algorithm, which was partly developed and programmed at the Cuban Center of Neurosciences.

To determine time changes in the intensity of oscillatory activity the evolutionary spectrum was used (Priestley, 1988). It is specifically assumed that the i-th recording epoch can be modeled by:

$$V_i(t) = \Pi(t) + \beta_i(t)$$

where $\Pi(t)$ is the mean evoked response (or the event-related potential) and $\beta_i(t)$ the trial-by-trial fluctuation around the mean. Since the focus was on oscillatory activity which is not deterministically time or phase locked to the stimuli, the usual estimate of $\Pi(t)$ was subtracted from each epoch. An estimate of the evolutionary spectrum of $\beta_i(t)$ was calculated by means of the Discrete Gabor Transform (Qian & Chen, 1993) which may be described as follows:

First, a time and frequency resolution compatible with the time/frequency uncertainty principle must be selected. In our case this was 64 ms for time and 3.9 Hz for frequency (highest frequency = 125 Hz with downsampling for analysis to 250 Hz). Then a *single* transformation is obtained which is equivalent to the following two steps:

1) A 256 ms sliding window $\gamma(t)$ is used to select segments of data centered around each time t and down weighted towards the extremes. $\gamma(t)$ is calculated as described in (Qian and Chen 1993) such that it has minimum energy, most closely approximates a Gaussian function, and ensures minimal crosstalk between adjacent frequencies.

2) The spectrum is computed for each segment. A combination of steps 1) and 2) yields the Discrete Gabor Transform coefficients $G_i(t, \omega)$, where ω is the frequency. It must be noted, an invertible Discrete Gabor Transform is thus ensured. Finally, the variance of the complex random variates $G_i(t, \omega)$

over all epochs i is computed in order to form a consistent estimate of the evolutionary spectrum. In population terms:

$$\sigma_{\beta}^{2}(t,\omega) = \mathbf{E}\left[\left|G_i(t,\omega)\right|^2\right]$$

where $\sigma_{\beta}^{2}(t,\omega)$ is the evolutionary spectrum of the $\beta_i(t)$, $\mathbf{E}[x]$ denotes the expected value operator of a random variable x and $|a|^2$ denotes absolute value of a complex number a.

Data reduction for statistical analysis

Unless otherwise stated, data reduction and statistical analysis in the frequency domain was performed in experiments 1 to 4 in the following manner:

For the analysis epoch, the mean spectral power for each frequency and electrode was calculated on the basis of the single trial evolutionary spectra. Two bands were chosen for statistical analysis: (1) a broad gamma band, which represents the averaged spectral power from 39-94 Hz, and (2), the alpha band from 8-12 Hz. The standing stimuli period served as a baseline (see Method sections in experiment 1 to 4). We divided the first 1472 ms while stimuli were in motion into seven time windows (192 ms each). These windows were obtained by averaging across 3 successive time points (64 ms each) in the frequency domain of the respective spectral power of each band. Thus, each 192 ms window contains 448 ms in the time domain. For every window, the natural logarithm was calculated to approximate a Gaussian distribution and the natural logarithm of the respective mean baseline power (i.e., the power while the stimulus was motionless) was subtracted. Thus, the normalized time windows represented the spectral power *relative to baseline*. These normalized time windows were subject to statistical analysis.

2.3.2. Experiment 1

First, the ability of the DGT to extract short bursts of induced gamma band activity by analysing local field potentials measured from area 17 of an awake fixating macaque monkey (macaca fascicularis) was tested. It was then investigated whether induced gamma band activity can be extracted from the human EEG with the "long bar" stimulus design. On the basis of the animal experiment (Gray, et al., 1989) it was hypothesized that the long bar induces gamma band responses in the human EEG.

Methods monkey recordings

The stimulus was a 1 deg by 1 deg light bar moving with a velocity of 1 deg/s over the receptive field. For intracortical extracellular recordings, glass insulated elgiloy electrodes (1 Mega Ohm at 100 Hz) were used. Data was recorded with a sampling frequency of 1000 Hz, and the raw signal was filtered from 10 to 100 Hz. The training of the animal, the implantation of the recording chamber and the description of the recording session was extensively reported in Kreiter (1992) and Kreiter and Singer (1992). All surgical and behavioral procedures were performed in accordance with the guidelines for the welfare of experimental animals.

Results monkey data

Figure 2.3.1 depicts three examples of an evolutionary spectrum of a single sweep and the grand mean of evolutionary spectra over 10 single sweeps from the monkey local field recordings.

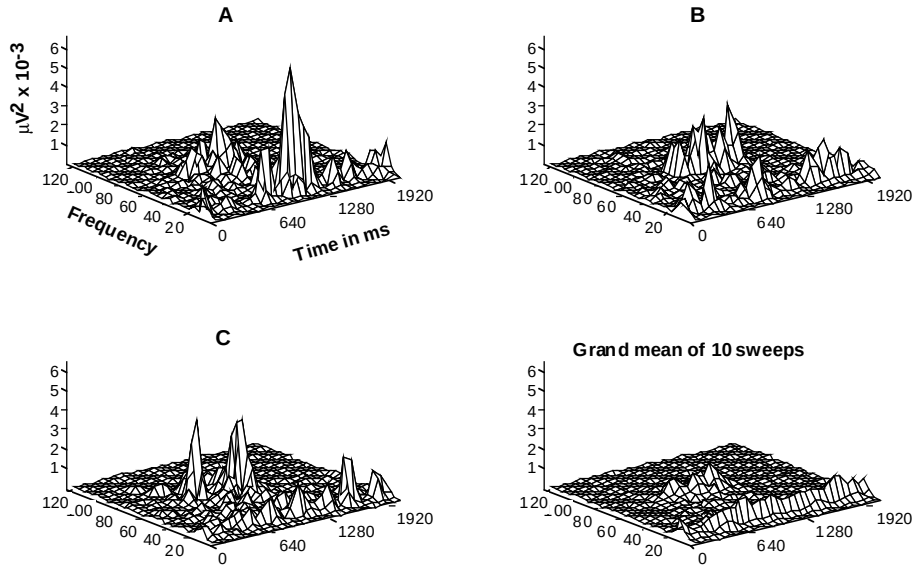

Figure 2.3.1. Evolutionary spectra of three single sweeps (panels a-c) and grand mean evolutionary spectra of ten single sweeps (panel d) of local field potentials from Area 17 of the awake behaving monkey while attending to a moving stimulus.

On average, spectral power was centered around 60 Hz. Figure 2.3.1 a-c clearly depicts the variance of frequency and time of onset of the induced gamma band activity in the single sweeps. These features correspond to the ones typically described in animal studies as well as parallel the findings of Kreiter (1992). Averaging of evolutionary spectra of 10 single sweeps resulted in a depression of the spectral power in the grand mean (Figure 2.3.1 d). Thus, it can be concluded that the Discrete Gabor Transform is able to extract synchronized oscillatory spindles in the gamma band range as they were observed in animal studies.

Methods EEG study

Subjects

EEG was recorded from seven human subjects (mean age 26.1 years, 4 males, 3 females) with normal or corrected-to-normal vision. Subjects received monetary compensation for participating in the experiment (25 DM). All subjects were naive with respect to the scientific goals of the experiment.

Stimuli and Design

The stimulus configuration corresponded to that used in animal studies (Gray, et al., 1989). There were two stimulus configurations. The first consisted of a single moving bar, which was expected to activate one single synchronously firing neuronal assembly. The second contained two identical bars moving in opposite directions (see Figure 2.3.2 and 2.3.3, inset). This stimulus was expected to evoke activity in at least two separate neuronal assemblies which are not synchronized, resulting in a reduction or even elimination of macroscopically visible gamma band responses. Bars were presented in the left visual hemifield in order to avoid cancellation of superimposed electrical vectors of cortical activity due to folding within the visual cortex.

The dimensions of the light bars were 9.8 deg x 0.46 deg for the coherent and 4 deg x 0.46 deg for the incoherent stimulus condition, and their velocity was 1.9 deg/s. Luminance of bars and background was 1.0 and 0.05 cd/sqm, respectively. Each condition comprised of 100 stimuli. The long bar and the two bars were presented in a random order with an interstimulus interval of 1750 ms. Prior to motion-onset, the bars were presented as standing stimuli for 260 ms. Motion-onset occurred directly thereafter, beginning 9.64 deg lateral to the fixation point and ending 3700 ms later (2.58 deg lateral to fixation point) with the disappearance of the bars. Stimuli and fixation point were presented on a 20 inch monitor with a frame rate of 60 Hz (non interlaced) one meter in front of the subject's eyes. Subjects were instructed to fixate on a cross at the center of a screen while attending to the presented stimuli.

Electrophysiological recordings and statistical analysis

EEG was recorded, using Ag-AgCl electrodes from Pz, Oz, P3, P4, T5, T6, O1, O2, VEOG (international 10-20 system) with a sampling rate of 1000 Hz (pass band: 0.3 to 300 Hz), referenced to linked earlobes. Electrode impedance for all electrodes was below 5 kOhms. Trials with EOG artifacts were rejected when the absolute value of the amplitude exceeded 75 µV. One subject, whose data contained more than 60% artifacts, was removed from further analysis. The evolutionary spectrum was calculated by means of the DGT across an epoch, defined as 256 ms pre-motion to 1792 ms after motion-onset of the bars.

Means comparisons across the 7 windows across all electrodes were calculated to test the difference between coherent and incoherent motion over time for the alpha- and the gamma band, respectively. P-values were adjusted by Huynh-Feldt correction. In addition, paired t-tests (coherent/incoherent) of mean values across electrodes were conducted for each time window.

Results

Grand mean normalized evolutionary spectra for our human subjects are shown in the next two Figures. Figure 2.2.2 represents the coherent (long bar) and Figure 2.2.3 the incoherent motion.

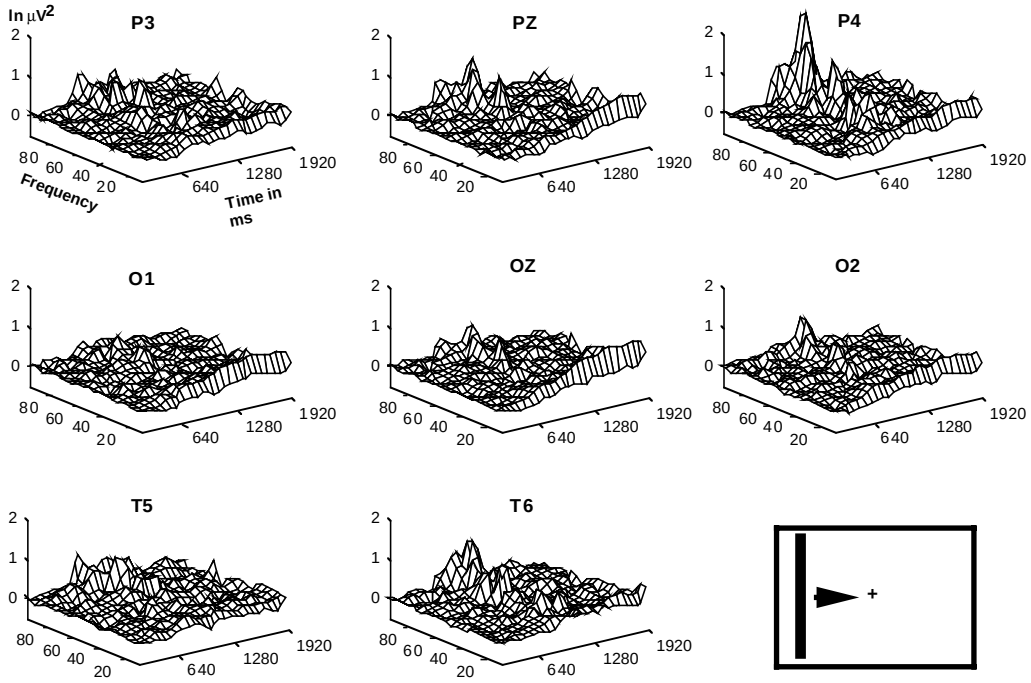

Figure 2.3.2. Grand mean normalized evolutionary spectra for the coherent motion.

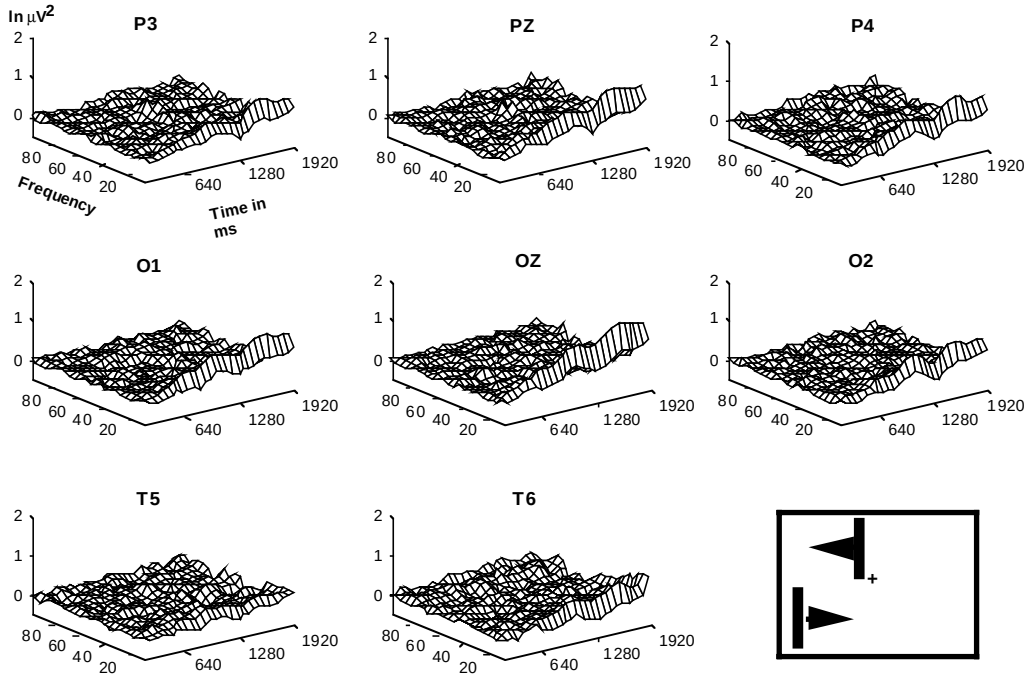

Figure 2.3.3. Grand mean normalized evolutionary spectra for the incoherent motion.

Relative to the standing stimuli, the grand averages of the evolutionary spectra for the different electrode positions revealed several important features:

(1) The single bar condition (Figure 2.3.2) was associated with enhanced gamma band (39-94 Hz) activity with two peaks, one in the 60 Hz range, and the other in the range of 80 Hz.

(2) This activity was most pronounced over the contralateral parietal scalp sites (P4, T6 and O2) in a time window between approximately 300 and 1000 ms post motion-onset and far exceeds the standing stimulus level, particularly in P4.

(3) In the presence of two incoherently moving bars, no comparable enhancement of activity in the gamma range was observed at any electrode site (Figure 2.3.3).

(4) Alpha activity was less pronounced in coherent as compared to incoherent motion.

(5) After a short period of little difference in alpha activity between standing and moving stimuli, alpha showed an ongoing recovery during the time course of motion.

(6) Topography and time course of alpha for both experimental conditions were not found in any other frequency.

Figure 2.3.4 depicts the normalized gamma band activity of the 7 time windows, and Figure 2.3.4 shows the same for the alpha band.

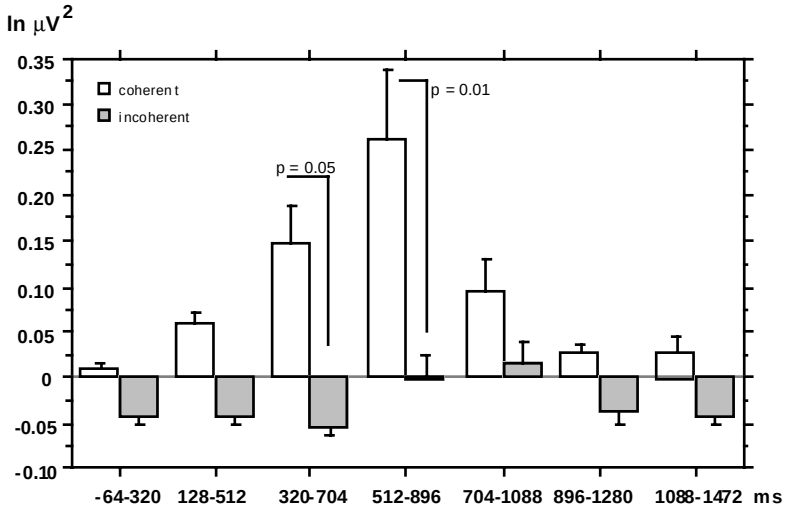

Figure 2.3.4. Means and standard errors across all subjects and electrodes for the normalized gamma band spectral power for the 7 time windows. *Note:* Time borders refer to the epoch in the time domain.

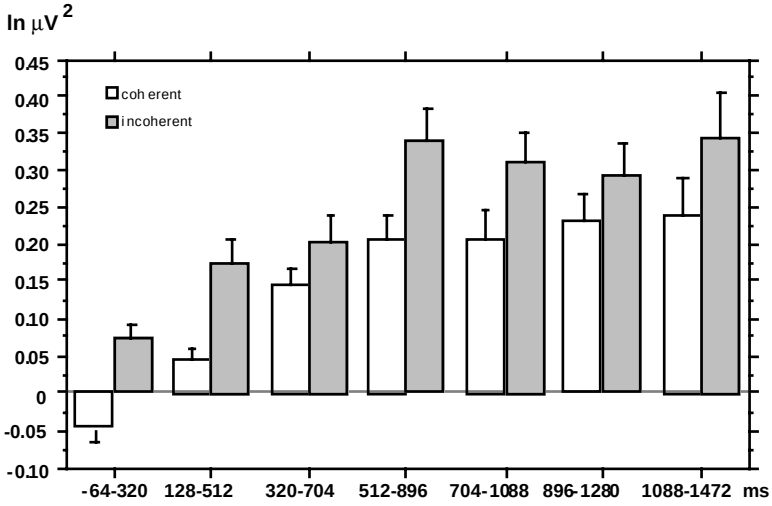

Figure 2.3.5. Means and standard errors across all subjects and electrodes for the normalized alpha band spectral power for the 7 time windows. *Note:* Time borders refer to the epoch in the time domain.

The statistical analysis of the normalized time windows showed significantly larger spectral power in the gamma band in all time windows for coherent motion as compared to incoherent motion ($F(1, 65) = 9.34$, $p < 0.05$). Differences were most pronounced in the time window between 320-704 ms ($t(6) = 2.0$, $p = 0.05$) and 512-896 ms post motion-onset ($t(6) = 2.5$, $p = 0.01$, Figure 2.3.4). In contrast, the relative changes in power over all time windows in the alpha band (8-12 Hz) was significantly lower in coherent as compared to incoherent motion ($F(1, 65) = 10.21$, $p < 0.01$, Figure 2.3.5).

Conclusion

These results prove that the DGT is able to extract short bursts of non time- and phase-locked gamma band activity. The results with respect to the human EEG data show that gamma band responses in the human EEG were induced by coherently moving bar stimulus, but disappear in the presence of two independently moving bars. The observation of stimulus induced gamma band activity in extracranial human EEG recordings suggests that many neurons have synchronized their activity in response to the single moving bar stimulus. The lack of macroscopically visible gamma band activity in the presence of two bars, moving simultaneously in opposite directions (incoherent stimulation), can be explained if each bar is producing an oscillatory activity in separate neuronal assemblies but the activity of these assemblies is not synchronized. In the macroscopically measurable activity, this results in a reduction or even cancellation of gamma band signals.

2.3.3. Experiment 2

Experiment 2 was designed to test the replicability of the findings of experiment 1. In addition, cortical alpha activity was again examined to test whether gamma band activity might reflect changes in harmonics of alpha waves. If so, the same temporal features of spectral power should occur for alpha- and for gamma band activity at the same electrode site and the intrasubjective topography of alpha- and gamma band should be significantly correlated.

Methods

Subjects

EEG was recorded from four healthy women (ages 20 to 32) with normal or corrected-to-normal vision. Subjects received monetary compensation for participating in the experiment (25 DM). All subjects were naive with respect to the scientific goals of the experiment.

Stimuli and Design

Stimuli and stimulus presentation was identical to experiment 1. Subjects were instructed to fixate on a cross at the center of a 20 inch monitor while attending to a single moving bar (coherent motion), or two identical bars, moving in opposite directions (incoherent motion). Stimulus motion-onset began 260 ms after the appearance of the bars and ended 3000 ms later with their disappearance. The standing stimulus served as a baseline period. For each condition, 100 trials were presented in the left visual field in a random order.

Electrophysiological recordings and data analysis

The EEG of one of the subjects was recorded from 20 Ag-AgCl electrodes (montage according to the international 10-20 system) integrated into an elastic cap (Electrocap). For the three other subjects a 27 channels montage was used to increase the spatial sampling rate for the topographical maps. Additional channels were CB1/2, POz, TO1/2, and CT5/6 (see Figure 2.2.1 and 2.3.9). To monitor horizontal and vertical eye-movements (EOG), electrodes were fixed above and below the left eye and as near as possible to the outer canthi. All electrodes were referenced to Fpz. A sampling rate of 1000 Hz (pass band: DC to 300 Hz) was used. Electrode impedance was kept below 5 kOhms. Trials with horizontal EOG exceeding 1 deg of lateral eye movements, blinks and EMG artifacts were rejected. Following this procedure, the data of one subject had to be rejected from further analysis. For the three other subjects an average of 78.5% of artifact free trials remained for further analysis.

Current source densities (CSDs) were calculated for each time point of each trial and electrode in order to obtain a reference free estimation of cortical

activity (Law, Rohrbaugh, Adams, & Eckhart, 1993). Frequency analysis, frequency bands and data reduction for statistical analysis were identical to experiment 1. Since electrodes T5, T6, O1, Oz and O2 showed the maximum of power in the gamma band at occipito-temporal electrodes, they were used for statistical analysis. In addition to the statistical tests described in experiment 1, the time course of the baseline corrected mean values across trials for both bands was tested by a three factor (ELECTRODE x TIME x COHERENT/INCOHERENT MOTION) repeated measurement ANOVA. P-values were adjusted by Huynh-Feldt correction.

Spherical spline (Perrin, et al., 1989) isocontour maps of the baseline corrected spectral power for the gamma band were calculated and the spectral power of both bands were normalized by means of a procedure suggested by McCarthy and Wood (1985), resulting in a value range between 0 and 1. Data were normalized separately for the two conditions in the time bin where gamma band activity was most pronounced. Similarity of intrasubjective scalp distributions of the two bands was examined by means of calculating the correlation across electrodes. Correlation coefficients were underwent a z-transformation for statistical evaluation.

Results

The mean time course of the gamma band across the 5 electrodes is illustrated in Figure 2.3.6, while the corresponding variations for the alpha band response are depicted in Figure 2.3.7.

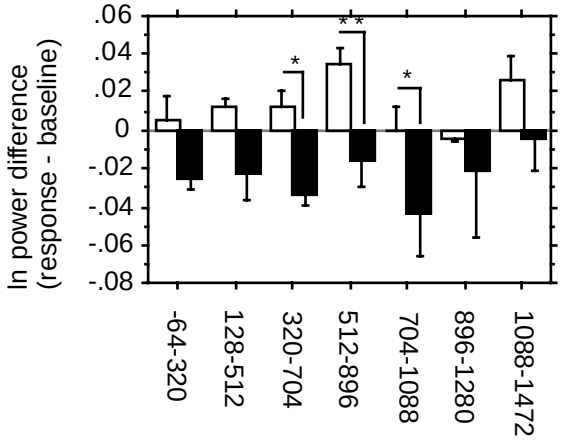

Figure 2.3.6. Means and standard errors across all subjects and electrodes T5, T6, O1, Oz and O2 for the normalized gamma band spectral power for the 7 time windows. *Note:* Time borders refer to the epoch in the time domain. White bars for coherent condition.

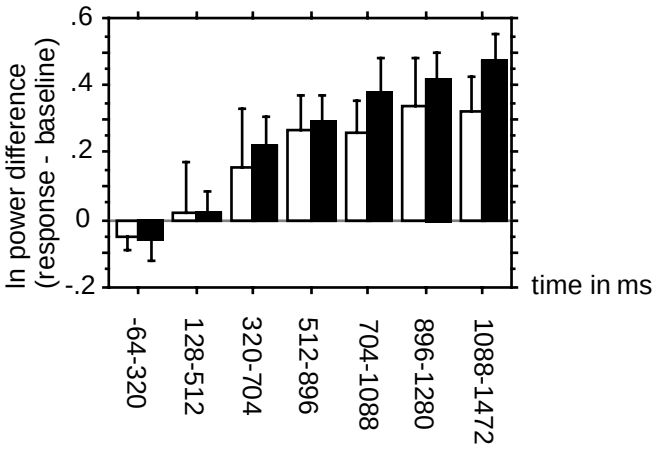

Figure 2.3.7. Means and standard errors across all subjects and electrodes T5, T6, O1, Oz and O2 for the normalized alpha band spectral power for the 7 time windows. *Note:* Time borders refer to the epoch in the time domain. White bars for coherent condition.

Gamma band activity was significantly more pronounced during coherent motion than during incoherent motion ($F(1, 26) = 22.66$, $p < 0.01$). The first time bin with a significant difference between conditions was the 320-704 ms time window ($t(2) = 4.63$, $p < 0.05$; time range refers to the time domain), while the most pronounced difference occurred in the following time bin of 512-896 ms ($t(2) = 9.1$, $p = 0.01$). A significant difference between conditions in the time window 704-1088 ms ($t(2) = 4.39$, $p < 0.05$) was due to a marked gamma suppression during the incoherent motion relative to baseline. In contrast, activity in the alpha band was somewhat higher for the incoherent motion as compared to the coherent motion, but this effect did not reach the significance level ($F(1, 26)=4.20$, $p = 0.08$). As in experiment 1, alpha suppression due to stimulus presentation was maintained at motion-onset (-64-320 ms time bin), but dissipated during the time course of motion, as confirmed by the main effect TIME ($F(6,12) = 27.90$, $p = 0.01$). No significant effect of the gamma band on time course was found.

The topographical maps of baseline corrected values in time bin 512-896 ms were normalized McCarthy and Wood (1985). This was done for gamma- and alpha band spectral power for the coherent motion. The maps are displayed in Figure 2.3.8 for all three subjects.

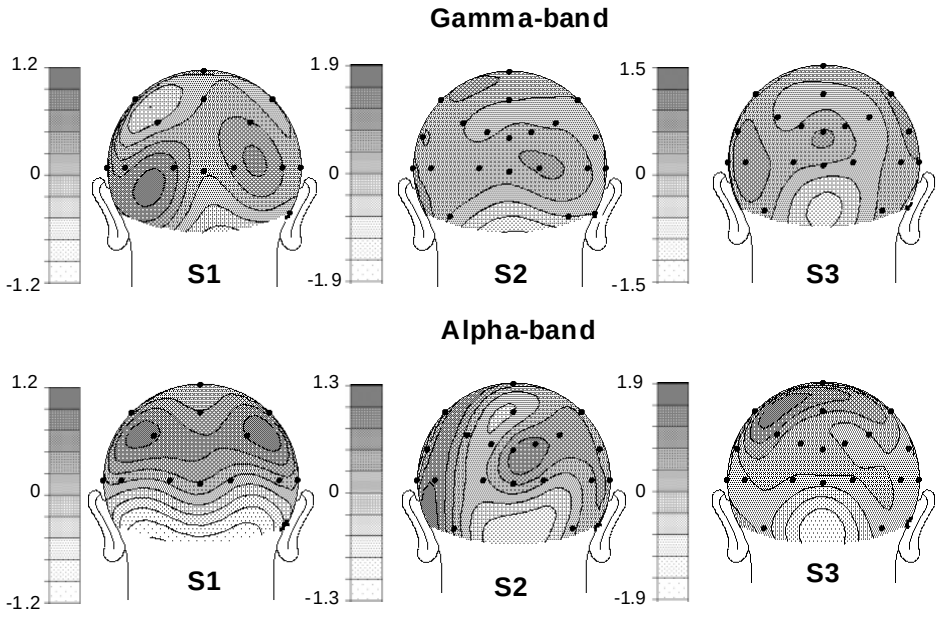

Figure 2.3.8. Spline interpolated isocontour maps of baseline corrected normalized gamma- and alpha band spectral power for all subjects for coherent motion in the time period of most pronounced gamma band activity (512-896 ms). *Note:* x-values are given in $(\mu A/m^3)^2$

As obvious from Figure 2.3.8, the scalp distribution of gamma- and alpha activity varied considerably between subjects. The intrasubjective correlation-coefficients did not reach the significance level and were ranging from 0.28 to -0.30, indicating that gamma band activity was not dominated by harmonics of the alpha waves. In contrast, intrasubjective consistency was high for the alpha band, as demonstrated by significant intrasubjective correlations between coherent and incoherent motion in all three subjects (S1: $r = 0.65$, $p = 0.003$; S2: $r = 0.64$, $p = 0.0004$; S3: $r = 0.88$, $p < 0.0001$). For the gamma band, no significant correlation was found between coherent and incoherent motion.

Conclusion

Experiment 2 demonstrates the replicability of induced gamma band activity while subjects were attending to a coherently moving long bar. The significant enhancement 320 ms post motion-onset parallels the results of Tallon-Baudry and co-workers (1996), who found induced gamma band activity in a visual search task within a latency of approximately 280 ms.

Gamma- and alpha band activity exhibited a different time course while bars were in motion and their topography was not correlated. Taken together, these results strongly suggest that gamma cannot be considered to be simply a harmonic of alpha waves. Furthermore, no significant intraindividual correlation between the gamma band topography during coherent and incoherent motion was obtained for any of the subjects. This indicates that generator structures are different for the two different conditions. It also provides further evidence that the induced gamma band activity is unlikely to result from muscle activity, since the topographical pattern of activity during the two conditions would be correlated, if one assumes that similar muscle groups are active. Unlike gamma, the topographical distribution of alpha for the coherent and incoherent condition was highly correlated within all subjects. This indicates that alpha generators do not differentiate between conditions and, thus, cannot be related to the specific type of processing.

2.3.4. Experiment 3

In contrast to the previous two experiments, which employed simple stimuli, this experiment used complex stimuli. The question was, whether a complex moving stimulus is also linked to enhanced induced gamma band activity as compared to a standing complex stimulus as was the case for simple stimuli (the long bar), or whether the complex moving stimulus is related to a decrease in gamma band power as predicted by the model of Vijn (1992; see section 1.2).

Methods

Subjects

12 subjects (three females) with normal or corrected-to-normal vision were recorded. Subjects received monetary compensation (DM 25) for participation and were naive with respect to the scientific goals of the study.

Stimuli and Design

Figure 2.3.9 depicts a schematic representation of the stimulus and the electrode positions.

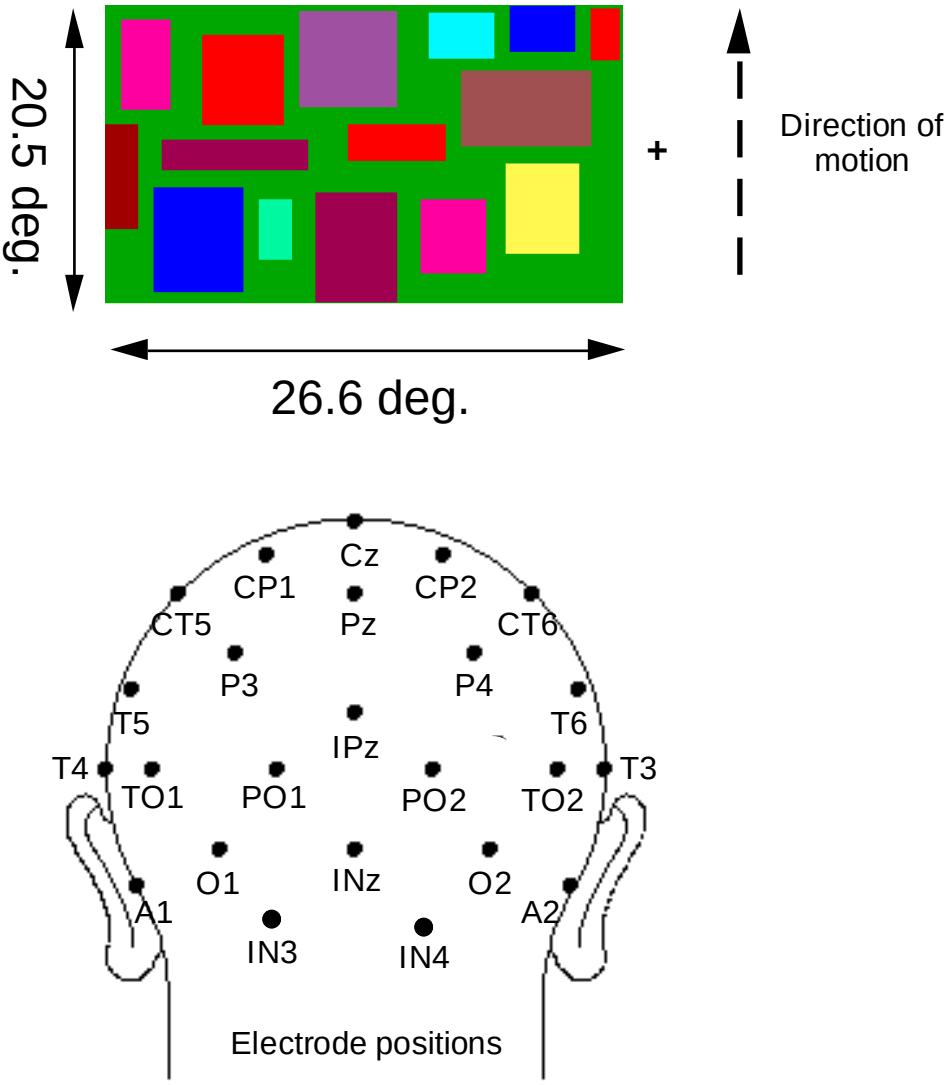

Figure 2.3.9. Schematic representation of the stimulus and electrode positions.

Colored squares and rectangles were presented on a 20 inch monitor on a green background. The screen subtended 20.5 x 26.9 degrees of the left visual field. Following a 1000 ms presentation as a standing stimulus, either (a) the entire moved upwards for a period of 2000 ms or (b) the stimulus remained motionless for an additional 2000 ms, followed by a dark screen for 1000 ms, respectively. Each condition was comprised of 100 trials, which were presented in a random order. Subjects were instructed to fixate on a fixation point affixed to the left border of the screen, and to avoid head/eye movements and blinks during stimulus presentation.

Electrophysiological recordings and data analysis

EEG was recorded from 27 electrodes (see Figure 2.3.9) referenced to Fpz. Additional electrodes were fixed to monitor horizontal and vertical eye-movements (EOG). The sampling rate was 1000 Hz (DC - 300 Hz). Electrode impedance was kept below 5 kOhms. Trials with horizontal EOG exceeding 1 deg of lateral eye movements, blinks and EMG artifacts were rejected. Three subjects were excluded from further analysis due to too many artifacts. For the remaining 9 subjects, an average of 81.2% of artifact free trials were analysed. Prior to transformation into the frequency domain, CSDs were calculated for every artifact free trial. Frequency analysis and bands, analysis epoch, data reduction and statistical analysis were conducted in a manner identical to experiments 1 and 2. Electrodes CT5/6, P3/4, T5/6 and TO1/2 were included for statistical analysis.

Results

Figure 2.3.10 depicts the time course of the GBR relative to baseline for the standing and moving stimulus.

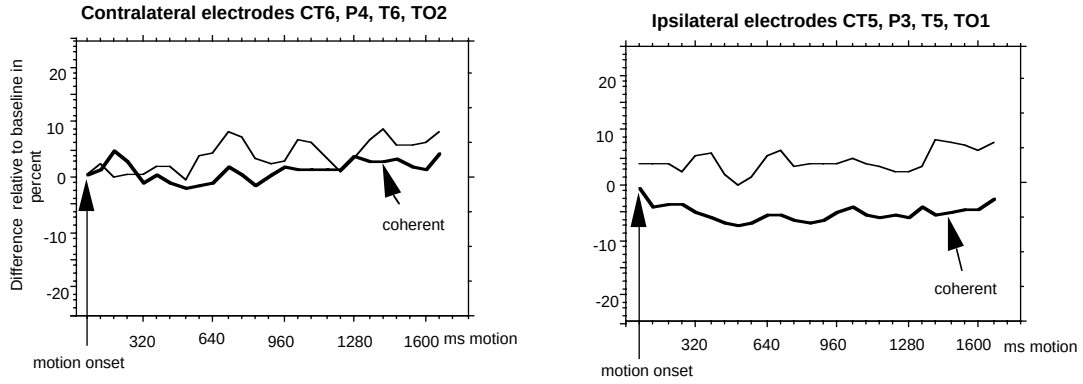

Figure 2.3.10. Time course of GBR (39-94 Hz) relative to baseline for the moving (bold) and standing (thin line) stimulus.

A significantly higher power across time and electrodes for the standing as compared to the moving stimulus ($F(1,8) = 6.0$, $p < 0.05$), not due to baseline differences, was found. The significant main effect TIME ($F(7,56) = 3.0$, $p < 0.05$) showed the most pronounced reduction in gamma band power in the time window 320-704 ms post motion-onset. This is exactly the same time window in which the first significant difference between coherent and

incoherent motion in experiments 1 and 2 was found. The reduction of gamma power in that time window was mainly due to the reduction in the motion condition, as was tested by an one group t-test ($t(8) = 0.8$, $p = 0.5$ for standing, and $t(8) = -3.5$, $p < 0.05$ for motion). As can be seen in Figure 2.3.10, there is a continuous increment of gamma power in the following time windows .

Conclusion

The results of experiment 3 were in line with the findings of Vijn et al. (1991; 1992, van Dijk, et al., 1994), who described a reduction in gamma band power when complex stimuli were in motion versus when they were motionless. However, the present experiment was not designed to fully test Vijn's model, so no conclusions can be drawn on the validity of that model based on the results of experiment 3. To test the model, complex and simple (e.g. a bar) standing and moving stimuli would need to be presented and their GBRs compared. Also, amplitude changes would need to be correlated to topographical changes from a broad to a more focused gamma band distribution.

2.3.5. Experiment 4

The functional relevance of induced GBRs is still under debate (see section 1). In the following experiment, the modulation of induced GBRs by spatial selective attention was tested. A modulation of induced gamma band activity by spatial selective attention would strongly suggest that the macroscopical recordings are linked to cortical activity with functional relevance and do not just represent an epiphenomenological by-product of neuronal activity. In contrast to animals, humans can easily be instructed to shift attention from one point to the other, and verbal reports of performance can be obtained. On the basis of our results from the SSVEP studies (see section 2.2) and the study of Beauchamp et al. (1995, see section 1.2), an augmentation of spectral power in the gamma band was expected, when subjects attended to a moving simple stimulus, versus when they ignored it. Unlike experiments 1 - 3, it was also examined, whether the effect of attention on the gamma band is related to a specific frequency band within the gamma band, or whether it is a broad-band phenomena.

Methods

Subjects

10 subjects (5 females) from 20 to 36 years of age with normal or corrected-to-normal vision participated in the experiment. All the subjects were naive with respect to the scientific goals of the study, and received monetary compensation (25 DM) for their participation.

Stimuli and Design

A 12 inch monitor was placed 80 cm in front of the subjects. A fixation rectangle (0.21 x 0.36 deg) was presented in the center of the screen. After 900 ms, a long bar (8 x 0.43 deg) occurred either in the left or right visual hemifield, either 1.43 deg or 5.3 deg lateral to the fixation rectangle. 600 ms after bar presentation, the bar started to move for 1578 ms from the center (1.43 deg lateral to the fixation rectangle) to the border of the screen (5.3 deg lateral to the fixation rectangle), or from the border to the center of the screen (1.43 deg lateral to the fixation rectangle), depending on the starting point (see Figure 2.3.11 and 2.3.12). The velocity of the bar was 2.45 deg/s. After motion, the bar disappeared but the fixation rectangle remained on the screen, always with the same color. 900 ms after the disappearance of the bar, a new bar was presented as a standing stimulus for 600 ms.

Synchronized with motion-onset, the bar and the fixation rectangle changed colors independently but synchronized to each other with a frequency of 3.2 Hz. Five isoluminant colors were presented, and subjects were instructed to detect and silently count the target color either in the bar, while ignoring the color changes in the fixation rectangle, or to silently count the same target color in the fixation rectangle while ignoring the moving bar, resulting in four experimental conditions (attend/unattend bar, left/right visual hemifield). Subjects were also instructed to avoid eye movements and blinks while performing the task. Each condition comprised of 200 trials and was presented as one block. The sequence of block presentation was counter balanced across subjects. Color changes for bar and fixation rectangle were presented in a random order with the restriction that the target color was never presented two times in a row, resulting in a inter-target interval of at least 625 ms. In order to check subjects' performance, the experiment was stopped from time to time (random interval) to ask for

the number of counted targets. Subjects received feedback on the accuracy of task performance.

Electrophysiological recordings and data analysis

EEG was recorded with 17 Ag/AgCl electrodes referenced against Fpz. Since our main interest was to record the cortical activity over the occipital lobes, electrodes were placed as follows (Lutzenberger, Pulvermüller, Elbert, & Birbaumer, 1995; Maier, Dagneli, Spekreijse, & van Dijk, 1987). In a square array, nine electrodes (3 x 3) were placed with a distance of 3.5 cm between each. The center electrode of the array was 6 cm anterior to the inion. In order to allow current source density analysis, additional electrodes were placed 3.5 cm above and below the first and the third column, as well as to the left and right of the first and third row (see Figure 2.2.11 and 2.3.12). Vertical eye movements were recorded with an electrode above and below the left eye (vertical EOG). Lateral eye movements were monitored with a left-right outer canthus montage (horizontal EOG). All channels were recorded with a sampling frequency of 500 Hz (DC - 200 Hz) and stored on disk for off-line analysis.

All trials with eyeblinks, EMG-artifacts and horizontal eye movements exceeding 1 deg were excluded from further analysis, which resulted in the exclusion of two subjects. For the remaining 8 subjects, 82.5% artifact free trials were analysed. Prior to transformation into the frequency domain, CSDs were calculated for every artifact free trial. The frequency analysis was conducted in an identical manner to the preceding experiments with two exceptions. First, the baseline period was extended to 512 ms prior to motion-onset to obtain a better estimate of the mean baseline power and the analysis epoch for motion lasted for 1536 ms. Second, the frequency range from 19.5 to 109.4 Hz was divided into six frequency bands, 19.5 - 31.3 Hz, 35.1 - 46.9 Hz, 50.8 - 62.5 Hz, 66.4 - 78.1 Hz, 82.0 - 93.7 Hz, and 97.6 - 109.4 Hz to test whether there is a specific frequency range in which a modulation occurs. The alpha band was extracted from 8-12 Hz as in the previous experiments. The time period where stimuli were in motion was devided into 5 windows, each of which was formed by the average of three consecutive 64 ms steps of the frequency domain data, starting with the first data point after motion-onset in the frequency domain, i.e. 64 ms. Therefore, one window contained an epoch of 448 ms in the time domain (see experiments 1 to 3). The natural logarithm was calculated for each time

window for each electrode and frequency band, in order to approximate a Gaussian distribution. Each time window was then normalized for each frequency band and electrode by subtracting the respective natural logarithm from the mean baseline value. For statistical analysis the nine electrodes which built the inner net were chosen.

To test whether the attentional manipulation was successful the visual evoked potentials (VEP), time locked to stimulus and motion-onset of the bar were extracted. For statistical analysis, three most left and three most right electrodes of the net were taken. For the VEP and the motion related components, the mean amplitude of the first 100 ms *prior to the appearance* of the bar served as a baseline. For stimulus onset, the mean baseline corrected amplitudes for the following epochs and components of the VEP were analysed: C1 (50-80 ms), P1 (100-130 ms), N1 (160-210 ms), P2 (220-280 ms), and N2 (330-380 ms). With respect to motion-onset the components P1 (170-200 ms) and N2 (260-310 ms after motion-onset) were tested. Besides the verbal record of performance we extracted the P300 for targets in the moving bar and fixation rectangle for the attended and unattended condition from the most upper electrode of the middle row (see Figure 2.3.11 and 2.3.12) as additional marker, that subjects really perform the task. Baseline for the P300 was defined as mean amplitude 100 ms prior to target onset.

Statistical analysis

First an omnibus-test over all 9 electrodes and five time windows was performed with a 2 (ATTEND/UNATTEND) x 2 (LEFT/RIGHT VISUAL HEMIFIELD) x 6 (FREQUENCY) repeated measurement ANOVA to see whether there was an effect on FREQUENCY. In the next step, all 6 frequency bands were subject to a 2 (ATTEND/UNATTEND) x 2 (LEFT/RIGHT VISUAL HEMIFIELD) repeated measurement ANOVA to test in which frequency band a significant effect for the attentional modulation over all 9 electrodes and 5 time windows occured. The frequency bands with a significant attention effect were put together in one band and a final 2 (ATTEND/UNATTEND) x 2 (LEFT/RIGHT VISUAL HEMIFIELD) x 3 (LEFT/MIDDLE/RIGHT ELECTRODE ROW) x 3 (ELECTRODE) x 5 (TIME WINDOW) repeated measurement ANOVA was conducted. This analysis was also calculated for the alpha band. VEPs and motion related components were subject to 2 (ATTEND/UNATTEND) x 2

(LEFT/RIGHT VISUAL HEMIFIELD) x 2 (IPSI-/CONTRALATERAL HEMISPHERE) x 3 (ELECTRODE) repeated measurement ANOVA. The P300 was tested with a paired t-test (ATTEND/UNATTEND) for targets in the bar and fixation rectangle, respectively. To obtain a more conservative estimation of interaction effects, all p-values were adjusted by Greenhouse-Geisser correction where necessary. Means and standard errors are presented.

Results

Performance and P300

The performance as measured by the verbal reports was equally good for all conditions. Taking over and underestimations into account, the average error rate was 4.6% for bar-targets in the left and 4.9% for bar-targets in the right visual hemifield. When subjects counted the targets in the fixation rectangle, the average error rate was 4.9% while the bar was in the left and 6.0% while the bar was in the right visual hemifield. This indicates that the task did not differ in terms of difficulty between the bar and the fixation rectangle. A highly significant P300 effect was obtained for the bar ($t(7) = 3.8$, $p < 0.01$) and the fixation rectangle condition ($t(7) = 3.5$, $p = 0.01$) for attended as compared to unattended targets, respectively, indicating that subjects really recognized and counted the targets and did not just estimate when asked for the number of targets.

Frequency analysis

The omnibus-test revealed a highly significant FREQUENCY effect ($F(5,35) = 8.31$, $p < 0.001$). The power was most pronounced for frequency bands 50.8 - 62.5 Hz, 66.4 - 78.1 Hz, and 82.0 - 93.7 Hz. For frequency band 19.5 - 31.3 Hz, the spectral power was below baseline level and for the remaining two bands, the increase in spectral power relative to baseline was only marginal. Next, the 6 frequency bands were tested separately. Table 2.3.1 presents the F- and p-values for the main effect ATTENTION for the 6 frequency bands.

Frequency band	df	F-value	p-value
19.5 - 31.3 Hz	1,7	0.6	p = 0.45
35.1 - 46.9 Hz	1,7	1.0	p = 0.35
50.8 - 62.5 Hz	1,7	5.5	p = 0.06
66.4 - 78.1 Hz	1,7	6.4	p = 0.03
82.0 - 93.7 Hz	1,7	8.6	p = 0.02
97.6 - 109.4 Hz	1,7	0.1	p = 0.73

Table 2.3.1. F- and p-values for main effect ATTENTION for 6 frequency bands.

Only the frequency bands 66.4 - 78.1 Hz and 82.0 - 93.7 Hz showed a statistically significant increase in spectral power when the moving bar was attended, as opposed to attending the fixation rectangle. Two additional points should be mentioned. First, there was no effect with respect to the hemifield in which the bar was presented for all frequency bands, indicating that both visual hemifields elicited equally strong or weak (depending on the frequency band) responses. Second, due to the diminishing of the attention effect in the last frequency band, it is highly unlikely that the result is an artifact of muscle activity.

For the final analysis, the two frequency bands 66.4 - 78.1 Hz and 82.0 - 93.7 Hz were combined by calculating the average of the two bands. Figure 2.3.11 shows the time course of the GBR and the evoked potentials for the left visual hemifield stimulation, Figure 2.3.12 the same for the right visual hemifield stimulation.

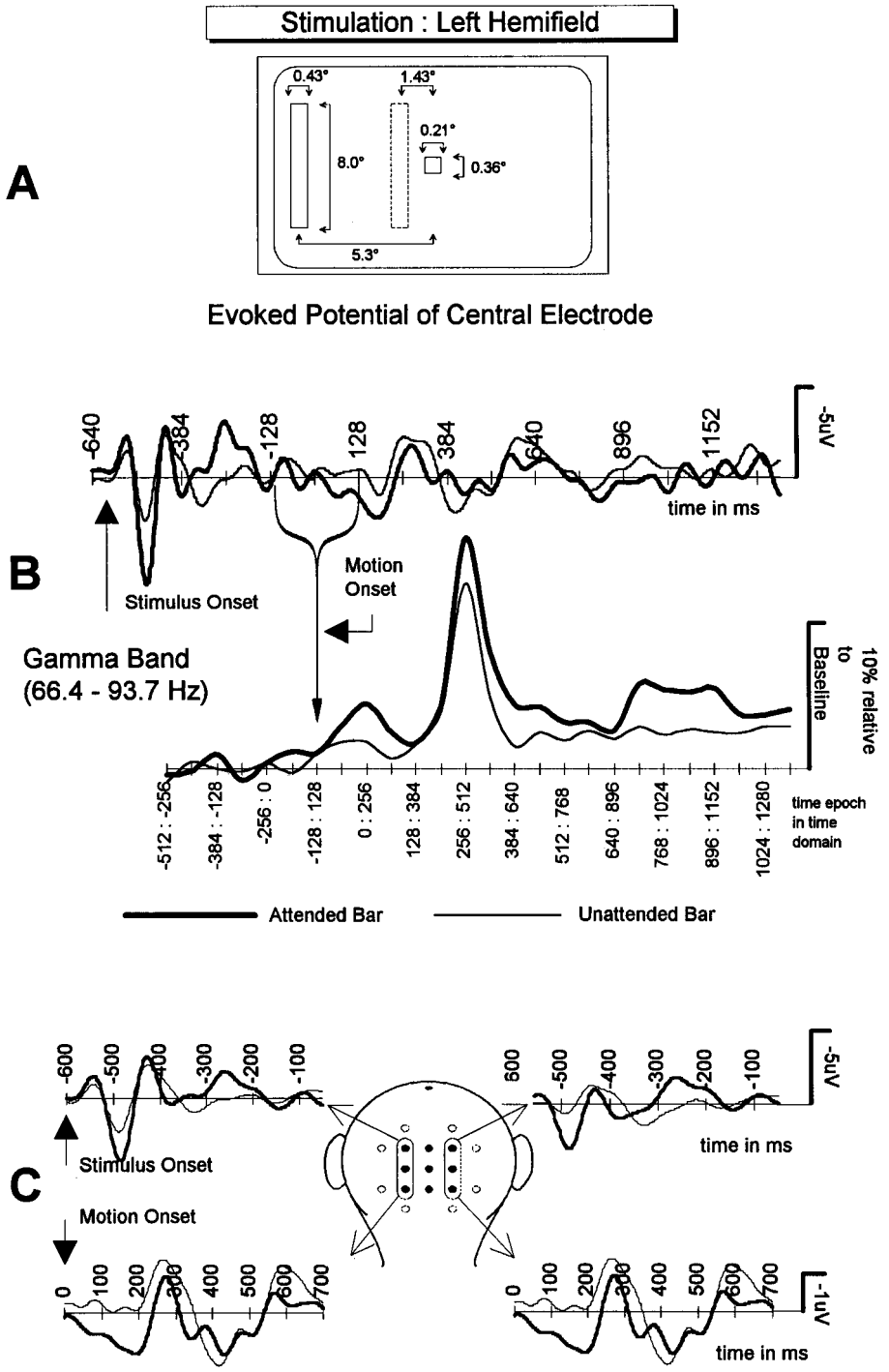

Figure 2.3.11. Upper panel: Schematic representation of the stimulus for the left visual hemifield. *Middle panel:* Evoked potential of the central electrode and time course of the 66.4 to 93.7 Hz gamma band response across 9 electrodes. *Lower panel:* Grand mean evoked potentials for stimulus occurrence and motion-onset averaged across the most left and right three electrodes of the net. *Note:* Negativity is plotted upwards. Bold lines correspond to attend bar condition, thin lines to the attend fixation rectangle condition.

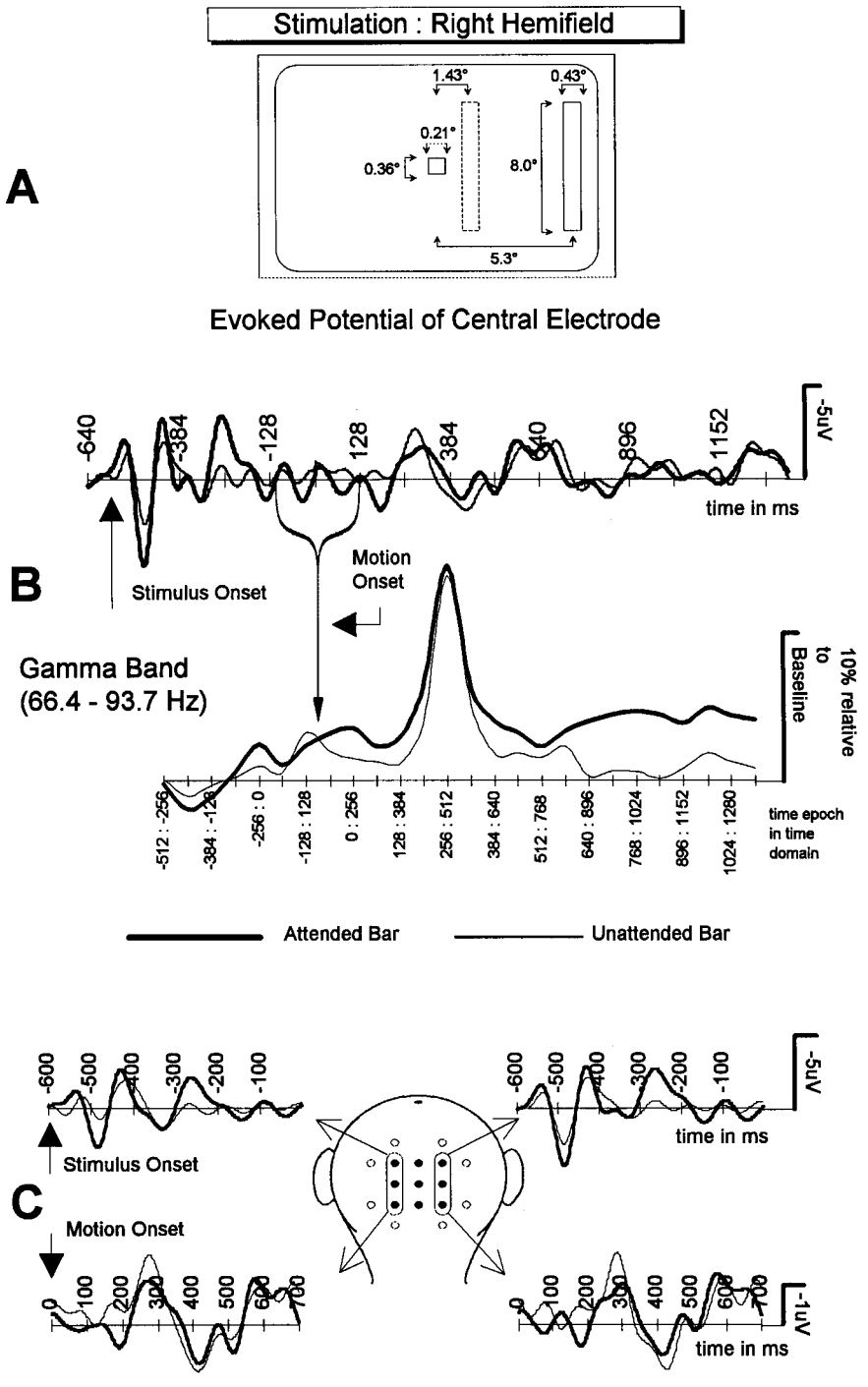

Figure 2.3.12. Same as Figure 2.3.11, but for the right visual hemifield.

Statistical analysis of the 66.4 to 93.7 Hz band revealed a significantly larger increase relative to baseline (4.9 ± 0.3%) when the moving bar was attended as compared to the unattended condition (3.2 ± 0.2%; $F(1,7) = 9.7$, $p = 0.01$) over time. Thus, the increase of power in the 66.4 to 93.7 Hz gamma band was 53% on the average when the moving bar was attended. Figure 2.3.11 and 2.3.12 shows the time course of the 66.4 to 93.7 Hz induced gamma band response. The biggest increase of spectral power relative to baseline was obtained in the 6th time bin after motion-onset, which is equivalent to a time epoch from 256 to 512 ms after motion-onset in the time domain. On the average, spectral power peaked with an increase of 17% for the attend left and for the attend right bar condition. The difference in spectral power over time was confirmed by a highly significant main effect TIME WINDOW ($F(4,28) = 13.2$, $p = 0.0001$). A highly significant ELECTRODE x TIME WINDOW interaction ($F(8,56) = 6.4$, $p < 0.001$) showed that the biggest increase in spectral power, relative to baseline, was present in the upper and middle row of electrodes during a time period of 128 to 704 ms after motion-onset. The power of the three electrodes in the lowest row exhibited only marginal fluctuations around baseline level. This indicates that artifacts of the neck muscles can not be responsible for the attention effect, since the lower row does not show any attention effect. This contrasts with the higher two rows, which are at greater distance the neck muscles[2]. In addition, the comparison left/right visual hemifield stimulation and ipsilateral/contralateral hemisphere revealed no statistically significant effect.

With respect to the alpha band, statistical analysis revealed a highly significant TIME effect ($F(4,28) = 7.2$, $p = 0.005$) indicating an increase of alpha activity over time starting with an increase of alpha power by 9.7 ± 1.0% relative to baseline in the time window -64 to 320 ms and ending with an increase of 23.9 ± 1.6% in the time window 704 to 1088 ms. The relative alpha power over time was slightly higher for the unattended condition (20.8 ± 0.8%) as compared to the attended condition (11.4 ± 0.08%; $F(1,7) = 4.9$, $p = 0.06$).

[2] In order to test this further we have also analysed the two lowest electrodes of the montage (see Figures 2.3.11 and 2.3.12). We have found no effect whatsoever.

VEP and motion related components analysis

With respect to the C1 component no significant effect was found. For P1, statistical analysis revealed alarger P1 when the bar was attended ($F(1,7) = 14.4$, $p = 0.007$), and this increase was greater for the hemisphere *ipsilateral* to the field of stimulation (ATTENTION x HEMISPHERE, $F(1,7) = 14.1$, $p = 0.007$; see Figure 2.3.11 and 2.3.12). For N1, amplitudes measured by ipsilateral electrodes were bigger than those recorded by contralateral electrodes (HEMISPHERE, $F(1,7) = 7.7$, $p < 0.05$), the most pronounced attention effect being for ipsilateral electrodes 1 and 2 (ATTENTION x HEMISPHERE x ELECTRODE, $F(2,14) = 5.1$, $p < 0.05$). P2 showed the most pronounced activity on *contralateral* electrodes 1 and 2 when the bar was attended (ATTENTION x HEMISPHERE x ELECTRODE, $F(2,14) = 7.0$, $p = 0.008$). N2 amplitudes were more pronounced when subjects attended the bar, (ATTENTION, $F(1,7) = 10.7$, $p < 0.05$). The biggest attention effects occurred for electrodes 2 and 3 (ATTENTION x ELECTRODE, $F(2,14) = 13.7$, $p = 0.001$) and for the *ipsilateral* hemisphere (ATTENTION x HEMISPHERE x ELECTRODE, $F(2,14) = 6.1$, $p < 0.05$) in particular. With respect to motion evoked components, a significant amplitude augmentation for the attended bar for P1 (ATTENTION, $F(1,7) = 8.7$, $p < 0.05$) was found, which was bigger for contralateral electrodes (ATTENTION x HEMISPHERE, $F(1,7) = 13.5$, $p = 0.008$) and most pronounced for contralateral electrodes 1 and 2 (ATTENTION x HEMISPHERE x ELECTRODE, $F(2,14) = 5.5$, $p < 0.05$).

Conclusion

In the present experiment, it was shown for the first time that visually induced gamma band responses can be altered by spatial attention, lending support to the functional relevance of these cortical activities. The finding that this effect is only present in a frequency range between 66.4 to 93.7 Hz parallels results from intracortical recordings from the visual cortex of the awake monkey in which the frequency range of induced oscillations varied between 60 and 90 Hz when moving stimuli were presented (Eckhorn, Frien, Bauer, Woelbern, & Kehr, 1993; Kreiter, 1992; Kreiter & Singer, 1992).

Evoked cortical responses served as a task control measure to ensure for the attention effects. The significant P300 effect proved that subjects were really detecting and counting the targets, since it otherwise would not have been present (as is the case for the unattended targets). The evoked potential

time locked to the appearance of the bar revealed the typical sequence of enhanced P1, N1, P2 and N2 components (Heinze, Luck, Münte, Gös, Mangun, & Hillyard, 1994; Heinze, Johannes, & Thinius, 1993; Hillyard, Mangun, Woldorff, & Luck, 1995; Luck, Fan, & Hillyard, 1993; Mangun, Hillyard, & Luck, 1990) when the subject was instructed to attend the bar. The motion-onset reveled a significant P1 effect which occurred in a time window between 170 to 200 ms after motion-onset. No effect was found on the later component. It appears obvious that the experimental manipulation was successful. Performance data indicated that the task was equally difficult for the bar and the fixation rectangle condition. The biggest increase in spectral power was obtained in a time window 256 to 512 ms after motion-onset. This was well after the P1 effect, which indicates, that different temporal structures are responsible for the respective effects. This will be discussed in the next section.

The present data also prove, that neither alpha band nor muscle activity contribute to the attention effect in the gamma band. The alpha band resembled a different time course, and the power was higher when subjects ignored the moving bar. Activity of the neck muscles would have the biggest effect in the most lower electrodes, which was not the case. Only marginal fluctuations around baseline level were found at this location. In addition, the effect is not present in the 97.6 to 109.4 Hz band, which is the frequency range in which muscle activity exhibits the highest power (Cacioppo, 1990). Thus, the results support the notion that attending to a moving stimulus is correlated with a higher activation of certain brain areas as opposed to when the moving stimulus is ignored. This result supports the notion that induced gamma band responses are related to cortical activities. On the basis of findings from Bauchamp et al. (1995), one might speculate that area V5 and V3 might have contributed to the present attention effect in the gamma band.

2.3.6. General summary and discussion of experiments 1 to 4

On the basis of intracranial local field recordings from area 17 of an awake behaving monkey, the ability of the DGT-algorithm to extract synchronized oscillating spindles in the gamma band was demonstrated. The thus obtained evolutionary spectra of single sweeps exhibited exactly the same features as those described in the animal literature (Kreiter, 1992; Kreiter &

Singer, 1992). Averaging the obtained spectra across ten single sweeps resulted in a reduced signal power as the time of onset and the frequency of the spindles varied from trial to trial.

Results of experiment 1 and 2 show that a coherently moving bar stimulus induces gamma band responses in the human EEG, which disappear in the presence of two independently moving bars. The observation of stimulus induced gamma band activity in extracranial human EEG recordings indicates that many neurons must have synchronized their activity in response to the single moving bar stimulus. The lack of macroscopically visible gamma band activity in the presence of two bars moving simultaneously in opposite directions (incoherent stimulation) can be explained if each bar is producing an oscillatory activity in separate neuronal assemblies but the activity of these assemblies is not synchronized. In the macroscopically measurable activity, this results in a reduction or even cancellation of gamma band signals. Animal experiments have indeed shown that cell groups in area 17 of the cat with non-overlapping receptive fields showed synchronous oscillation if they were activated by a single continuous stimulus (long bar). If two bars moving in opposite directions were presented, firing was uncorrelated (Gray, et al., 1989; Engel, et al., 1992). Evidently, cells join one assembly when they are activated by a single coherent stimulus, whereas they couple to two different assemblies when activated by two incoherent stimuli. These two assemblies are spatially disjunct and desynchronized relative to each other. Similar effects were observed even when the cell groups had overlapping receptive fields (Gray, et al., 1990).

The present study is the first which demonstrates a replication of former findings in human subjects with respect to induced gamma band activity. Gamma- and alpha band activity exhibited a different time course while bars were in motion and the topography was not correlated. In experiment 4, alpha power was higher when the bars were not attended. All results strongly suggest that gamma is not simply a harmonic of alpha waves, as has been indicated by Jürgens et al. (1995). In addition, no significant intrasubjective correlation was found between the gamma band topography of the coherent and incoherent motion (experiment 2). This can be interpreted in two ways. First, a different structure of the generator(s) for alpha and gamma is responsible for the topographical distribution, and, second, induced gamma band activity is not due to muscle activity, since

muscle activity most certainly would result in correlated topographical features (see also the general discussion of experiment 4 with respect to muscle artifacts). Unlike gamma, the topographical distribution of alpha for the coherent and incoherent condition was highly correlated in all subjects. This indicates, that identical alpha generators were active in both conditions.

The results of experiment 1 and 2 are also in line with Pulvermüller and co-workers (1995) who have also shown that contrary to gamma, alpha does not differ when words or pseudowords were presented. Pfurtscheller and Neuper (1992) demonstrated a simultaneous alpha desynchronization and enhanced *evoked* 40 Hz (gamma band) activity during finger movement and concluded that alpha band activity is characteristic for cortical areas at rest while gamma band activity represents the "working brain," e.g., the activity of cell assemblies which encode sensory information or to perform a motor task. Thus, the two frequencies are related to different functional meanings of cortical activity.

On the basis of the results of experiment 3 and the model of Vijn (1992), one might speculate that different coding mechanisms underlie simple and complex stimuli. There was less gamma band activity for the moving complex stimulus as compared to the complex standing stimulus. This fits in perfectly with the findings of Vijn and colleagues (van Dijk, et al., 1994; Vijn, et al., 1991; Vijn, et al., 1992; Vijn, 1992) who also found a reduction in spectral power up to 40 Hz when a complex stimulus started to move.

In the long bar experiment (experiment 1 and 2), the induced gamma band activity was most pronounced in a time window beginning 320 ms post motion-onset. In experiment 4, the gamma power was most pronounced in a time window starting 256 ms after motion-onset. The observed latencies of the present work parallel those reported by Tallon-Baudry et al. (1997), who found induced gamma band activity in a visual search task with a latency of approximately 280 ms. Pulvermüller (1996) reported an enhanced power in the gamma band for words as compared to pseudo-words in the latency range of 300 to 500 ms. In the visual cortex of the cat, the reported latencies for the first oscillatory spindles, not phase locked to a moving stimuli, occured at approximately 400 ms (Bauer, et al., 1995; Eckhorn, et al., 1990), which is consistent with the findings in the human EEG, where induced gamma band activity does not appear earlier than 256 ms.

However, stimulus evoked activity (i.e. responses phase locked to the stimulus) occur within the first 100 ms after stimulus presentation (Bauer, et al., 1995; Eckhorn, et al., 1990; Pantev, et al., 1995). The late appearance of stimulus induced activity suggests a fundamental difference between evoked and induced oscillations. Eckhorn and co-workers (1990) speculated on the complementary features of the two types of oscillations. They assumed that

> "evoked responses serve to define crude instantaneous 'preattentive percepts', and stimulus-induced oscillatory synchronization mainly support the formation of more complex, 'attentive percepts' that require iterative interactions among different processing levels and memory" (page 302).

A similar interpretation was provided by Pulvermüller (1996) with respect to word processing. He assumes that the first fast evoked responses may be related to the activation or ignition of a cell assembly and the later induced responses are related to the sustained activity of the network which might also include further cognitive processes.

For now it seems that induced gamma band activity occurs later than the evoked cortical activity. Differences in latencies of induced GBRs across studies may be attributed to different tasks and the respective time resolution of the analysis method used. However, the relation between early evoked components and late induced components remain speculative until further research provides clearer evidence.

The functional relevance of induced gamma band responses is still under debate (e.g. Singer & Gray, 1995; Bair, et al., 1994; Tovee & Rolls, 1992; Young, et al., 1992). Evidence that induced gamma band responses may be linked to feature binding was recently put forth by Tallon and co-workers (1995). The presentation of an illusory triangle (Kanizsa triangle) produced 30 Hz-activity most pronounced around the vertex (Cz). A control stimulus without the illusory quality (achieved by rotation of the inducing disks) elicited no such gamma band response. In a subsequent study, Tallon-Baudry et al. (1997) found induced gamma band responses when subjects had to perceive a Dalmation. In addition, it was shown that induced gamma band activity is related to word processing (Eulitz, Maess, Pantev, Friederici, Feige, & Elbert, 1996; Lutzenberger, Pulvermüller, & Birbaumer,

1994; Pulvermüller, 1996; Pulvermüller, Eulitz, Pantev, Mohr, Feige, Lutzenberger, et al., 1996a; Pulvermüller, Preissl, Lutzenberger, & Birbaumer, 1996b) and to a sensory motor task (Kristeva-Feige, Feige, Makeig, Ross, & Elbert, 1993). The present work has shown that induced gamma band activity is also altered by spatial visual attention. These findings are lending strong support to the hypothesis that macroscopically visible gamma band activity is functionally relevant. Nonetheless, more conclusive evidence is needed to determine whether this response is actually linked to feature binding.

3. General discussion

The present work consists of a series of experiments conducted to investigate the steady-state response in the auditory and visual modality and visually induced gamma band responses. It has been shown that although the underlying mechanisms which generate the respective response might be different, these oscillatory rhythms provide information about cortical processes which exceed or complement the information obtained with event related potentials, e.g to investigate the temporal characteristics of attentional processes. All three responses are similar in such that they can be altered by attention. For the auditory SSR, this was true for an oddball task and for a self paced voluntary movement[1]. Although the mechanism which generates auditory SSRs is still not fully resolved (see section 2.1.5 for a discussion), the generator(s) of the auditory SSR have been reliably located in the primary auditory cortex (Pantev, Bertrand, Eulitz, Verkindt, Hampson, Schuierer, et al., 1995; Pantev, Elbert, Makeig, Hampson, Eulitz, & Hoke, 1993; Pantev, Roberts, Elbert, Ross, & Wienbruch, 1996). Therefore, the present results suggest that attentional processes modulate information processing in the auditory cortex prior to the initial stages of cortical processing. This parallels earlier findings, which have shown a modulation of the middle-latency Pa component by focused auditory attention (Woldorff, Gallen, Hampson, Hillyard, Pantev, Sobel, et al., 1993; Woldorff & Hillyard, 1991). Evidence of which physiological mechanisms are responsible for the CERP perturbations remains inconclusive. Possible mechanisms were discussed (see section 2.1.5), and will not be repeated here. However, it appears obvious that attentional modulation mechanisms in the auditory and visual modality are different. In the auditory cortex, the first component which can be modulated by attention has a latency of about 30 to 40 ms. For the visual modality it was frequently reported that the first component which can be altered by visual spatial attention has a latency of about 80 ms after stimulus onset and has its generator in the extrastriate cortex (Hillyard, et al., 1995; Mangun, et al., 1990; 1992; Heinze, et al., 1993).

It was demonstrated that steady-state visual evoked potentials can be elicited with a variety of frequencies (see 2.2.1). This constitutes another difference

---

[1] Since subjects were instructed to press a button about every 10 seconds, one might assume, that the execution of the motor response draws attention away from the auditory stimulus train.

to the auditory modality, in which the only stimulation frequency for SSRs is around 40 Hz, indicating that auditory and visual SSRs can not have the same underlying generating mechanisms. Regan (1989) suggested three frequency bands for the SSVEPs with amplitude maxima in the low (5-12 Hz), medium (12-25 Hz) and high (30-50 Hz) frequency band. As of yet, there is no clear theory of how the visual SSR is generated. Spekreijse and co-workers speculated that the 30 ms early component of the visual evoked potential corresponds to the high frequency band, the 100 to 120 ms component to the medium, and the rhythmic afterdischarge of a flash visual evoked potential in the alpha range corresponds to the low frequency band (Spekreijse, Estevez, & Reits, 1977).

The present work has shown that the equivalent current dipoles of SSVEPs elicited by 6.0 and 11.9 Hz had a different location as compared to the 15.2 Hz SSVEP, which can be considered to lend support to the notion of different frequency bands. Van Djik and Spekreijse (1990) have localized the equivalent current dipole of a 40 Hz flicker in the primary visual cortex (Area 17). In addition, the eccentricity of the driving stimulus was in agreement with the retinotopic map of area 17, i.e. the most foveal stimulus evoked occipital responses whereas the more eccentric stimuli (2-4 deg) generated activity on the medial wall (van Dijk & Spekreijse, 1990). However, it might be also possible that higher frequency flickers would preferentially activate the magnocellular (M) visual pathways, whereas lower frequencies would produce relatively greater activity in parvocellular (P) pathways (Silberstein, 1995). Further research needs to determine, whether one can devise the SSVEP locations into two clusters, or whether there is a low, medium and high frequency cluster. It is also possible that more than three clusters which track different visual pathways can be identified. A tracking of visual pathways by means of the SSVEP would allow to get a much better understanding of attentional processes in the visual cortex. If it holds true that higher stimulation frequencies (around 40 Hz) produce an activation in the primary visual cortex, the SSVEP can be used to investigate whether striatal activity is modulated by attention (see below and footnote 5).

SSVEP amplitudes of Regan's low and middle frequency band have been increased when the flickering stimulus was attended as compared to when

this stimulus was not attended[2]. For both bands, the amplitude of the SSVEP almost doubles when the stimulus is attended. The cortical activation occurs in a very focused area over the posterior scalp, indicating that sources of the striate cortex can not account for that activity (see section 2.2.2). Based on these distributions, the intracranial sources of these SSVEPs were estimated using the recently developed Variable Resolution Electrical Tomography (VARETA)[3] technique (Riera, Aubert, Valdes, Casanova, & Lins, 1996; Valdes-Sosa, Marti, Garcia, & Casanova, 1996) to further examine the question of whether the 20.8 and 27.8 Hz SSVEPs derive from focal brain areas or represent the resonant activity of widespread brain regions[4]. The intracranial sources of the attended SSVEPs as estimated with VARETA are shown for the grand average data in Figure 3.1.

---

[2] The attentional modulation of SSVEPs in the low frequency band was shown by Morgan, et al. (1996).

[3]The VARETA technique provides a discrete spline-interpolated solution that estimates the spatially smoothest intracranial current distributions compatible with the observed scalp distributions. This approach extends the Low Resolution Electromagnetic Tomography (LORETA) technique (Pascual-Marqui, Michel, & Lehmann, 1994) by placing anatomical constraints on the allowable solutions. The constraints used here restricted the source currents to probability estimates of the cortical mantle that were derived from the average-brain data set produced at the Montreal Neurological Institute (Collins, Neelin, Peter, & Evans, 1994; Evans, Collins, Mills, Brown, Kelly, & Peters, 1993; Mazziotta, Toga, Evans, Fox, & Lancaster, 1995). The VARETA analysis has the general form of an iterative nonlinear estimator, which under certain simplifications can be estimated linearly. Both distributed and discrete sources may be estimated with equal accuracy using VARETA depending on the degree of spatial smoothing, which may be allowed to vary from point to point in gray matter (hence the name "Variable Resolution"). This variable resolution allows for spatially adaptive nonlinear estimates of current sources that eliminate "ghost solutions" that may be present in linear inverse solutions.

[4] For a more detailed description of the VARETA analysis with respect to the current work see Müller, M.M., Picton T.W., Valdes-Sosa, P., Riera, J., Teder-Salejarvi, W., Hillyard, S.A.: Effects of spatial selective attention on the steady-state visual evoked potentials in the 20-28 Hz range (submitted for publication). This section is an adapted version of this article.

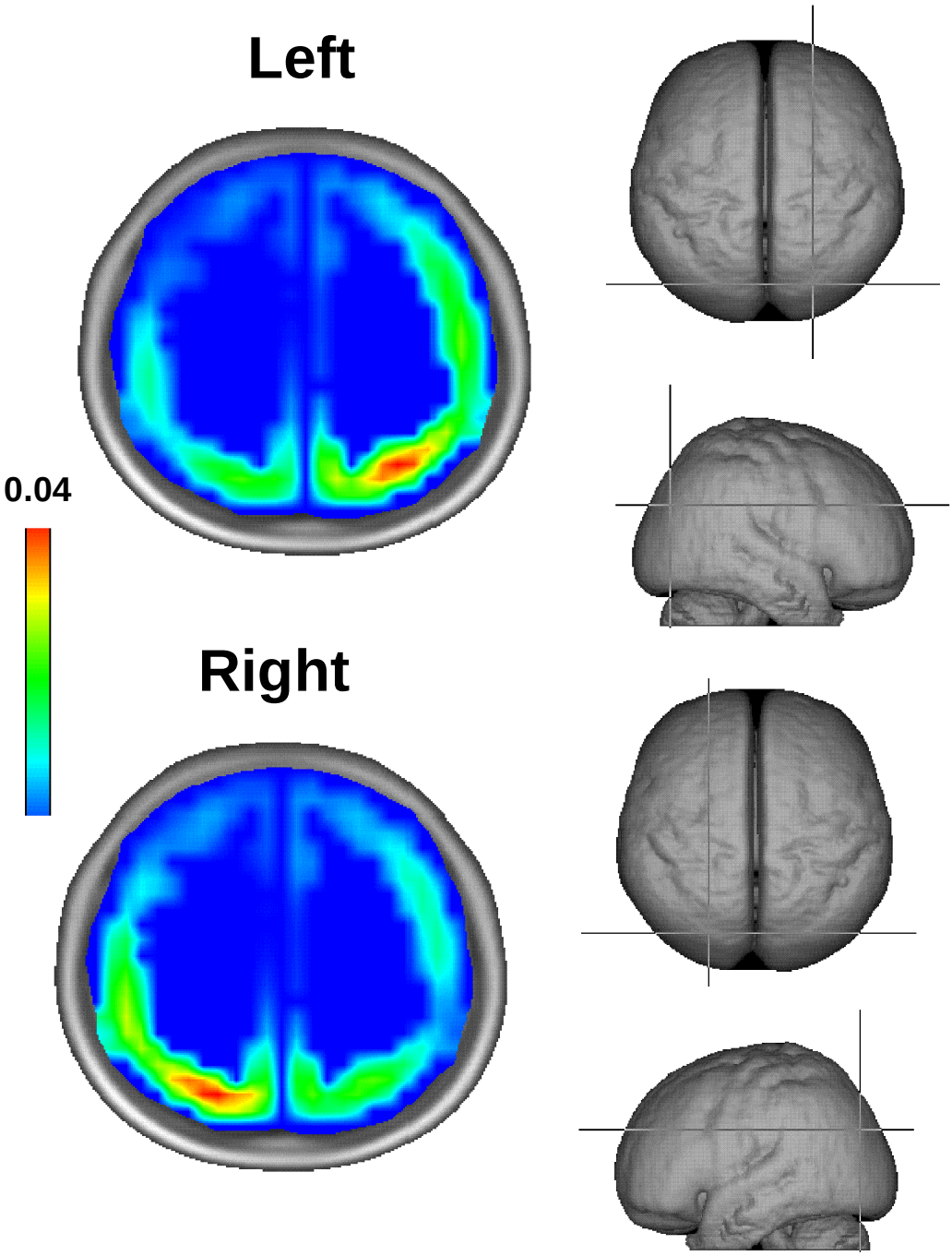

Figure 3.1. Source analysis of SSVEPs for grand average SSVEP scalp distributions over all 10 subjects in response to attended left and attended right field stimuli (see section 2.2.3) using VARETA. Color maps show estimated intracranial current distributions in tomographic sections where currents were maximal. Color scale is adjusted to span range of zero to maximum current density observed in each condition. Scale values are only approximate since precise geometry and conductivities of scalp, skull and brain were not determined. Using estimates of skin conductivity of 0.15 Siemens/meter and skin thickness of 0.1 cm, multiplying the scale values by 1.5 approximates the current density in picoamps/cm^2 . Planes of section are illustrated on surface renditions of the "average brain" produced at the Montreal Neurological Institute (Evans, et al., 1993), which was used to constrain the VARETA analysis.

In both cases, maximal current flows were situated in focal areas of parietal-occipital cortex contralateral to the attended stimulus. Since VARETA is designed to reveal distributed rather than discrete sources (see footnote 3), this approach would be more likely to give veridical solutions for distributed sources than analysis techniques based on modeling intracranial sources in terms of discrete dipoles (Picton, Lins, & Scherg, 1995) would. Despite its sensitivity to distributed sources, VARETA revealed rather focal sources for the 20.8/27.8 Hz SSVEP, which provides strong evidence for a focal origin of these attention-sensitive responses to flicker. The exact location of these sources in parieto-occipital cortex should be viewed with caution, but their position does appear to be somewhat dorsal to the occipito-temporal sources determined for the 8.6/12 Hz SSVEP in the Morgan et al. (1996) study. This difference may have to do with a different frequency selectivity for dorsal and ventral visual pathways[5] (see also section 2.2.2).

The present findings are in accordance with previous studies of spatial attention that support an extrastriate rather than a striate locus of attentional modulation of visual processing. Enhanced neural activity in extrastriate cortex to attended-location stimuli has been revealed using transient ERPs (Clark & Hillyard, 1996; Mangun, Hillyard, & Luck, 1993), combined SSVEPs and fMRI (Hillyard, Hinrichs, Tempelmann, Morgan, Hansen, Scheich, et al., in press), and PET imaging (Clark & Hillyard, 1996; Heinze, Mangun, Burchert, Hinrichs, Scholz, Münte, et al., 1994; Mangun, Hopfinger, Kussmaul, Fletchert, & Heinze, in press; Woldorff, Fox, Matzke, Lancaster, Veeraswamy, Zamarripa, et al., in press). No modulation of evoked neural activity was observed in primary visual cortex in any of these studies. This evidence supports an attentional mechanism that acts by biasing the extrastriate visual pathways so that inputs coming from attended locations receive enhanced processing relative to unattended locations.

The present work showed the time course of the so-called "attentional blink" (Raymond, Shapiro, & Arnell, 1992; Shapiro, Caldwell, & Sorensen,

---

[5] It should be mentioned, that the inter-flicker intervall for the 27.8 Hz stimulus was 36 ms, which is about the time latency for a superposition of early visual evoked potential components. Spekreijse et al. (1977) have proposed that the visual evoked potential component with a latency of about 30 ms is part of the high frequency band. If the high frequency band really has its generator primarily in the primary visual cortex, one would expect a location of the source of the 27.8 Hz flicker at least closer to Area 17. This, however, was not the case.

1997; Shapiro, Raymond, & Arnell, 1994) on the cortical level. The increase of the SSVEP amplitude after the direction cue did not occur earlier then 240 ms for the right (27.8 Hz) and 288 ms for the left visual hemifield stimulus (20.8 Hz). The time bin in which subjects reached their maximum performance level correlated highly significantly with the latency of the SSVEP amplitude peak. It was also shown that subjects who reached their maximum performance earlier (fast responders) had an shorter latency for the SSVEP amplitude maximum as compared to subjects who reached their maximum performance level in a later time bin (slow responders). As discussed in section 2.2.5, experiments using rapid serial stimuli have shown that the "attentional blink" was related to the probe stimulus *following* the target cue, whereas the difficulty to detect the target cue had no influence on the time period of the "attentional blink" (Broadbent & Broadbent, 1987; Raymond, et al., 1992; Shapiro, et al., 1997; Shapiro, et al., 1994; Sperling & Reeves, 1980; Weichselgartner & Sperling, 1987). In experiment 4 (see 2.2.4), left bar targets were more difficult to detect as compared to right bar targets, which found expression in slower reaction times and a higher error rate for left bar targets. However, given the somewhat poor time resolution of our behavioral data, subjects reached their maximum performance 432 ms after the attention direction cue for both bars. A closer inspection of figure 2.2.14 and 2.2.15 shows that this was also the approximate time range in which the SSVEP amplitude reached its maximum. Therefore, it can be concluded that the SSVEP serves as a powerful tool to investigate not only the spatial, but also the temporal characteristics of visual attention processes.

It has been proposed that the attentional blink does not reflect a suppression of perceptual processing, rather it reflects a loss of information at a postperceptual stage (Raymond, et al., 1992; Shapiro, et al., 1994). In an elegant study, Luck, Vogel, and Shapiro (1996) investigated this matter by presenting words either 83, 249 or 581 ms after a target among a series of distractors. The words were either related or unrelated to a given first word at the beginning of each trial. After each trial, subjects were asked to indicate by a button-press whether or not the word was related to the given first word. Aside from the behavioral response, the N400 event related potential, an indicator of mismatch between a word and a previously given semantic context served as the dependent variables. In concordance with previous reports, the attentional blink was most prominent in words presented 249 ms after the target. Subjects were not able to correctly indicate whether or

not the word was related to the first word at the start of the trial. Most interestingly, the N400 amplitude was not reduced for those words, which indicates that perceptual processing was not suppressed in the time period of the attentional blink. Since subjects were not able to correctly relate the words to the first word given at the beginning of the trial, it was concluded that the attentional blink reflects a loss of information at a postperceptual stage of stimulus processing.

In addition to driven oscillatory cortical activities, the present work has also investigated visually induced cortical responses in the gamma band range. These responses are elicited by but are not time- and phase locked to a stimulus. In section 1.2 four hypothesis were presented to explain why cell assemblies oscillate. On the basis of animal studies and theoretical models, it has been proposed that these synchronized oscillations represent the physiological substrate and computational mechanism of how the brain binds different features of an object together. In the present work, induced gamma band responses were reliably extracted from the human EEG when a moving long bar was attended. In contrast, two short bars moving in opposite directions produced a significant reduction of gamma spectral power as compared to the long bar (supporting hypothesis 1 and/or 2). The implications were discussed in section 2.3.6. However, a moving complex stimulus was correlated with a reduction in gamma power as compared to when the same complex stimulus was standing, which might support hypothesis 2 of a coding of the stimulus itself. On the basis of Vijn's model (1992) one would rather conclude that the brain remained in the scanning state when the standing stimulus was presented. However, as has been discussed in section 2.3.6, experiment 3 of the present work was not designed to entirely test Vijn's model (see 2.3.4). To test this model, one should combine complex and simple stimuli, and further investigate the time course of the topography of the spectral power in the gamma band range. One would expect a change in topography from a very broad distribution to a more focused distribution of the gamma spectral power.

The model by Vijn brings a problem into mind, namely what would a "correct" baseline for such experiments be. In the present work, the baseline was always the standing stimulus. According to Vijn, the visual cortex would be in the scanning state during that time period, which is functionally different from the detection state, when the stimuli are in motion. The alternative would be to take the period during which the

screen is black as a baseline. However, one might speculate that this would not change much since the brain would also be in the scanning state during this epoch "waiting" for the stimulus to occur. After the stimulus appears on the screen, one should expect that the brain switches to the detection state and then, when the standing stimulus is presented for a longer epoch, one would expect a switch back to the scanning state. So one can doubt, whether the black screen provides a better baseline. However, studies using evoked potentials have the same problem, since the time epoch before stimulus onset should also be related to the scanning state of the brain. Vjin (1992) provides no temporal information in his model. Therefore, the question arises as to how long a stimuls has to be present without any change, for the brain function to remain in the scanning state? Again, this could be investigated in scanning the time course of the topographical distribution of the gamma power. However, one should keep in mind that the gamma band topography showed no systematic patterns between subjects in the present and in the work of Tallon-Baudry et al. (1997), which makes it somewhat difficult to draw clear solutions from topographical distributions.

It was demonstrated here that GBRs do not represent higher harmonics of the alpha band, are most certainly not muscle artifacts, and might have a functional role (i.e. stimulus processing) since one can alter induced gamma band responses by visual spatial attention (supporting hypothesis 3, against hypothesis 4). This last experiment of section 2.3 (see 2.3.5) has demonstrated that the attentional modulation is not reflected in a broad gamma band range, rather it was only seen in a frequency range between 66 and 94 Hz. This finding parallels the result by Eckhorn et al. (1993) who reported induced gamma band responses in the visual cortex of the awake behaving monkey in a frequency range between 60 and 90 Hz, which is a considerably higher range as compared to the frequency reported in cat visual cortex (see Singer & Gray, 1995 for an overview).

In section 2.3.6, a possible relationship between induced gamma band responses and early evoked potentials was discussed. As of yet, all proposed relations are purely speculative. The same holds true for the relationship between evoked potentials and the steady-state response. Some findings of the present work suggest that SSR provide information which can not be obtained by evoked potentials. First, one can investigate the time course of cortical activities. Second, SSVEPs might track different visual pathways,

which allows the investigation of normal visual function as well as pathological deviations. Third, one can underlay SSRs to each task without interference, and fourth, it seems obvious that a system which is permanently in action provides different information than one with only short periods of activation. With respect to induced gamma band responses one might speculate that the relatively late occurrence of these activities must be related to a different functional role as compared to evoked potentials. Nonetheless, more conclusive evidence that these oscillations are related to feature binding is needed. Neither animal nor human experiments have been able to provide this evidence of yet.

4. Summary

In the present work, three types of oscillatory cortical activity were investigated: (a) auditory SSR, (b) visual steady-state evoked potentials, and (c) visually induced gamma band rhythms. It was demonstrated that all three responses can be altered by attention thereby providing different information about attentional processes. Auditory steady-state responses have been found to have their generator(s) in the primary auditory cortex. The findings of the present work suggest that in the auditory modality, attentional modulations were already active in the primary auditory cortex. This differs from the visual modality, where attentional modulations have only been found in cortical responses with a latency of about 80 ms, which have their generator(s) in the extrastriate visual cortex. Unlike the auditory steady-state response, the visual steady-state response can be elicited with a large variety of frequencies, suggesting that the steady-state response of the two modalities is generated by different mechanisms. With respect to the steady-state visual evoked potential, it has been shown that the location of an equivalent current dipole changed systematically as a function of frequency, which may be interpreted as a sign that they track different visual pathways. High frequency steady-state visual evoked potentials (20.8 and 27.8 Hz) were altered by visual spatial attention, with a narrow focus of cortical activity over the posterior scalp contralateral to the stimulation side, suggesting extrastriate generators. The continuous cortical steady-state activity is used to track the temporal characteristics of attentional processes. The present work is the first to demonstrate temporal characteristics of visual spatial attention on the cortical level. The amplitude augmentation was highly correlated with the time window in which subjects achieved their best performance level, suggesting that the attentional shifting (or attentional blink) period is not a fixed time constant, but related to the features of the task *following* the shifting cue.

Synchronized oscillatory neuronal activity is discussed as the key mechanism by which the brain binds information processed in different cortical areas together to form a percept. The present work has demonstrated that so-called induced gamma band responses can be extracted from the human EEG. Using an identical stimulation design, as used in animal studies, it was shown that human induced gamma band responses resembled the same features as those reported from intracortical recordings from animals. The functional relevance of induced gamma band responses

is still under debate. The present work has shown that they are not higher harmonics of the alpha band and that they can be modulated by spatial visual attention. These results support the notion that gamma band activity is not just a by-product of neuronal activity and that alpha- and gamma band activities represent different cortical functional states.

5. References

Bair, W., Koch, C., Newsome, W., & Britten, K. (1994). Power spectrum analysis of bursting cells in area MT in the behaving monkey. The Journal of Neuroscience, 14, 2870-2892.

Bauer, R., Brosch, M., & Eckhorn, R. (1995). Different rule of spatial summation from beyond the receptive field for spike rates and oscillation amplitudes in cat visual cortex. Brain Research, 669, 291-297.

Beauchamp, M. S., & DeYoe, E. A. (1995). fMRI reveales feature-specific attentional modulation of area MT, V3/V3a and parietal visual areas. Soc Neurosci Abstr, 21, 1760.

Berg, P. (1986). The residual after correcting event-related potentials for blink artefacts. Psychophysiology, 23, 354-364.

Berger, H. (1929). Über das Elektenkephalogramm des Menschen. Arch. Psychiat. Nervenkr., 87, 527-570.

Broadbent, D. E., & Broadbent, M. H. P. (1987). From detection to identification: Response to multiple targets in rapid serial visual presentation. Perception & Psychophysics, 42, 105-113.

Bullock, T. H., Karamürsel, S., Achimowicz, J. Z., McClune, M. C., & Basar-Eroglu, C. (1994). Dynamic properties of human visual evoked and omitted stimulus potentials. Electroencephalography and Clinical Neurophysiology, 91, 42-53.

Cacioppo JT. (1990) The skelemotor system. In: Cacioppo JT, Tassinary LG (eds) Principles of psychophysiology. Cambridge University Press, Cambridge. pp 325-384.

Clark, V. P., & Hillyard, S. A. (1996). Spatial selective attention affects early extrastriate but not striate components of the visual evoked potential. J. Cog. Neurosci., 8, 387-402.

Collins, D. L., Neelin, P., Peter, T. M., & Evans, A. C. (1994). Automatic 3D registration of MR volumetric data in standardized talairach space. J. Comput. Assist. Tomogr., 18, 192-205.

Corbetta, M., Miezin, F. M., Shulman, G. L., & Petersen, S. E. (1993). A PET study of visuospatial attention. The Journal of Neuroscience, 13, 1202-1226.

Deecke, L., Kornhuber, H. H., Schreiber, H., Lang, M., Lang, W., Kornhuber, A., Heise, B., & Keidel, M. (1986). Bereitschaftspotential associated with writing and drawing. Cerebral Psychophysiology, EEG Suppl. 38, 245-247.

Deecke, L., Lang, W., Heller, H. J., Hufnagl, M., & Kornhuber, H. H. (1987). Bereitschaftspotential in patients with unilateral lesions of the supplementary motor area. Journal of Neurology, Neurosurgery, and Psychiatry, 50, 1430-1434.

Deecke, L., Scheid, P., & Kornhuber, H. H. (1969). Distribution of readiness potential, pre-motion positivity, and motor potential of the human cerebral cortex preceding voluntary finger movements. Experimental Brain Research, 7, 158-168.

Eckhorn, R., Bauer, R., Jordan, W., Brosch, M., Kruse, W., Munk, M., & Reitboeck, H. J. (1988). Coherent oscillations: a mechanism of feature linking in the visual cortex? Biological Cybernetics, 60, 121-130.

Eckhorn, R., Frien, A., Bauer, R., Woelbern, A., & Kehr, H. (1993). High frequency (60-90 Hz) oscillations in primary visual cortex of awake monkey. NeuroReport, 4, 243-246.

Eckhorn, R., Reitboeck, H. J., Arndt, M., & Dicke, P. (1990). Feature linking via synchronization among distributed assemblies: simulations of results from cat visual cortex. Neural Computation, 2, 293-307.

Eckhorn, R., Schanze, T., Brosch, M., Salem, W., & Bauer, R. (1992). Stimulus-specific synchronizations in cat visual cortex: multiple microelectrode and correlation studies from several cortical areas. In E. Basar & T. H. Bullock (Eds.), Induced Rhythms in the Brain (pp. 47-82).

Elbert, T., Pantev, C., Wienbruch, C., Rockstroh, B., & Taub, E. (1995). Increased cortical representation of the fingers of the left hand in string players. Science, 270, 305-307.

Engel, A. K., König, P., Gray, C. M., & Singer, W. (1990). Stimulus-dependent neuronal oscillations in cat visual cortex: inter-columnar interaction as determined by cross-correlation analysis. European Journal of Neuroscience, 2, 588-606.

Engel, A. K., König, P., Kreiter, A. K., & Singer, W. (1991b). Interhemispheric synchronization of oscillatory neuronal responses in cat visual cortex. Science, 252, 1177-1179.

Engel, A. K., König, P., Kreiter, A. K., Gray, C. M., & Singer, W. (1991a). Temporal coding by coherent oscillations as a potential solution to the binding problem: physiological evidence. In H. G. Schuster (Ed.), Nonlinear dynamics and neuronal networks (pp. 3-25). Weinheim: VHC Verlagsgesellschaft.

Engel, A. K., König, P., Kreiter, A. K., Schillen, T. B., & Singer, W. (1992). Temporal coding in the visual cortex: new vistas on integration in the nervous system. TINS, 15, 218-226.

Engel, A. K., Kreiter, A. K., König, P., & Singer, W. (1991c). Synchronization of oscillatory neuronal responses between striate and extrastriate visual cortical areas of the cat. Proceedings of the National Acadamy of Science USA, 88, 6048-6052.

Eulitz, C., Maess, B., Pantev, C., Friederici, A. D., Feige, B., & Elbert, T. (1996). Oscillatory neuromagnetic activity induced by language and non-language stimuli. Cognitive Brain Research, 4, 121-132.

Evans, A. C., Collins, D. L., Mills, S. R., Brown, E. D., Kelly, R. L., & Peters, T. M. (1993). 3D statistical neuroanatomical models from 305 MRI volumes. In Proc. IEEE-Nuclear Science Symposium and Medical Imaging Conference.

Freeman, W. J. (1975). Mass action in the nervous system. New York: Academic Press.

Freeman, W. J. (1992). Predictions on neocortical dynamics derived from studies in paleocortex. In E. Basar & T. H. Bullock (Eds.), Induced Rhythms in the Brain (pp. 183-200).

Freeman, W. J. (1996). Feedback models of gamma rhythems. TINS, 19(11), 468.

Freeman, W. J., & Dijk, B. W. v. (1987). Spatial patterns of visual cortical fast EEG during conditioned reflex in a rhesus monkey. Brain Research, 422, 267-276.

Freeman, W. J., & Prisco, G. V. d. (1986). EEG spatial pattern differences with discriminated odors manifest chaotic and limit cycle attractors in olfactory bulb of rabbits. In G. Palm & A. Aertsen (Eds.), Brain theory (pp. 97-119). Berlin: Springer.

Galambos, R. (1992). A comparison of certain gamma band (40-Hz) brain rhythms in cat and man. In E. Basar & T. H. Bullock (Eds.), Induced Rhythms in the Brain (pp. 201-216). Boston: Birkhäuser.

Galambos, R., Makeig, S., & Talmachoff, P. (1981). A 40-Hz auditory potential recorded from the human scalp. Proc. Natl. Acad. Sci. USA, 78, 2643-2647.

Gray, C. M., & McCormick, D. A. (1996). Chattering Cells: Superficial pyramidal neurons contributing to the generation of synchronous oscillations in the visual cortex. Science, 274, 109-113.

Gray, C. M., & Singer, W. (1989). Stimulus-specific neuronal oscillations in orientation columns of cat visual cortex. Proceedings of the National Acadamy of Science USA, 86, 1698-1702.

Gray, C. M., Engel, A. K., König, P., & Singer, W. (1990). Stimulus-dependent neuronal oscillations in cat visual cortex: receptive field properties and feature dependence. European Journal of Neuroscience, 2, 607-619.

Gray, C. M., Engel, A. K., König, P., & Singer, W. (1992). Synchronization of oscillatory neuronal responses in cat striate cortex: temporal properties. Visual Neuroscience, 8, 337-347.

Gray, C. M., König, P., Engel, A. K., & Singer, W. (1989). Oscillatory responses in cat visual cortex exhibit inter-columnar synchronization which reflects global stimulus properties. Nature, 338, 334-337.

Hackley, S. A. (1993). An evaluation of the automaticity of sensory processing using event-related potentials and brain-stem reflexes. Psychophysiology, 4, 415-428.

Hari, R., & Salmelin, R. (1997). Human cortical oscillations: a neuromagnetic view through the scull. TINS, 20, 44-49.

Hari, R., Hämäläinen, M., & Joutsiniemi, S.-L. (1989). Neuromagnetic steady-state responses to auditory stimuli. J. Acoust. Soc. Am., 86, 1033-1039.

Hazemann, P., Audin, G., & Lille, F. (1975). Effect of voluntary self-paced movements upon auditory and somatosensory evoked potentials in man. Electroenceph. clin. N□europhysiol., 39, 247-254.

Hebb, D. O. (1949). The organization of behavior. Chichester: John Wiley & Sons.

Heinze, H. J., Johannes, S., & Thinius, R. (1993). Neurale Mechanismen visueller selektiver Aufmerksamkeit: Untersuchungen mit ereigniskorrelierten Potentialen. Zeitschrift fuer EEG und EMG, 24, 16-23.

Heinze, H. J., Mangun, G. R., Burchert, W., Hinrichs, H., Scholz, M., Münte, T. F., Gös, A., Scherg, M., Johannes, S., Hundeshagen, H., Gazzaniga, M. S., & Hillyard, S. A. (1994). Combined spatial and temporal imaging of brain activity during visual selective attention in humans. Nature, 372, 543-546.

Heinze, H. J., Mangun, G. R., Burchert, W., Hinrichs, H., Scholz, M., Münte, T. F., Gös, A., Scherg, M., Johannes, S., Hundeshagen, H., Gazzaniga, M. S., & Hillyard, S. A. (1994). Combined spatial and temporal imaging of brain activity during visual selective attention in humans. Nature, 372, 543-546.

Heinze, H.-J., Luck, S. J., Münte, T. F., Gös, A., Mangun, G. R., & Hillyard, S. A. (1994). Attention to adjacent and seperate positions in space: An electrophysiological analysis. Perception & Psychophysics, 56, 42-52.

Hillyard, S. A., Hinrichs, H., Tempelmann, C., Morgan, S. T., Hansen, J. C., Scheich, H., & Heinze, H. J. (in press). Combining steady-state visual evoked potentials and fMRI to localize brain activity during selective attention. Hum. Brain Mapping.

Hillyard, S. A., Mangun, G. R., Woldorff, M. G., & Luck, S. J. (1995). Neural systems mediating selective attention. In M. S. Gazzaniga (Ed.), The Cognitive Neurosciences (pp. 665-681). Cambridge: MIT Press.

Hillyard, S. A., Mangun, G. R., Woldorff, M. G., & Luck, S. J. (1995). Neural systems mediating selective attention. In M. S. Gazzaniga (Ed.), The Cognitive Neurosciences (pp. 665-681). Cambridge: MIT Press.

Ikeda, A., Shibasaki, H., Nagamine, T., Terada, K., Kaji, R., Fukuyama, H., & Kimura, J. (1994). Dissociation between contingent negative variation and Bereitschaftspotential in a patient with cerebellar efferent lesion. Electroenceph. clin. Neurophysiol., 90, 359-364.

Jokeit, H., & Makeig, S. (1994). Different event-related patterns of gamma-band power in brain waves of fast- and slow-reacting subjects. Proceedings of the National Acadamy of Science USA, 91, 6339-6343.

Jürgens, E., Rösler, F., Hennighaus, E., & Heil, M. (1995). Stimulus-induced gamma oscillations: harmonics of alpha activity? NeuroReport, 6, 813-816.

Kirschfeld, K. (1992). Oscillations in the insect brain: do they correspond to the cortical gamma-waves of vertebrates? Proceedings of the National Acadamy of Science USA, 89, 4764-4768.

König, P., Engel, A. K., & Singer, W. (1995). Relation between oscillatory activity and long-range synchronization in cat visual cortex. Proceedings of the National Acadamy of Science USA, 92, 290-294.

Kreiter, A. K. (1992). Kodierung neuronaler Assemblies durch kohärente Aktivität: Korrelationsanalysen im Sehsystem von Säugetieren. Ph.D., Eberhard-Karls-Universität, Tübingen.

Kreiter, A. K., & Singer, W. (1992). Oscillatory neuronal responses in the visual cortex of the awake macaque monkey. European Journal of Neuroscience, 4, 369-375.

Kristeva-Feige, R., Feige, B., Makeig, S., Ross, B., & Elbert, T. (1993). Oscillatory brain activity during a motor task. NeuroReport, 4, 1291-1294.

Law, S. K., Rohrbaugh, J. W., Adams, C. M., & Eckhart, M. J. (1993). Improving spatial and temporal resolution in evoked EEG responses using surface Laplacians. Electroencephalogr. Clin. Neurophysiolog., 88, 309-322.

Livingstone, M., & Hubel, D. (1988). Segregation of form, color, movement, and depth: anatomy, physiology, and perception. Science, 240, 740-749.

Llinas, R. R. (1992). Oscillations in CNS Neurons: a possible role for cortical interneurons in the generation of 40-Hz oscillations. In E. Basar & T. H. Bullock (Eds.), Induced Rhythms in the Brain (pp. 269-286).

Llinas, R. R., & Ribary, U. (1992). Rostrocaudal scan in human brain: a global characteristic of the 40-Hz response during sensory input. In E. Basal & T. H. Bullock (Eds.), Induced Rhythms in the Brain (pp. 147-154).

Llinás, R., & Ribary, U. (1993). Coherent 40-Hz oscillation charcterizes dream state in humans. Proceedings of the National Acadamy of Science USA, 90, 2078-2081.

Luck, S. J., Fan, S., & Hillyard, S. A. (1993). Attention-related modulation of sensory-evoked brain activity in a visual search task. Journal of Cognitive Neuroscience, 5, 188-195.

Luck, S. J., Hillyard, S. A., Mouloua, M., Woldorff, M. G., Clark, V. P., & Hawkins, H. L. (1994). Effects of spatial cuing on luminance detectability: Psychophysical and electrophysiolgical evidence for early selection. Journal of Experimental Psychology: Human Perception and Performance, 20, 887-904.

Luck, S. J., Vogel, E. K., & Shapiro, K. L. (1996). Word meanings can be accessed but not reported during the attentional blink. Nature, 383, 616-618.

Lutzenberger, W., Preissl, H., Birbaumer, N., & Pulvermüller, F. (1997). High-frequency cortical responses: do they not exist if they are small? Electroencephalography and clinical Neurophysiology, 102, 64-66.

Lutzenberger, W., Pulvermüller, F., & Birbaumer, N. (1994). Words and Pseudowords elicit distinct patterns of 30-Hz EEG responses in humans. Neuroscience Letters, 176, 115-118.

Lutzenberger, W., Pulvermüller, F., Elbert, T., & Birbaumer, N. (1995). Visual stimulation alters local 40-Hz responses in humans: an EEG-study. Neuroscience Letters, 183, 39-42.

Maier, J., Dagneli, H., Spekreijse, H., & van Dijk, B. W. (1987). Principal component analysis for source localization of VEPs in man. Vision Research, 27, 165-177.

Makeig, S. (1989). Changes in auditory steady-state responses during neuroleptic treatment. Schizophrenia Research, 84.

Makeig, S. (1993). Auditory event-related dynamics of the EEG spectrum and effects of exposure to tones. Electroencephalography and clinical Neurophysiology, 86, 283-293.

Makeig, S. (1994). Effects of attention and stimulus probability on the auditory complex event-related potential. unpublished manuscript.

Makeig, S., & Galambos, R. (1989). The CERP: event-related perturbations in steady-state responses. In E. Basar & T. H. Bullock (Eds.), Brain dynamics: progress and perspectives (pp. 375-400). Berlin: Springer-Verlag.

Makeig, S., & Inlow, M. (1993). Lapses in alertness: coherence of fluctuations in performance and EEG spectrum. Electroenceph. clin. Neurophysiol., 86, 23-35.

Makeig, S., Müller, M.M., & Rockstroh, B. (1996). Effects of voluntary movements on early auditory brain responses.Experimental Brain Research, 110, 487-492.

Mäkelä, J. P., & Hari, R. (1987). Evidence for cortical origin of the 40Hz auditory evoked response in man. Electroenceph. clin. Neurophysiol., 66, 539-546.

Malsburg, C. v. d., & Schneider, W. (1986). A neural cocktail-party processor. Biological Cybernetics, 54, 29-40.

Mangun, G. R., Hillyard, S. A., & Luck, S. J. (1990). Electrocortical substrates of visual selective attention. In D. E. Meyer & S. Kornblum (Eds.), Attention and Performance XIV (pp. 219-242). Cambridge, Massachusetts: The MIT Press.

Mangun, G. R., Hillyard, S. A., & Luck, S. J. (1993). Electrocortical substrates of visual selective attention. In D. Meyer & S. Kornblum (Eds.), Attention and Performance XIV (pp. 219-243). Cambridge: MIT Press.

Mangun, G. R., Hopfinger, J., Kussmaul, C. L., Fletchert, E., & Heinze, H. J. (in press). Covariations in ERP and PET measures of spatial selective attention in human extrastriate visual cortex. Hum. Brain Mapping.

Mazziotta, J. C., Toga, A., Evans, A. C., Fox, P., & Lancaster, J. (1995). A probabilistic atlas of the human brain: Theory and rationale for its development. Neuroimage, 2, 89-101.

McCarthy, G., & Wood, C. C. (1985). Scalp distributions of event-related potentials: an ambiguity associated with analysis of variance models. Electroencephalography and Clinical Neurophysiology, 62, 203-208.

Menon, V., Freeman, W. J., Cutillo, B. A., Desmond, J. E., Ward, M. F., Bressler, S. L., Laxer, K. D., Barbaro, N., & Gevins, A. S. (1996). Spatio-temporal correlations in human gamma band electrocorticograms. Electroenceph. clin. Neurophysiol., 98, 89-102.

Milner, P. M. (1974). A model for visual shape recognition. Psychological Review, 81, No.6, 521-535.

Morgan, S. T., Hansen, J. C., & Hillyard, S. A. (1996). Selective attention to stimulus location modulates the steady state visual evoked potential. PNAS, 93, 4770-4774.

Müller, M. M., Rockstroh, B., Berg, P., Wagner, M., Elbert, T., & Makeig, S. (1994). SSR-modulation during slow cortical potentials. In C. Pantev, T. Elbert, & B. Lütkenhöner (Eds.), Oscillatory event-related brain dynamics New York: Plenum Press.

Müller, M.M., Rockstroh, B., Elbert, T. (1994). Don't move while listening! Journal of Psychophysiology, 8, 354-355.

Müller, M.M., Valdes-Sosa, M., Bosch, J., Riera, J., Bobes, M.A. (1994). Eliciting induced gamma band responses with the movement of a coherent stimulus in humans. Psychophysiology, 31 (suppl. 1), 69-70.

Müller, M.M., Bosch, J., Elbert, T., Kreiter, A., Valdes Sosa, M., Rockstroh, B. (1995). Human visually induced gamma band responses measured by EEG. Journal of Psychophysiology, 9, 358

Müller, M.M., Bosch, J., Elbert, T., Kreiter, A., Valdes Sosa, M., Valdes Sosa P., Rockstroh, B. (1996). Visually induced gamma band responses in human EEG - A link to animal studies. Experimental Brain Research, 112, 96-112.

Müller, M.M., Junghöfer, M., Elbert, T., & Rockstroh, B. (1997). Visually induced gamma-band responses to coherent and incoherent motion: a replication study. NeuroReport, 8, 2575-2579.

Müller, M. M., Teder, W., & Hillyard, S. A. (1997). Magentoencephalographic recording of steady-state visual evoked cortical activity. Brain Topography, 9, 163-168.

Müller, M.M., Elbert, T., Rockstroh, B. (in press). Visuell induzierte Gammabandaktivität im menschlichen EEG - Ausdruck corticaler Reizrepräsentation? Zeitschrift für Experimentelle Psychologie.

Müller, M.M., Picton, T.W., Valdes-Sosa, P.. Riera, J., Teder-Sälejärvi, W., & Hillyard,.S.A. (submitted). Effects of spatial selective attention on the steady-state visual evoked potential in the 20-28 Hz range.

Neshige, R., Lüders, H., & Shibasaki, H. (1988). Recording of movement-related potentials from scalp and cortex in man. Brain, 111, 719-736.

Neuenschwander, S., & Varela, F. J. (1993). Visually triggered neuronal oscillations in the pigeon: an autocorrelation study of tectal activity. European Journal of Neuroscience, 5, 870-881.

Neuenschwander, S., Engel, A. K., König, P., Singer, W., & Varela, F. J. (1996). Synchronization of neuronal responses in the optic tectum of awake pigeons. Visual Neuroscience, 13, 575-584.

Otavio, O. G., & Picton, T. W. (1995). Auditory steady-state responses to multiple simultaneous stimuli. Electroencephalography and clinical Neurophysiology, 96, 420-432.

Pantev, C., Bertrand, O., Eulitz, C., Verkindt, C., Hampson, S., Schuierer, G., & Elbert, T. (1995). Specific tonotopic organizations of different areas of the human auditory cortex revealed by simultaneous magnetic and electric recordings. Electroenceph. clin. Neurophysiol., 94, 26-40.

Pantev, C., Elbert, T., Makeig, s., Hampson, S., Eulitz, C., & Hoke, M. (1993). Relationship of transient and steady-state auditory evoked fields. Electroenceph. clin. Neurophysiol., 88, 389-396.

Pantev, C., Makeig, S., Hoke, M., Galambos, R., Hampson, S., & Gallen, C. (1991). Human auditory evoked gamma band magnetic fields. Proc Natl Acad Sci USA, 88, 8996-9000.

Pantev, C., Roberts, L. E., Elbert, T., Ross, B., & Wienbruch, C. (1996). Tonotopic organization of the sources of human auditory steady-state responses. Hearing Research, 101, 62-74.

Pascual-Marqui, R. D., Michel, C. M., & Lehmann, D. (1994). Low resolution electromagnetic tomography: a new method for localizing electrical activity in the brain. International Journal of Psychophysiology, 18, 49-65.

Perrin, F., Pernier, J., Bertrand, O., & Echallier, J. F. (1989). Spherical splines for scalp potential and current source density mapping. Electroencephalography and clinical Neurophysiology, 72, 184-187.

Pfurtscheller, G. (1992). Event-related synchronization (ERS): an electrophysiological correlate of cortical areas at rest. Electroenceph. clin. Neurophysiol., 83, 62-69.

Pfurtscheller, G., & Aranibar, A. (1979). Evaluation of event-related desynchronization (ERD) preceding and following voluntary self-paced movement. Electroenceph. clin. Neurophysiol., 46, 138-146.

Pfurtscheller, G., & Klimesch, W. (1992). Event-related synchronization and desynchronization of alpha and beta waves in a cognitiv task. In E. Basar & T. H. Bulock (Eds.), Induced Rhythms in the Brain (pp. 117-128).

Pfurtscheller, G., & Neuper, C. (1992). Simultaneous EEG 10 Hz desynchronization and 40 Hz synchronization during finger movements. NeuroReport, 3, 1057-1060.

Pfurtscheller, G., Flotzinger, D., & Kalcher, J. (1993). Brain-computer interface - a new communication device for handicapped persons. Journal for Microcomputer Applications, 16, 293-299.

Pfurtscheller, G., Stancak Jr. , A., & Edlinger, G. (1997). On the existence of different types of central beta rhythms below 30 Hz. Electroenceph.clin.Neurophysio., 102, 316-325.

Picton, T. W., Champagne, S. C., & Kellett, A. J. C. (1992). Human auditory evoked potentials recorded using maximum length sequences. Electroenceph. clin. Neurophysiol., 84, 90-100.

Picton, T. W., Lins, O., & Scherg, M. (1995). The recording of evevt-related potentials. In F. Boller & J. Grafman (Eds.), Handbook of Neuropsychology, Vol.10 (pp. 3-73). Amsterdam: Elsevier.

Picton, T. W., Vajsar, J., Rodriguez, R., & Campbell, K. B. (1987). Reliability estimates for steady-state evoked potentials. Electroenceph. clin. Neurophysiol., 68, 119-131.

Plourde, G., Stapells, D. R., & Picton, T. W. (1991). The human auditory steady-state evoked potentials. Acta Otolaryngnol. (Stockh), Suppl. 491, 153-160.

Prechtl, J. C. (1994). Visual motion induces synchronous oscillations in turtle visual cortex. Proceedings of the National Acadamy of Science USA, 91, 12467-12471.

Press, W. H., Teukolsky, S. A., Vetterling, W. T., & Flannery, B. P. (1992). Numerical recipes in C: The art of scientific computing. Cambridge: Cambridge University Press.

Priestley, M. B. (1988). Non-linear and non-stationary time series analysis. London: Academic Press.

Pulvermüller, F. (1996). Hebb´s conceptof cell asssemblies and the psychophysiology of word processing. Psychophysiology, 33, 317-333.

Pulvermüller, F., Eulitz, C., Pantev, C., Mohr, B., Feige, B., Lutzenberger, W., Elbert, T., & Birbaumer, N. (1996a). High-frequency cortical responses reflect lexical processing: a MEG study. Electroenceph. clin. Neurophysiol., 98, 76-85.

Pulvermüller, F., Lutzenberger, W., Preissl, H., & Bierbaumer, N. (1995). Spectral responses in the gamma-band: Physiological signs of higher cognitive processes. NeuroReport, 6, 2059-2064.

Pulvermüller, F., Preissl, H., Lutzenberger, W., & Birbaumer, N. (1996b). Brain rhythms of language: Nouns versus verbs. Europ. J. of Neurosci., 8, 937-941.

Qian, S., & Chen, D. (1993). Discete Gabor Transform. IEEE Transactions on Signal Processing, 41, 2429-2438.

Raymond, J. E., Shapiro, K. L., & Arnell, K. M. (1992). Temporary suppression of visual processing in an RSVP task: an attentional blink ? Journal of Experimental Psychology: Human Perception and Performance, 18, 849-860.

Regan, D. (1989). Human brain electrophysiology: Evoked potentials and evoked magnetic fields in science and medicine. New York: Elsevier Pubs.

Ribary, U., Ioannides, A. A., Singh, K. D., Hasson, R., Bolton, J. P. R., Lado, F., Mogilner, A., & Llinás, R. (1991). Magnetic field tomography of coherent thalamocortical 40-Hz oscillations in humans. Proc. Natl. Acad. Sci. U, 88, 11037-11041.

Riera, J. J., Aubert, E., Valdes, P., Casanova, R., & Lins, O. (1996). Discrete spline electric-magnetic tomography (DSPET) based on realistic neuroanatomy. In BIOMAG, Santa Fee, New Mexico.

Rockstroh, B., Müller, M., Heinz, A., Wagner, W.; Elbert, T. (1996). Modulation of auditory responses during oddball tasks. Biological Psychology, 43, 41-56.

Rohrbaugh, J. W., Varner, J. L., Paige, S. R., Eckardt, M. J., & Ellingson, R. J. (1990a). Auditory and visual event-related perturbations in the 40 Hz auditory steady-state response. Electroenceph. clin. Neurophysiol., 76, 148-164.

Rohrbaugh, J. W., Varner, J. L., Paige, S. R., Eckhardt, M. J., & Ellingson, R. J. (1990b). Event-related perturbations in an electrophysiological measure of auditory sensitivity: effects of probability, intensity and repeated sessions. International Journal of Psychophysiology, 10, 17-32.

Sarvas, J. (1987). Basic mathematical and electomagnetic concepts of biomagnetic inverse problem. Physics in Medicine and Biology, 32, 11-22.

Shapiro, K. L., Caldwell, J., & Sorensen, R. E. (1997). Personal names and the attentional blink: a visual "cocktail party" effect. Journal of Experimental Psychology: Human Perception and Performance, 23, 504-514.

Shapiro, K. L., Raymond, J. E., & Arnell, K. M. (1994). Attention to visual pattern information produces the attentional blink in rapid serial visual presentation. Journal of Experimental Psychology: Human Perception and Performance, 20, 357-371.

Shibasaki, H., Barrett, G., Halliday, E., & Halliday, A. M. (1980). Cortical potentials following voluntary and passive finger movements. Electroencephalography and Clinical Neurophysiology, 50, 201-213.

Silberstein, R. B. (1995). Steady-state visually evoked potentials, brain resonances, and cognitive processes. In P. L. Nunez (Ed.), Neocortical Dynamics and Human EEG Rhythms (pp. 272-303). Oxford: Oxford University Press.

Silberstein, R. B., Ciorciari, J., & Pipingas, A. (1995). Steady-state visually evoked potential topography during the Wisconsin card sorting test. Electroenceph. clin. Neurophysiol., 96, 24-35.

Silberstein, R. B., Schier, M. A., Pipingas, A., Ciorciari, J., Wood, S. R., & Simpson, D. G. (1990). Steady-state visually evoked potential topography associated with a visual vigilance task. Brain Topography, 3, 337-347.

Singer, W. (1990). Search for coherence: a basic principle of cortical self-organization. Concepts in Neuroscience, 1, 1-26.

Singer, W. (1995). Development and plasticity of cortical processing architectures. Science, 270, 758-764.

Sinkkonen, J., Tiitinen, H., & Näätänen, R. (1995). Gabor filters: an informative way for analysing event-related brain activity. Journal of Neuroscience Methods, 56, 99-104.

Snyder, A. Z. (1992). Steady-state vibration evoked potentials: description of technique and characterization of responses. Electroenceph. clin. Neurophysiol., 84, 257-268.

Spekreijse, H., Estevez, O., & Reits, D. (1977). Visual evoked potentials and the physiological analysis of visual processes in man. In J. E. Desmedt (Ed.), Visual evoked potentials in man (pp. 16-89). Oxford: Claredon.

Sperling, G., & Reeves, A. (1980). Measuring the reaction time of a shift of visual attention. In R. S. Nickerson (Ed.), Attention and performance VIII Hillsdale: Erlbaum.

Steriade, M. (1996). Awakening the brain. Nature, 383, 24-25.

Steriade, M., Amzica, F., & Contreras, D. (1996). Synchroization of fast (30-40 Hz) spontaneous rhythms during brain activation. The Journal of Neuroscience, 16, 392-417.

Steriade, M., Contreras, D., & Amzica, F. (1994). Synchronized sleep oscillations and their paroxysmal developments. TINS, 17, 199-208.

Steriade, M., Gloor, P., Llinás, R. R., Lopes da Silva, F. H., & Mesulam, M.-M. (1990). Basic mechanisms of cerebral rhythmic activities. Electroenceph. clin. Neurophysiol., 76, 481-508.

Steriade, M., McCormick, D. A., & Sejnowski, T. J. (1993). Thalamocortical oscillations in the sleeping and aroused brain. Science, 262, 679-685.

Szczepaniak, W. S., & Moller, A. R. (1993). Interaction between auditory and somatosensory systems: a study of evoked potentials in the inferior colliculus. Electroenceph. clin. Neurophysiol., 88, 508-515.

Tallon, C., Bertrand, O., Bouchet, P., & Pernier, J. (1995). Gamma-range activity evoked by coherent visual stimuli in humans. European Journal of Neuroscience, 7, 1285-1291.

Tallon-Baudry, C., Bertrand, O., Delpuech, C., & Pernier, J. (1996). Stimulus Specifity of Phase-Locked and Non-Phase-Locked 40 Hz Visual Response in Human. The Journal of Neuroscience, 16 (13), 4240-4249.

Tallon-Baudry, C., Bertrand, O., Delpuech, C., & Pernier, J. (1997). Oscillatory gamma-band (30-70 Hz) activity induced by a visual search task in human. The Journal of Neuroscience, 17, 722-734.

Tapia, M. C., Cohen, L. G., & Starr, A. (1987). Attenuation of auditory-evoked potentials during voluntary movement in man. Audiology, 26, 369-373.

Tiitinen, H., Sinkkonen, J., May, P., & Näätänen, R. (1994). The auditory transient 40-Hz response is insensitive to changes in stimulus features. NeuroReport, 6, 190-192.

Tobimatsu, S., Tomoda, H., & Kato, M. (1996). Normal variability of the amplitude and phase of steady-state VEPs. Electroenceph. clin.Neurophysio., 100, 171-176.

Tovee, M. J., & Rolls, E. T. (1992). Oscillatory activity is not evident in the primate temporal visual cortex with static stimuli. NeuroReport, 3, 369-372.

Valdes-Sosa, P., Marti, F., Garcia, F., & Casanova, R. (1996). Variable resolution electric-magnetic tomography. In BIOMAG, Santa Fee, New Mexico.

van Dijk, B. W., & Spekreijse, H. (1990). Localization of electric and magnetic sources of brain activity. In J. E. Desmedt (Ed.), Visual evoked potentials (pp. 57-74). New York: Elsevier.

van Dijk, B. W., Vijn, P. C. M., & Spekreijse, H. (1994). Low temporal frequency desynchroisation and high temporal frequency synchronization accompany processing of visual stimulation in anaesthetized cat visual cortex. In C. Pantev, T. Elbert, & B. Lütkenhöner (Eds.), Oscillatory event-related brain dynamics (pp. 183-204). New York: Plenum Press.

Vijn, P. C. M., van Dijk, B. W., & Spekreijse, H. (1991). Visual stimulation reduces EEG activity in man. Brain Research, 550, 49-53.

Vijn, P. C. M., van Dijk, B. W., & Spekreijse, H. (1992). Topography of occipital EEG reduction upon visual stimulation. Brain Topography, 5, 117-181.

Vijn, P. M. C. (1992). Coherent neuronal activity underlying the EEG. Ph.D. thesis, University of Amsterdam.

Walter, W. G. (1959). Intrinsic rhythms of the brain. In J. Field (Ed.), Handbook of Physiology (pp. 279-298). Washington: American Physiological Ass.

Weichselgartner, E., & Sperling, G. (1987). Dynamics of automatic controlled visual attention. Science, 238, 778-780.

Weichselgartner, E., & Sperling, G. (1987). Dynamics of automatic controlled visual attention. Science, 238, 778-780.

Weichselgartner, E., & Sperling, G. (1987). Dynamics of automatic controlled visual attention. Science, 238, 778-780.

Williamson, S. J., & Kaufman, L. (1990). Theory of neuroelectric and neuromagnetic fields. In F. Grandori, M. Hoke, & G. L. Romani (Eds.), Auditory Evoked Magnetic Fields and Electric Potentials Basel: Karger.

Wilson, G. F., & O`Donnell, R. D. (1986). Steady-state evoked responses: Correlations with human cognition. Psychophysiology, 23, 57-61.

Woldorff, M. G., & Hillyard, S. A. (1991). Modulation of early auditory processing during selective listening to rapidly presented tones. Electroenceph. clin. Neurophysiol., 79, 170-191.

Woldorff, M. G., Fox, P. T., Matzke, M., Lancaster, J. L., Veeraswamy, S., Zamarripa, F., Seabold, M., Glass, T., Gao, J. H., Martin, C. C., & Jerabek, P. (in press). Retinoptic organization of the early visual-spatial attention effects as revealed by PET and ERPs. Hum. Brain Mapping.

Woldorff, M. G., Gallen, C. C., Hampson, S. A., Hillyard, S. A., Pantev, C., Sobel, D., & Bloom, F. E. (1993). Modulation of early sensory processing in human auditory cortex during auditory selective attention. Proceedings of the National Acadamy of Science USA / Neurobiology, 90, 8722-8726.

Yantis, S., & Jonides, J. (1990). Abrupt visual onsets and selective attention : Voluntary versus automatic allocation. J. Exper. Psychol.: Hum. Percept. Perform., 16, 121-134.

Young, M. P., Tanaka, K., & Shigeru, Y. (1992). On oscillating responses in the visual cortex of the monkey. Journal of Neuroscience, 67, 1464-1474.

Zeki, S. (1993). A Vision of the Brain (1 ed.). Oxford: Blackwell.